SECURITY MARKING

The classified or limited status of this report applies to each page, unless otherwise marked.
Separate page printouts MUST be marked accordingly.

THIS DOCUMENT CONTAINS INFORMATION AFFECTING THE NATIONAL DEFENSE OF THE UNITED STATES WITHIN THE MEANING OF THE ESPIONAGE LAWS, TITLE 18, U.S.C., SECTIONS 793 AND 794. THE TRANSMISSION OR THE REVELATION OF ITS CONTENTS IN ANY MANNER TO AN UNAUTHORIZED PERSON IS PROHIBITED BY LAW.

NOTICE: When government or other drawings, specifications or other data are used for any purpose other than in connection with a definitely related government procurement operation, the U. S. Government thereby incurs no responsibility, nor any obligation whatsoever; and the fact that the Government may have formulated, furnished, or in any way supplied the said drawings, specifications, or other data is not to be regarded by implication or otherwise as in any manner licensing the holder or any other person or corporation, or conveying any rights or permission to manufacture, use or sell any patented invention that may in any way be related thereto.

AFAPL-TR-65-40
VOLUME I

AEROSPACE EXPANDABLE STRUCTURES AND MAINTENANCE SUPPORT DEVICES

VOLUME I. EXPANDABLE SELF-RIGIDIZING SOLAR ENERGY CONCENTRATORS AND AEROSPACE SHELTERS FROM HONEYCOMB TYPE FABRIC

RONALD ROCHON, ROBERT C. CLARK, and NELS S. HANSSEN

GCA VIRON DIVISION
GCA CORPORATION

WILLIAM J. McKILLIP

ARCHER-DANIELS-MIDLAND COMPANY

TECHNICAL REPORT AFAPL-TR-65-40, VOLUME I

JULY 1965

AIR FORCE AERO PROPULSION LABORATORY
RESEARCH AND TECHNOLOGY DIVISION
AIR FORCE SYSTEMS COMMAND
WRIGHT-PATTERSON AIR FORCE BASE, OHIO

NOTICES

1. When Government drawings, specifications, or other data are used for any purpose other than in connection with a definitely related Government procurement operation, the United States Government thereby incurs no responsibility nor any obligation whatsoever; and the fact that the Government may have formulated, furnished, or in any way supplied the said drawings, specifications, or other data is not to be regarded by implication or otherwise as in any manner licensing the holder or any other person or corporation, or conveying any rights or permission to manufacture, use, or sell any patented invention that may in any way be related thereto.

2. Qualified requesters may obtain copies of this report from the Defense Documentation Center (DDC), (formerly ASTIA), Cameron Station, Bldg. 5, 5010 Duke Street, Alexandria, Virginia, 22314.

3. Many of the items compared in this report were commercial items that were not developed or manufactured to meet any Government specification, to withstand the tests to which they were subjected, or to operate as applied during this study. Any failure to meet the objectives of this study is no reflection on any of the commerical items discussed herein or on any manufacturer.

4. Copies of this report should not be returned to the Research and Technology Division, Wright-Patterson Air Force Base, Ohio, unless return is required by security considerations, contractual obligations, or notice on a specific document.

200 - September 1965 - AF33(615)773-5-89

FOREWORD

This document is Volume 1 of a two volume report entitled "Aerospace Expandable Structures and Maintenance Support Devices" completed under Contract No. AF33(615)-1243. Volume 1 was prepared by Ronald Rochon, Robert C. Clark, and Nels S. Hanssen of GCA Viron Division, GCA Corporation, the prime contractor, and Dr. William J. McKillip of Archer-Daniels-Midland (ADM) Company, the sub-contractor. Both companies are located in Minneapolis, Minnesota. The effort was initiated under:

Project No. 8170, "Aerospace Site Support Techniques"
Project No. 3145, "Dynamic Energy Conversion Technology", and
Project No. 8174, "Limited War Support Techniques".

In particular, it was a development effort in compliance with:

Task No. 817004, "Expandable and Modular Structures for Aerospace",
Task No. 314502, "Solar Dynamic Power Units", and
Task No. 817403, "Experimental Structural Techniques".

The study was administrated under the direction of the Technical Support Division and the Aerospace Power Division of the Air Force Aero Propulsion Laboratory, Research and Technology Division, Air Force Systems Command, Wright-Patterson Air Force Base, Ohio. The Air Force project engineer was Mr. Fred W. Forbes, This report covers work conducted from 9 December 1963 to partial contract termination on 2 November 1964.

Mr. Ivan W. Russell, Expandable Structures Group Leader and Project Manager at GCA Viron, and Dr. E. B. Dunning, Group Leader of the Basic Research Section and Technical Project Manager at ADM contributed materially to the study by providing technical assistance and directing the program to fruition.

The authors wish to acknowledge the assistance that was received from project monitors Mr. Fred W. Forbes, 1/Lt. Ian Thompson, 1/Lt. Anthony Zappanti, and 2/Lt. Wayne Lauderback in scheduling Air Force facilities for experimental work, providing the necessary supporting equipment, and lending their knowledge to the study.

This report was submitted by the authors June 1965.

ABSTRACT

Materials and Techniques were improved to advance the concept of expandable, self-rigidizing honeycomb type structures. The strength to weight ratio of structures was markedly improved through the correct utilization of inflatable configurations with a high degree of structural rigidity. A rigidizing resin was developed with an improved strength/weight ratio, a more rapid cure time, and a good shelf life. Solar collectors with reasonably good optical reflectivity and aerospace shelters were fabricated, expanded, and rigidized.

Two large sized structures suitable for space application were constructed as end items of this study. Those structures were a 10 foot diameter, 60^{o} rim angle solar energy concentrator and a 13 x 15 ft semi-cylindrical aerospace maintenance dock. Both structures utilized a resin impregnated honeycomb type fabric construction and were inflated and rigidized from a packaged configuration. The maintenance dock was successfully designed for 30 psf gravity and 100 mph wind loads. Both structures significantly advanced the concept of expandable, self-rigidizing structures by their size, construction, and performance.

This report has been reviewed and is approved:

Peter N. Van Schaik

Peter N. Van Schaik, Chief
Space Technology Branch
Technical Support Division

TABLE OF CONTENTS

LIST OF FIGURES

LIST OF FIGURES (CONT'D)

LIST OF FIGURES (CONT'D)

LIST OF TABLES

LIST OF TABLES (CONT'D)

SECTION 1

INTRODUCTION

The problems and requirements of space exploration have caused attention to be focused on the concept of lightweight, expandable structures. These specialized structures can be grouped into a number of varieties of which the expandable, self-rigidizing honeycomb structure is one. It features a strong, light-weight, fibrous substrate material impregnated throughout with a flexible resin. It can be deployed, packaged, transported, and then rigidized on command. Generally, the deployment and rigidization are independent of each other, however, both are accomplished by internally pressurizing the structure.

A previous study, AF33(657)-10409 (APL TDR 64-29), by GCA Viron Division, GCA Corporation and Archer-Daniels-Midland Company proved the feasibility of this type of expandable structure and suggested many ways to further improve the concept. That study also suggested that the concept be applied to large size structures. The present study, conducted under AF Contract 33(615)-1243, has developed the expandable, honeycomb concept from small structures to large structures. These structures were completed after the partial termination of this contract with corporate funds and consequently are not fully discussed herein.

The concept of the expandable, self-rigidizing, honeycomb structure was co-invented by Sydney Allinikov and Fred Forbes of the Research and Technology Division, Air Force Systems Command, Wright-Patterson Air Force Base, Ohio.

SECTION 2

OBJECTIVES

The objective of this study was to advance the "state-of-the-art" in the area of inflatable, self-rigidizing expandable structures. In particular, fabrication and rigidization techniques were to be improved, preliminary structural design data was to be compiled, the substrate and the rigidizing resin were to be optimized, and large size structures were to be constructed.

Specific items were: 1) A number of solar energy concentrators, and 2) an aerospace maintenance dock.

1. The solar concentrators were to be paraboloidal surfaces of revolution two feet and ten feet in diameter, constructed with a reflective surface of aluminized Mylar and a drop thread or fluted honeycomb core fabric sandwich material for structural rigidity. These were to be inflated and rigidized in a vacuum environment.

2. The aerospace maintenance dock was to be semi-cylindrical, quonset type structure of 26 x 30 ft plan dimensions. It was to be designed for terrestrial deployment and use.

SECTION 3

RESIN SYSTEM RESEARCH

A. Introduction

The resin system research was a part of the overall effort to optimize the structural material. The other part of this effort was the optimization of the substrate materials used in the construction of the solar collectors and the aerospace maintenance dock. These two structures each required a different substrate material because of the difference in the end requirements of each type of structure. The optimization of the respective substrates was an integral part of the development of the solar collectors and the aerospace maintenance dock. A discussion of each substrate optimization is incorporated in its respective section. The optimization of the rigidizing resin is discussed entirely in this section since one resin was intended to satisfy the requirements of both the solar collectors and the aerospace maintenance dock.

The chemical research and development performed under this contract have been concerned with resinous prepolymer design. The objective of the program was to develop an impregnant for honeycomb aerospace structures so they could be maintained in a flexible, packaged form, deployed under a hard vacuum, and inflated and rigidized by means of a gaseous catalyst upon command.

To meet these objectives, a candidate resin system must possess several properties. Those include:

storage stability,
adhesion to the fiber surface,
low tackiness,
rapid reactivity with gaseous type catalysts,
cross-linking ability,
adequate physical strengths,
cured and uncured environmental stability, and
low shrinkage.

The approach used in this study was based on the background acquired under a previous contract. The result of this initial research effort showed the gas-catalyzed chemical rigidization concept to be feasible. The improvement of resin performance has been the goal of the present effort.

B. Summary of Accomplishments

Two classifications of laminating resins, urethane and polyester, have been developed which rapidly polymerize in a hard vacuum through cross-linking initiated by gaseous catalyst. The most effective resin to date has been a soluble urethane prepolymer which is capable of further polymerization when reacted with water vapor. The feasibility of using a urethane prepolymer, moisture cured, one-component system was demonstrated earlier. Only commercially available prepolymer reactants were screened in that initial effort. Although vapor cured rates of glass and nylon reinforced laminates were fast in comparison to any other resin system screened for this application, they were not rapid enough. The physical strengths (tensile and flexural) of the vapor cured urethane reinforced laminates

might be considered poor when compared to urethane laminates prepared by pressure-temperature cycling; however, it should be pointed out that cross-linking a resinous impregnant multi-ply laminate through the use of a volatile catalyst within a hard vacuum is not the best approach toward preparing good laminates. The volatile product formed during the isocyanate-water reaction and the continuing removal of the volatile solvents tends to delaminate the prepared specimen and thus physically weaken the structure. In addition, surface irregularities formed by gaseous by-products create an inferior sample preparation. Thus, data obtained from samples prepared by this procedure cannot be directly compared to flexural data compiled on resin systems in commercial use since pressure-temperature cycle laminations removes volatiles without adversely affecting sample preparation.

Unsaturated polyester resins were only partially effective in as much as reproducibility of gaseous peroxide catalyzed cures under vacuum conditions could not be realized. The method of polymerization and the availability of catalyst appear to be the important factors in both systems.

The primary objective for the resin research was to optimize the gas-cured resin, particularly with respect to rate of cure and reinforced resin laminate physical strength. This objective was met since continued research on urethane resin design has led to definite improvement in the cure rate of prepolymers and physical strengths of a polyurethane polymer. Rigidization times of urethane impregnated small prototype structures cured by water vapor while in a vacuum environment were reduced by more than 50 percent, and flexural strengths of vapor cured urethane laminates have increased three fold. Resin saturated prototype structures were cured within 1/2 hour under laboratory vacuum conditions at ambient temperature. Flexural strengths, obtained from three ply 181 glass-urethane impregnated laminates cured with water vapor, averaged 35,000 psi with a flexural modulus of 2,000,000 psi.

This resin performance optimization was forecast from experimental resin design concepts. It was proposed that improved cure rate and physical strength could be achieved by first developing a prepolymer from a more reactive diisocyanate. This task was performed and cure rates were improved during this work effort. Secondly, development of a prepolymer possessing rigid structural components and utilization of polyols possessing high hydroxyl equivalents was proposed to attain polymer backbone rigidity and maximum cross-linking density respectively. This task was accomplished by synthesis of polyfunctional acyclic polyols which were specifically propoxylated for rigid urethane formulation. The results of this research has led to the improved physical strengths that were achieved.

These major material improvements were accomplished without unduely sacrificing the resin shelf stability of resin usability. Under the most stringent anhydrous conditions, long term shelf stability can be realized. Canned resin has remained ungelled in excess of 12 months under rigorously dry conditions, and in the absence of catalyst. Glass fiber, resin impregnated specimens have been sealed under nitrogen and stored in vapor permeable bags for a duration in excess of 10 months.

Good adhesion to glass was generally obtained and a low degree of resin tack observed when vacuum impregnated onto honeycomb woven glass fabric. No serious problems were experienced when folding and unfolding resin saturated reinforced structures. Most of the prepared urethane prepolymers when evaluated as cast free films showed negligible visible shrinkage in planar directions. However, the amine accelerating agent was not utilized in obtaining these sample cures.

Other urethane improvements recorded during this study included utilizing high boiling, non-reactive and reactive type plasticizers without adversely affecting the shelf life of the resin or the properties of the polymerized urethane.

Finally, urethane resin design has been initiated which hopefully will extend the life of the polymer system in a high radiation environment.

An unsaturated polyester, cross-linked by gassing with a volatile peroxide received considerable emphasis during this work effort. Acceptable cure times and physical strengths were achieved; however, rigidization reliability was not established. The most commonly used monomeric reactant, styrene, was replaced with polyfunctional methacrylates. It was found that methacrylate esters of diols and triols are sufficiently non-volatile, have satisfactory solvent properties, and are fast reacting. The dimethacrylate ester of tetraethylene glycol and the trimethacrylate of trimethylol propane were used most extensively in this application. The acrylic esters were necessary in concentrations as high as 60-70 percent of total resin weight to provide a workable viscosity. Small amounts of styrene (up to 10 percent) aided solvency and seemed to accelerate a more complete cure in these systems. Methacrylate and acrylate monomers exhibited a strong tendency to homopolymerize in the absence of styrene, leaving significant amounts of unpolymerized polyester to act as a plasticizer or inert diluent. This explains the lack of complete cure experienced when the polyester system was solvated with only methacrylate monomers.

The polyester resins containing specific combinations of several accelerators were found to have good shelf-life at a variety of accelerator levels. The fastest curing systems available have been formulated and evaluated. The volatile catalyst employed has been methyl ethyl ketone peroxide available as a 60 percent active material in an aromatic ester plasticizer. This catalyst volatilizes moderately well at room temperature and 10^{-5} to 10^{-6} mm Hg.

Small structures, impregnated with the resins, were rigidized in 30 minutes when gassed with peroxide vapors in a high vacuum. The rigid structures continued to harden over a 24 hour period, probably via the absorbed peroxide which promotes a type of post curing.

A limited effort of research was spent developing a displaceable isocyanate blocked group. Most blocked isocyanates commercially available rely on high temperature conditions to effect unblocking and regeneration of free isocyanate. This is the basis of the stable two component urethane system. A system was developed which employed imidazole as the blocking group for active isocyanate sites. This resulting blocked isocyanate was found to be labile to nucleophilic displacement. Although of interest in bulk polymerization reactions, this development was found to be ineffective for use in a vapor phase catalyst program.

Furthering development with gas cured epoxy resin systems led to the evaluation of both reactive and non-reactive epoxy diluents. It was established that modification of the diluent altered physical properties of the epoxy resin.

Several difunctional epoxides were synthesized for ultimate use in the preparation of epoxy resin.

The bulk of this research is covered in detail in the following discussion of results section.

C. Technical Discussion

1. Urethane

A polyurethane has a polymer backbone consisting of urethane linkages. In addition, urea, ester, ether, methylene and aromatic groups may be included. The arrangement of this spectrum of structures and the choice of monomer units determines the property-structure relationship. The significant structural features influencing the urethane polymer properties include intermolecular forces, stiffness of chain units, molecular weight, crystallization, and ease of rotation of chain segments. The ether groups are relatively flexible and offer no chain stiffness; the aromatic groups are rigid and offer resistance to rotation, while the urea, urethane, aromatic and ester groups contribute strong intermolecular forces. The relative contribution of the various groups to intermolecular forces may be illustrated by the "molar cohesive energy" of the different groups in small molecules. Urea and urethane groups have high numerical values for molar cohesive energy and thus possess strong intermolecular attractions. This can be seen in Table 1.

TABLE 1

MOLAR COHESIVE ENERGY OF ORGANIC GROUPS

Group	Cohesion, kcal/mole
$-CH_2-$	0.68
-O-	1.00
-COO-	2.90
$-C_6H_4-$	3.90
-CONH-	8.50
-HNHCONH-	9.21

Modulus (tensile, shear, and compression), tear strength, hardness, melting point, crystallinity, and glass transition temperature have been shown to increase with increasing effective intermolecular forces which are pronounced in functional groups with high molar cohesive energy. The term "effective intermolecular force" is used to indicate a combination of the intermolecular attractive forces that are possible for the structural groups present, combined with the geometric structure of "fit" that regulates the extent to which these forces can operate. This type of bond, formed through electrostatic attraction, is called a secondary valence bond and contributes significantly to property strength.

Most mechanical properties change with molecular weight up to a limiting value, then do not change as the molecular weight increases further. The degree of polymerization must initially be maintained low to be useful in this application (vapor phase catalysis) in order to insure a soluble, impregnable laminating resin. Ideally a high degree of polymerization is desired during the gassing reaction which occurs on command after structure deployment.

These discussed properties are obtainable in polyurethane polymers. The specific requirements of a gas-phase chemical rigidization have best been met by employing a one-component urethane prepolymer system that cures with water vapor. This system shall be discussed in detail.

2. Urethane Prepolymer

The urethane prepolymer will be discussed in terms of a) composition, b) cross-linking mechanism, c) relative reaction rates, d) effect of catalysts on reaction rate, e) plasticizer additive effect, and f) physical properties of resin and mechanical properties of gas-cured specimens.

a. Composition

Di- or poly-isocyanates can be reacted with certain combinations of polyols to form a solid, but soluble isocyanate terminated resin. A solution of this resin provides a one component vehicle which is stable as long as it is kept anhydrous. Further polymerization occurs through the remaining terminal isocyanate groups.

The basic composition of the prepolymers evaluated consisted of the following:

(1) Isocyanates
(2) Polymeric Polyols
(3) Short Chain Diols

The NCO/OH ratio based on equivalents was maintained at a level greater than 1.5 to insure against gelation of the prepolymer. Viscosity of the prepolymer is also dependent upon NCO/OH ratio. The greater the ratio, the lower the viscosity as an increase of lower molecular fragments are formed. Active NCO content of the prepolymers ranged from 4 to 23 percent based on 100 percent resin solids.

(1) Isocyanates

Aromatic diisocyanates were preferred in resin formulation over aliphatic diisocyanates because of the greater reactivity and greater rigidity in the polymer backbone due to the aromatic ring. The search for increased reactivity led to evaluation of several aromatic diisocyanates including 2,4-toluene diisocyanate, 4,4'-diphenyl methane diisocyanate, m-phenylene diisocyanate, and chlorinated m-phenylene diisocyanate. Figures 1, 2, and 3 indicate comparative degree of reactivities.

Prepolymers containing m-phenylene diisocyanate and chlorinated m-phenylene diisocyanate registered most rapid gel times when reacted with varying ratios of aqueous triethyl amine. Table 2 and Figure 4 compare gelation times observed with prepolymers containing m-phenylene diisocyanate, toluene diisocyanate and 4,4'-diphenyl methane diisocyanate.

Very slight changes in flexural strength data were observed in prepolymer systems wherein only the aromatic diisocyanate was changed. The one exception to this statement was the case of chlorinated phenylene diisocyanate (Table 3) where flexural data indicated drastically reduced physical strengths of laminates. This system undoubtedly showed poor performance because of the inferior quality

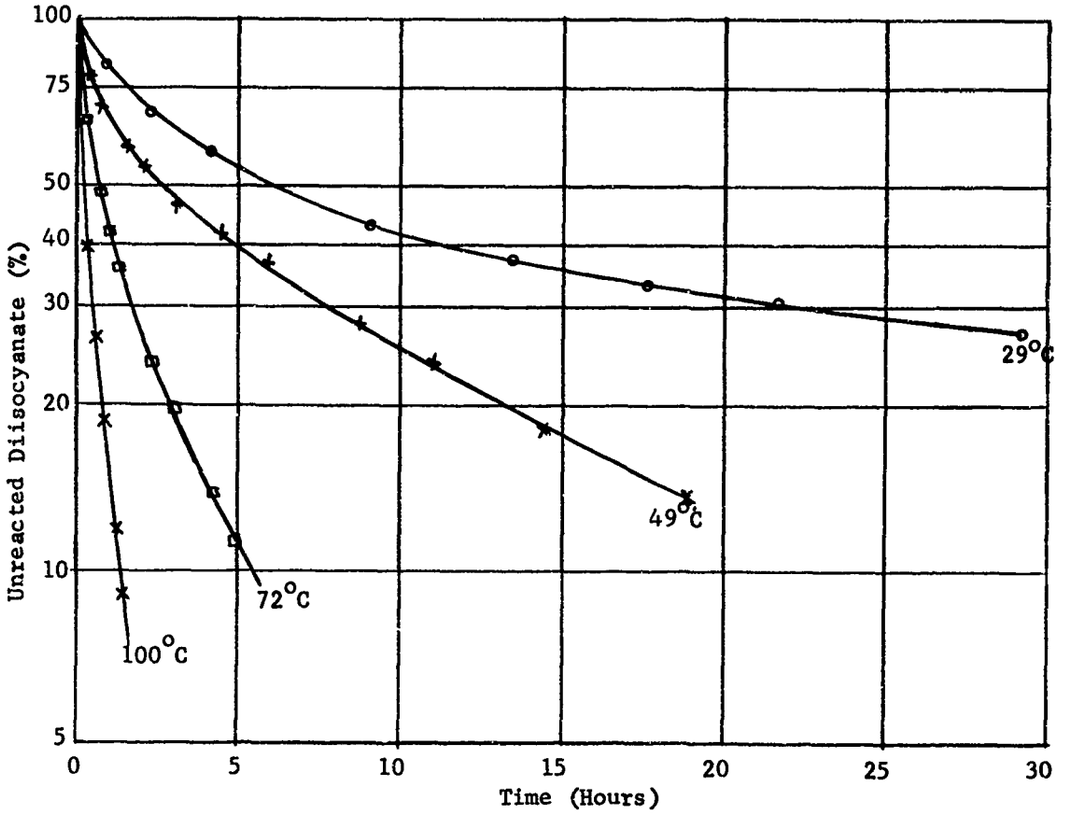

Figure 1 - Reactivity Of 2,4-Toluene Diisocyanate With Diethylene Glycol Adipate

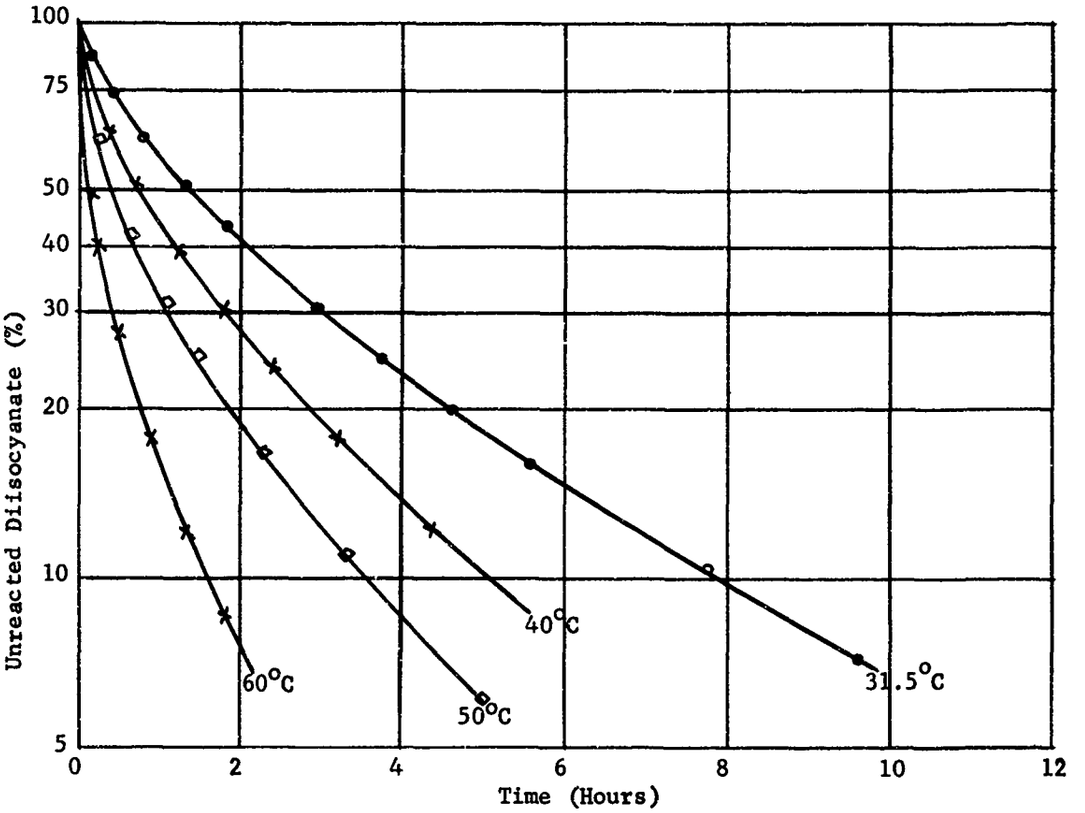

Figure 2 - Reactivity Of m-Phenylene Diisocyanate With Diethylene Glycol Adipate

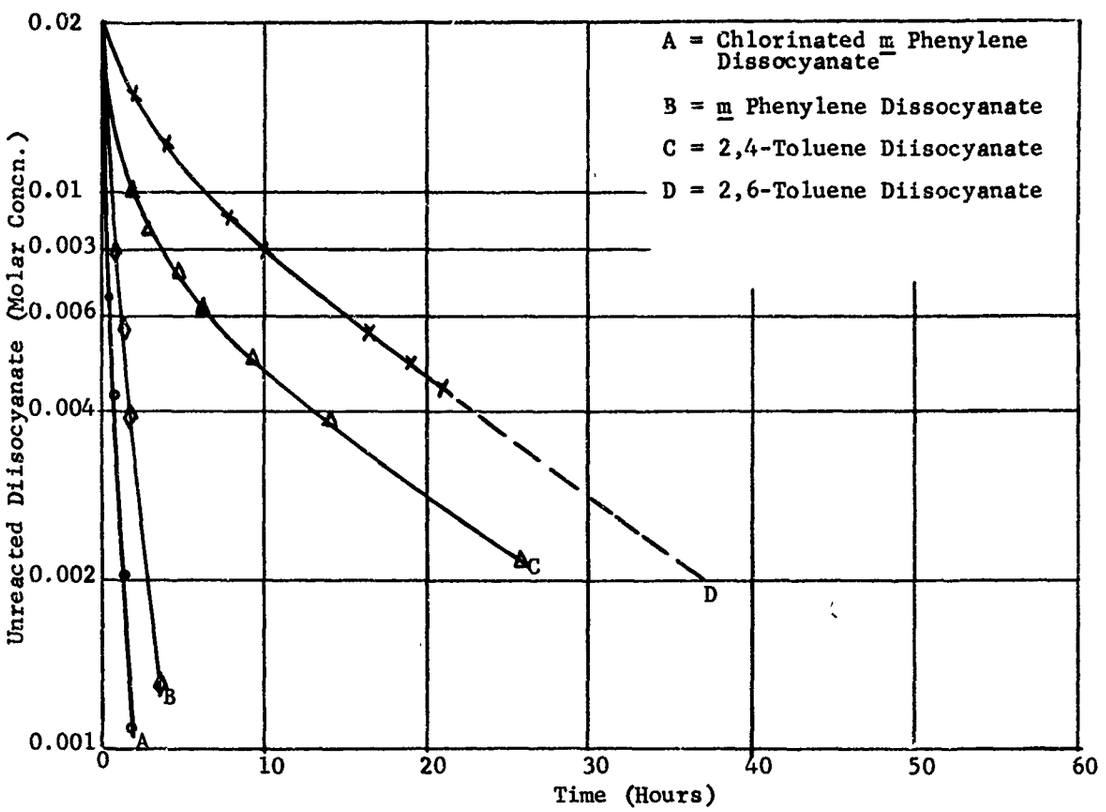

Figure 3 - Reactivity Of Aromatic Dissocyanate With 2-Ethyl Hexyl Alcohol In Benzene

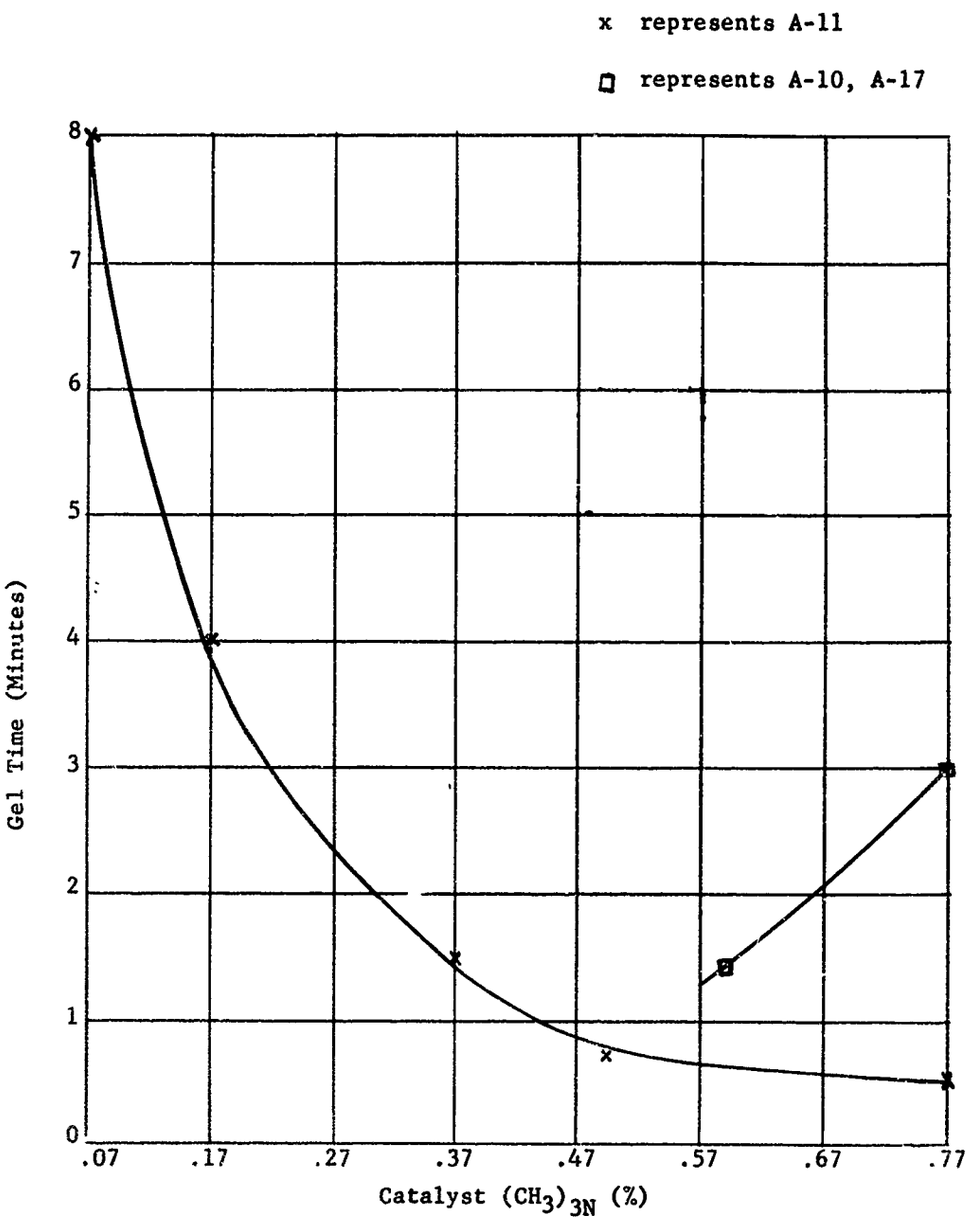

Figure 4 - Gelation Time Evaluation of Urethane Prepolymer

TABLE 2

GELATION TIME EVALUATIONS

Sample	NCO/OH	Catalyst*	Gel Time
A-11	3	0.075%	8 min.
A-11	3	0.17%	4 min.
A-11	3	0.375%	1.5 min.
A-11	3	0.50%	0.7 min.
A-11	3	0.77%	0.5 min.
A-10	2	0.77%	3.0 min.
A-17	1.75	0.60%	1.5 min.

*Catalyst represents aqueous trimethylamine

TABLE 3

VARIATION OF PHYSICAL PROPERTIES OF CURED POLYURETHANE LAMINATES BY STRUCTURAL MODIFICATION

Sample Designation	Laminated Tensile Strength		Laminate Flexural		% Resin
	psi	% Elong.	Strength psi	Modulus psi x 10^6	
A-1	19,000	3.2			32
A-2	18,000	2.8			30
A-3	17,500	3.1	20,460	2.1	32
A-4	17,000	3.0	21,880	2.2	30
A-5			16,200	1.3	37
A-6a			24,570		
A-6			25,700	1.7	40
A-7			33,700	2.1	40
A-8			38,200	3.0	37
A-9			6,900	1.5	33
A-10			22,200	1.4	
A-11			6,940	1.6	
A-12			19,000	1.35	
A-13			29,900	1.6	
A-14			27,000	1.8	
A-15			18,000	1.2	
A-16			23,000	1.7	
A-17			25,000	1.5	
A-18			22,000	1.7	
A-19			18,700	1.1	
A-20			28,300	1.3	
A-21	26,800	3.2	23,500		
A-22	27,300	3.4	24,500		
A-23	19,400	3.2			
A-24	24,260	3.0			

of the laminate. The reaction of the laminating resin was so rapid with moisture that the gas-off product, carbon dioxide, caused severe delamination of the test specimen. Another contributing factor may have been poor adhesion of the particular resin to the glass fiber. It is possible that the highly chlorinated aryl diisocyanate prevents good surface adhesion. Further investigation of the reactant will be necessary.

The primary function of the diisocyanate in prepolymers is to increase reaction rate. The secondary contribution of aromatic diisocyanates is to aid in contributing to polymer rigidity.

Inorganic diisocyanates were considered briefly in the early stages of this contract; however, unavailability and high cost greatly retarded any progress. In addition, the phosphoryl and sulfuryl isocyanates were ineffective in prepolymer systems due to the poor nucleophilic character of the amines formed from the isocyanate-water reaction. ($X\text{-}NCO + H_2O \longrightarrow X\text{-}NH_2 + CO_2$ where X = $O{=}P$, $O{=}S{=}O$ etc). The degree of cross-linking necessary for further polymerization could not be achieved due to the poor nucleophilic character of the resultant amine caused by the strong electron withdrawing phosphoryl and sulfuryl groups.

(2) Polymeric Polyols

The polymeric polyols considered for polyurethane applications were divided into polyether type and nonetheral type classifications. Commercially available and specifically synthesized materials were evaluated.

(a) Polyether Type

Polyether polyols are derived readily from polyfunctional hydroxyl containing monomers by treatment with alkylene oxides (ethylene or propylene oxide) under pressure and usually in the presence of catalytic amounts of base. Most commercially available polyethers evaluated were based on tri, tetra, hexa, or octafunctional polyols. A pentafunctional polyether derived from a known pentol was also evaluated.

During an earlier study, a linear polyoxypropylene diol (PPG 400) was employed in conjunction with a high percentage of trimethylol propane. The trifunctional trimethylol propane was used to introduce branching and the PPG 400 was used to control the degree of rigidity. This system, although successful in demonstrating feasibility, did not display physical strength sufficient to meet design goal requirements. In addition, a reduction of cure time was desired. Commercially available poly (oxypropylene oxide) adducts of glycerol (3-functionality), α methyl glucoside (4-functionality), and sorbitol (6-functionality), were formulated into prepolymers and evaluated. A propylene oxide adduct of unknown composition, Actol 51-530, obtained from Allied Chemical Company was also evaluated. This material, with a hydroxyl value of 530, was assumed to be polyfunctional. Prepolymer prepared from m-phenylene diisocyanate and this polyether were chosen as candidate resins for deliverable items under this study. Water vapor catalyzed vacuum cure times of under one hour were observed. Flexural strengths of moisture cured, 3-ply 181 glass laminates averaged 18,000 psi. These were significant accomplishments over the previous effort. Octafunctional sucrose polyethers, obtained from

Dow Chemical, were screened for application in prepolymers; however, the residue of basic catalyst contained in these polyols caused early gelation in every instance. Attempts to neutralize basicity interfered with prepolymer reaction rates. These materials are primarily for use in rigid foam systems where shelf stability is not critical and in that application perform very well.

Several specific polyfunctional polyols were synthesized and propoxylated. A methylolated derivative of cyclohexanone, 2,2,6,6-tetramethylol cyclohexanol, was propoxylated with propylene oxide and evaluated. Results obtained from the data tabulated on prepolymers derived from this reactant and m-phenylene diisocyanate were very promising, and demonstrated best efforts to date. Flexural strengths of moisture cured 3-ply 181 glass laminates averaged 34,000 psi and a flexural modulus of 2×10^6 psi. This demonstrated superior performance over previous efforts and showed a developing trend which was forecast earlier.

Finally, a novel glucoside derived from starch was propoxylated and formulated into prepolymers. These systems showed properties with marked improvement over standard items previously evaluated. Table 4 lists composition of all urethane prepolymers derived from polyethers. Table 3 records physical properties of these prepolymers.

(b) Non-Ethereal Type

(i) Polyester Polyols

Polyester polyols are derived from polyfunctional hydroxyl containing monomers by condensation with dibasic acids. Commercial esters evaluated were trifunctional, generally based on trimethylol propane. The several polyesters evaluated included: Multron R-12, R-4 Amoco Trimellitic Anhydride Polyester, and several specifically prepared polyesters.

Prepolymers from trifunctional polyesters gave flexural strengths of 24,300 psi as compared to flexural strengths of 10,000 to 12,000 psi obtained from comparable trifunctional polyethers. Physical properties and the composition of prepolymers are tabulated in Tables 3 and 4.

(ii) Nitrogen Containing Hydroxy Terminated Polymers

Several amido and urea polyols were synthesized by the reaction of omega-lactones with alkanol amines and by the reaction of 4,5-dihydroxy-2-imidazolidone with glycols. The repeating polymer units for polyimidazolidone glycol is represented by the following structure.

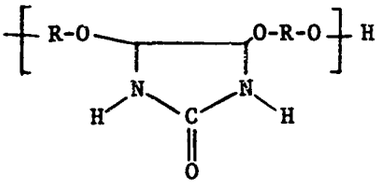

It was hoped that the reaction with glycols would give polyethers with cross-linking potential through the urea hydrogens. Generally, prepolymer stability was poor; however, insufficient data was obtained to be conclusive.

TABLE 4

COMPOSITION OF URETHANE PREPOLYMERS

Sample Designation	Diisocyanate	P.O. Polyether	OH#	Chain Extender
A-1	MPDI		525	
A-2	TDI	Sorbitol	475	
A-3	"	PPG 425	400	Butylene glycol
A-4	"	"	400	" "
A-5	MPDI	Actol 51-530	530	" "
A-6	"	" "	530	Bis-hydroxymethyl-trimethylene sulfide
A-6a	TDI	PPG 425	400	Butylene glycol
A-7	MPDI	Tetramethylolcyclohexanol	510	
A-8	"	"	510	Butylene glycol
A-9	Cl-MPDI	Actol 51-530	530	Butylene glycol
A-10	MPDI	Tetramethylolcyclohexanol	510	
A-11	"	"	510	
A-12	"	"	510	
A-13	"	"	510	
A-14	"	"	510	
A-15	"	Actol 51-530	530	Butylene glycol
A-16	"	Tetramethylolcyclohexanol	510	
A-17	"	"	510	
A-18	"	Starch glucoside	469	
A-19	"	" "	510	
A-20	"	Tetramethylolcyclohexanol	510	Butylene glycol
		Polyester Polyol		
A-21	TDI	Multron R-12	166	Butylene glycol
A-22	"	" R-4	280	" "
A-23	"	Amoco Polyester 300	300	" "
A-24	"	2093-7	200	

TABLE 4 (Cont'd)

COMPOSITION OF URETHANE PREPOLYMERS

Sample Designation	NCO/OH	%NCO	%NV	Cross-linking Monomer	Plasticizer %	Storage Stability
A-1	1.6	16.3	40			Gel 5 mos.
A-2	2.0	15.8	60			Gel 6 mos.
A-3	2.0	11.4	50	Trimethylolpropane (TMP)	15% Tridecyl phthalate	8 mos.
A-4	1.8	6.87	50	"	15% " "	8 mos.
A-5	1.6	9.0	50	"		8 mos.
A-6	2.0	10.8	50	"		Gel 4 mos.
A-6a	1.8	6.0	50	"	20% Dioctyltrimellitate	6 mos.
A-7	2.3	13.8	60			3½ mos.
A-8	2.0	10.6	60			Gel 3 mos.
A-9	1.5	9.1	60			3 mos.
A-10	2.0	9.3	60			Gel 2 mos
A-11	3.0	5.7	60			Gel 2 mos.
A-12	2.0	10.4	60		60% Dioctyl phthalate	2 mos.
A-13	2.0	9.5	60		25% " "	1½ mos.
A-14	2.0	9.5	60		40% " "	1½ mos.
A-15	1.5	6.0	60	"		9 mos.
A-16	2.5	10.6	60			3 mos.
A-17	1.7	7.6	60			Gel 2 mos.
A-18	2.0	9.6	60			1½ mos.
A-19	2.0	9.8	60			1 mo.
A-20	2.0	10.1	60			1½ mos.
A-21	1.8	10.6	60	"		9 mos.
A-22	1.8	10.3	50	"		9 mos.
A-23	3.0	22.0	70			Gel 1 mo.
A-24	2.0	11.6	50	"		7 mos.

In the collected data presented in Table 2 through 5, several trends can be observed. Enhanced physical strengths of urethane polymers obtained by replacing linear aliphatic polyols with cyclic polyols have been demonstrated. Increasing the cross-link density of the urethane-resin system will give increased rigidity. This has been accomplished by using poly-functional materials with high hydroxyl equivalents. Small ratios of short chain diols added in the formulation appear to give superior properties to those formulations containing no chain extender. Polyesters containing equivalent hydroxyl functionality compared to polyether seem to have slightly superior properties. The properties of the one-component urethane polymer seem to depend mainly upon three properties of the polyol. Those properties are: equivalent weight, functionality, and chemical composition.

Equivalent Weight of Polyols

Synthesized polyols having an equivalent weight in the range of 40-50 were propoxylated to obtain polymeric polyols in the range of 100-120. Higher equivalent weight polyols yielded softer and more flexible films while lower equivalent weight polyols yielded brittle films of little practical use.

Functionality of Polyols

The use of tetrols and pentols in prepolymers induced a shorter pot life than experienced when using diols of the same equivalent weight. Cured coatings containing tetrols and pentols gave harder, more rigid films.

Chemical Composition of Polyols

Polyols containing acyclic rings contribute increased rigidity to coating systems. The use of a highly branched polyol propoxylated in a propylene oxide/OH, mole equivalent ratio of 1/1, so increases the cross-linking density that the ultimate film strengths are obtained. In addition, more urethane groups per molecule are formed and as the proportion of urethane groups is increased, the film becomes generally harder and tougher. With increased functionality, as present in the chemical composition of the polyols evaluated, less moisture is necessary to form an efficient cross-linked structure.

(3) Short Chain Diol

The use of a diol for extension of the prepolymer affects the degree of flexibility. That method of chain extension was not generally advocated in the research program as the utmost rigidity was desired. Diols were employed only when necessary to improve shelf life. In most instances, this was not necessary; however superior strengths resulted from those formulations containing only small percentages of chain extender.

In an attempt to achieve increased environmental stability, short chain diols containing labile disulfide linkages were synthesized and incorporated into prepolymer formulations and cured.

TABLE 5

PLASTICIZER ADDITIVE EFFECT ON PHYSICAL PROPERTIES

Urethane Sample No.	% Plasticizer	Storage Stability	Flexural Strength psi	Flexural Modulus psi x 10^6
Comparative Standard	No Plasticizer		12,300	1.3
A-3	Ditridecyl Phthalate		20,460	2.1
A-4	Ditridecyl Phthalate	9 mo.	21,880	2.2
A-6a	Trioctyl trimellitate	9 mo.	24,570	
A-12	60% Dioctyl Phthalate	Gel 2½ mo.	19,000	1.3
A-13	25% Dioctyl Phthalate	1½ mo.	29,900	1.6
A-14	40% Dioctyl Phthalate	1½ mo.	27,000	1.8

Monomers prepared and evaluated as chain extenders for prepolymer formulation under this work effort included the following:

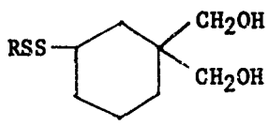

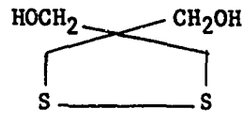

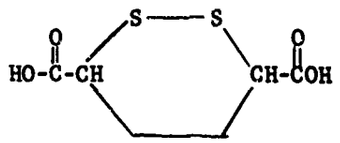

These prepolymers exhibited satisfactory shelf stability, gel times, and physical strength properties. The contribution to environmental stability of these systems has not been determined.

b. Cross-Linking Mechanism

Urethane prepolymers can be further reacted to produce higher molecular weight polymers at some later time. The cure of a urethane prepolymer in coatings application usually involves the reaction of some percentage of the isocyanate with atmospheric moisture. The initial reaction of the water and terminal NCO is one of addition to form a carbamic acid which dissociates readily to form an amine plus carbon dioxide. The free amino groups then add to additional NCO and create cross-linkages and ultimately a high molecular weight build up.

The effective cross-linking of the moisture cured prepolymer is due to the slow rate of reaction of water with isocyanate compared to the fast reaction which is shown in the following equations:

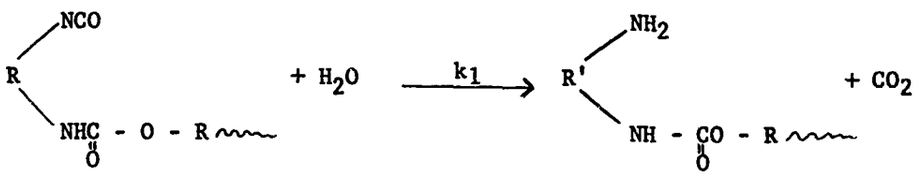

(A) (B)

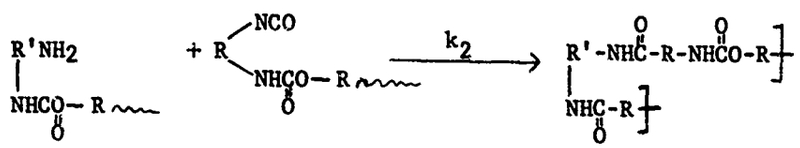

If k_2 were not much faster than k_1, a moisture cured urethane prepolymer would be ineffective as sufficient quantity of reactant (A) would be unavailable for the reaction represented by the second equation to take place. The reaction fundamental to cross-linking the prepolymer is represented by the second equation. The real advantage of a urethane prepolymer-water vapor cure system lies in the fact that the cross-linking reactant (B) is generated in situ as part of the resin.

c. Relative Reaction Rates

The reaction rates of a urethane prepolymer depend on the structure of the diisocyanate utilized in its preparation. The reaction rates of several diisocy-

anates with actively chosen compounds taken from the literature were discussed previously. Table 2 indicated data pertaining to gelation times of evaluated prepolymer systems.

It is shown in Table 6 that the kinetics of the phenyl isocyanate-water reaction is dependent on the water concentration and upon temperature.

TABLE 6

REACTION OF PHENYL ISOCYANATE WITH WATER
(0.5M Isocyanate in Dioxane)

Water/Isocyanate Mole Ratio	Temperature, °C	k x 10^4 liters/Mole/Sec
4:1	25	1.42
2:1	25	0.77
1:1	25	0.41
1:1	35	0.73
1:1	50	1.53

In the case of moisture-cured prepolymer systems, the rate of cure might be expected to be proportional to the relative humidity through a wide range of humidity, although no extensive investigation of this has been conducted. Temperature has a distinct effect on the rate of cure--the higher the temperature--the faster the cure. For cures initiated by gassing with water vapor under vacuum, the water vapor concentration available for any given time (t) is critical for reasonable reaction rates. This factor has not been determined to this date.

d. Effect of Catalyst

The choice of catalyst in a urethane coating system must be one that favors the NCO/water reaction. Tertiary amines have been employed to accelerate this reaction. Many metallic compounds were found to be catalysts for the isocyanate-water reaction. A tertiary amine of small size and low molecular weight is more effective in the gas cure of a urethane prepolymer since it is volatile and possesses the appropriate size to effectively form a complex with the available isocyanate.

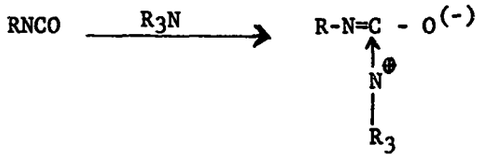

Trimethylamine, triethylamine, and N-methyl ethyleneimine have been successfully employed as isocyanate-water reaction accelerators.

Dibutyl tin diacetate was most effective when pre-mixed with the resin. When used in conjunction with tertiary amines, a catalytic synergistic effect was observed. However, the limited shelf life shown in dibutyl tin diacetate catalyzed systems prevented full utilization.

A specifically synthesized tin containing polyester

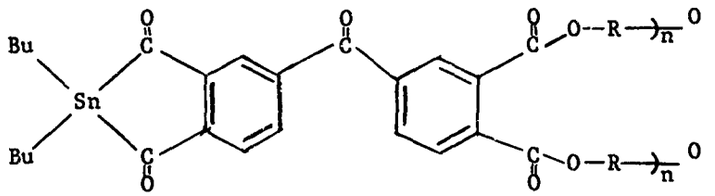

was ineffective as a catalyst for isocyanate reactions. The bulky nature of the molecule undoubtedly negated its catalyzing ability. A condensation product of boric acid and dibutyl tin oxide

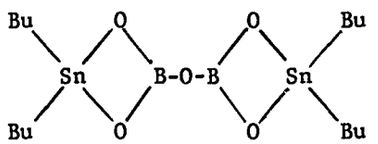

shows more promise as a catalyst; however, the mechanism involved in catalysis is not thoroughly understood. It is thought that the diborate hydrolyzes with water to form a mixture of tin containing derivates.

e. Plasticizer Additive

One component, urethane prepolymers are generally diluted with urethane grade solvents to permit a workable viscosity. The usual solvents are the low boiling acetates (ethyl, butyl, hexyl, or cellosolve) in combination with aromatic solvents such as toluene or xylene. These solvents have fairly high rates of evaporation which are necessary for coating applications, the prime use for urethane prepolymer moisture cure systems. These high rates of evaporation produce disadvantages when vacuum cures of impregnated structures are attempted, due to surface cooling caused by rapid volatilization. It would be an added bonus if the toxic, high vapor pressure solvents could be partially replaced by a nontoxic plasticizer. In addition, the selection of a high boiling plasticizer as a partial solvent system would aid in porosity control of an impregnated fibrous structure. By definition, a plasticizer is a high molecular weight, high boiling liquid composition that displays compatibility with the resin in question.

Prepolymers were synthesized in a 30 percent solvent system consisting of 15 parts by weight of hexyl acetate and 15 parts of ditridecyl phthalate. This non-reactive plasticizer has a molecular weight of 530 and a boiling point of 286°C at 5 mm Hg. Thus, at 10^{-10} mm Hg this slow evaporation rate prevents loss of heat of vaporization. Trioctyl trimellitate which was similarly used has a molecular weight of 546 and a boiling point of 260°C at 1 mm Hg. Free films of these polyurethanes were too brittle for tensile evaluation. Prepolymers were formulated containing as high as 35 percent of the plasticizers mentioned. It was anticipated that a loss of physical properties (flexural strength) would occur, but the reverse was true. With identical systems, the plasticizer containing

prepolymers demonstrated a two-fold increase in flexural strengths. Whether this is achieved by some electrostatic interaction such as dipole-dipole attraction, or whether some actual chemical interaction occurs is unknown at this time, although the latter explanation is very dubious. These test results are recorded in Table 5 and Figure 5.

In addition to "non-reactive" type plasticizers (e.g., the phthalates), reactive type plasticizers such as polyfunctional acrylates were then evaluated. The methacrylate of trimethylol propane and the dimethacrylate of tetraethylene glycol were both formulated with urethane prepolymer, A-5 (Table 4), in 35 percent by weight ratios. Five months shelf stability was recorded on these systems. Rapid gelation initiated by a combination of an aqueous tertiary amine and a peroxide occurred with this modified prepolymer. Moisture curing of 30 mil thick "wet" films cast on glass panels resulted in a cured film flexibilized by the unreacted acrylate monomer. The unreacted acrylate monomer was incompatible with the cured urethane and exuded from the surface of the film. This unreacted acrylate is capable of subsequent homopolymerization in the presence of free radical initiators and/or an energy source.

f. Physical Properties Of Resin And Mechanical Properties Of Gas-Cured Specimens

Table 3 includes physical properties of gas cured laminates. Flexural data was obtained on 3-ply 181 glass fabric laminates, moisture cured at 50 percent RH and 75°F for five days. Percent resin contained in the laminate was determined by ash content and ranged from 30-40 percent by weight of glass. Glass fabric used was pretreated with Volan A. The surface treatment of the fiber glass remains a critical parameter in obtaining optimum physical strengths. Volan (amino silane) treated glass-urethane laminates demonstrated significantly superior flexural strengths in comparison with identically prepared laminates made from Garan (vinyl silane) treated 181 glass. Thus, adhesion of the resin to the individual glass fibers plays a most significant role in determining physical strengths of laminates. All test evaluations were conducted on an Instron testing machine.

The feasibility of gas-curing a urethane prepolymer under hard vacuum has been demonstrated repeatedly on small scale laboratory samples. Structures were fabricated from a three-dimensional glass fabric with flutes connecting the two parallel facings. The reinforcing fabric was out-gassed for several hours prior to use. The structures were then packaged, vacuum impregnated with resin, and sealed under nitrogen. Storage tests on various prepolymer systems vary depending upon the reactivity of the system. Successful storage tests of urethane impregnated fabric containing no accelerator have been in progress for ten months with no loss of flexibility. Storage tests of urethane impregnated fabric containing varying proportions of dibutyl tin diacetate remain flexible for three weeks. The increased reactivity of prepolymers developed under this contract prohibit the use of tertiary amine as catalyst. No reasonable storage stability at room temperature can be achieved with systems containing tertiary amines.

3. Blocked Isocyanates

Urethane polymer systems with indefinite shelf stabilities were obtained by preparation of labile blocked isocyanates capable of regeneration through nucleophilic displacement. This was accomplished by reacting di- or poly-

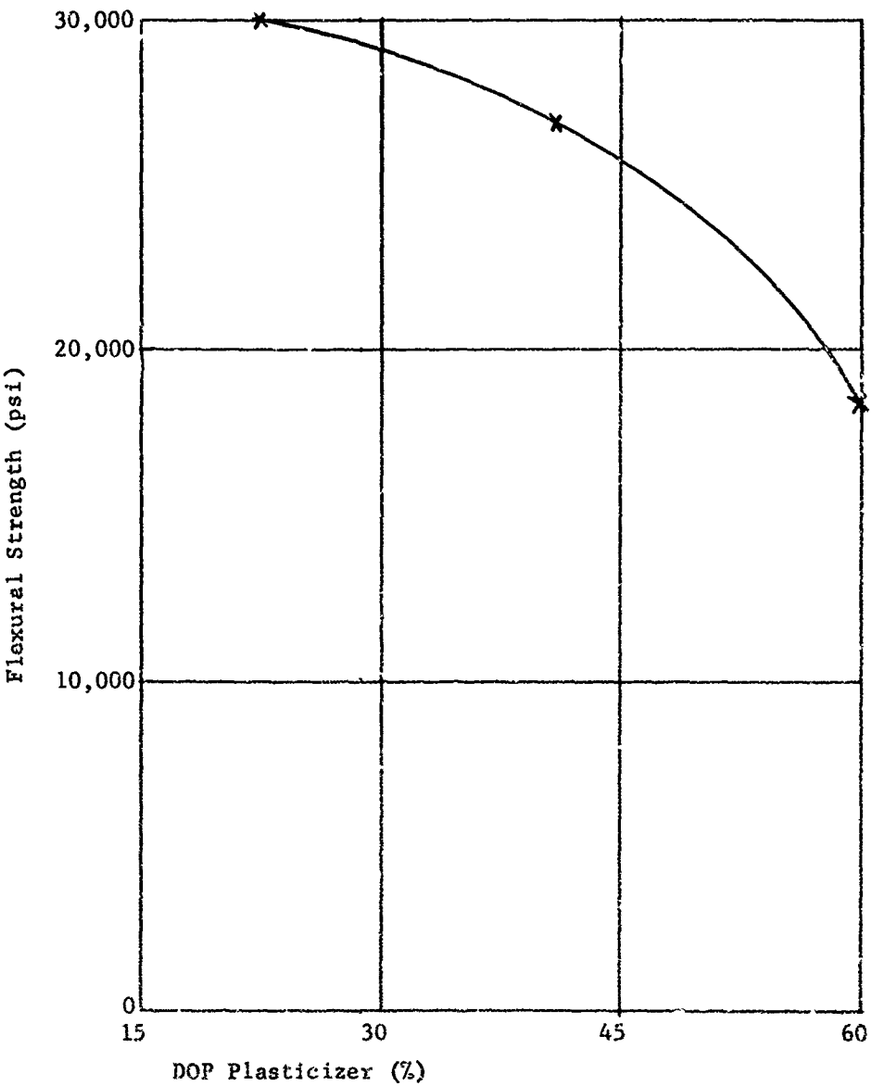

Figure 5
Effect Of Varying Weight % Plasticizer Additive On
Resin-Laminate Flexural Strengths Of Samples A-12,-13,-14.

isocyanates with imidazole in a ratio of one mole of imidazole for every available NCO. These blocked isocyanates are stable to heat, ultraviolet, and moisture and are, in most instances, soluble in polar organic solvents. De-blocking occurs through displacement of the imidazole anion by a nucleophile such as an amine. The use of a difunctional nucleophile initiates polymer formation. Rather high yields of polymers possessing excellent polymer properties were obtained when a bisimidazole urea (formed by reacting a diisocyanate with two equivalents of imidazole) was reacted with a difunctional amine (aryl or aliphatic).

Attempts to gas catalyze this reaction by volatilizing the difunctional nucleophile failed to give a sufficient degree of polymerization. No successful rigidization procedure could be achieved. All other blocking systems were thermolabile and required heat to regenerate the isocyanate.

4. Unsaturated Polyesters

A second major polymer classification of significant reactivity to be considered for this application was unsaturated polyester. Those resins are polyester polymers dissolved in unsaturated reactive monomeric materials. The polyester chain is a condensation product of diol and mixtures of saturated and unsaturated dibasic acids. (Aromatic acids were considered saturated since they are not reactive with free radical catalysts.) A typical unsaturated polyester for structural applications could be prepared from a 1:1:2 ratio of isophthalic acid, maleic anhydride, and propylene glycol. Styrene is the common unsaturated monomer used in polyester resins, but acrylic monomers and polyallyl esters have also been used. The unsaturated monomer functions as a reactant and a solvent, thus providing, in theory, a 100 percent reactive polymer system.

Polyester resins are converted from a solution of a thermoplastic polyester in reactive monomers to a cross-linked thermoset plastic material by the action of free-radical generating initiators. The decomposition of the initiators into polymer-creating free radicals is achieved by the use of heat or of chemical accelerators. Heat provides energy to break the weak bonds in the peroxide or azo compounds into free radicals, while the chemical accelerators probably act by electron transfer mechanisms to create the free radicals. Heavy metal salts (cobalt, manganese, lead, etc) are effective accelerators for hydroperoxide containing materials and tertiary amines are commonly used accelerators for peroxides. There are no effective chemical accelerators for azo type catalysts.

Because polyester impregnated materials have found a wide range of use in structural applications and because of the very satisfactory performance of polyesters in a variety of uses, a program to investigate their use for gas-catalyzed-curing in a vacuum atmosphere was undertaken. Three approaches were apparent for initial investigation: heat-initiated cure of a catalyzed resin system, volatilization of an accelerator for resins containing a catalyst, and volatilization of a catalyst for a resin containing the accelerator. Two approaches are discussed separately below, the second approach being most applicable and successful.

The presence of a monomeric reactant, such as styrene, is necessary since the unsaturation in the polyester chain will not homopolymerize via free radical catalysis to a cross-linked network. The low molecular weight of styrene and other commonly used reactive monomers preclude their use due to high volatility at reduced pressure. Attempts to cure styrenated polyesters by volatile catalysts were completely unsuccessful. Allyl esters, such as diallyl pathalate and triallyl cyanurate, were satisfactory from a volatility standpoint, but are not reactive

enough under the necessary conditions, nor do they provide satisfactory solvent action. Polyester systems including allyl esters are generally cured with heat and pressure. It has been found that methacrylate esters of diols and triols are sufficiently non-volatile, have satisfactory solvent properties, and are fast reacting. Synthesized aryl trisubstituted acrylates and hexafunctional aliphatic acrylates were completely unacceptable as monomeric diluents. They would not copolymerize with unsaturated polyesters containing maleic functionality. These monomers could be successfully homopolymerized to very brittle solids. It was concluded that these monomers contained too high an aromatic character and were, in addition, too functional for use in this application. The dimethacrylate ester of tetraethylene glycol and the trimethacrylate of trimethylol propane have been used most extensively in this application. The acrylic esters were present in as high as 60-70 percent of total resin weight to provide a workable viscosity. Small amounts of styrene (up to 10 percent) aided solvency and seemed to accelerate cure in these systems.

Eighteen polyester resin compositions based on varying proportions of maleic anhydride and isophthalic acid were synthesized for physical testing. Styrene modified resins were prepared as standards for comparison with less volatile reactive monomers. None of the above resins compared favorably with respect to the physical properties of the commercially available Aropol 7230 MC. Flexural strengths of a standard polyester copolymerized with less volatile reactive monomers are similar to those polyesters copolymerized with styrene. Table 7 shows flexural strength data on 6 ply laminates. The laminates were cured for one hour at 80°C with 1 percent of a non-oxidative catalyst. The resin diluted with 60 percent A-209 (tetraethylene glycol dimethacrylate) compared favorably with a styrene diluted polyester (Aropol 7200 MC). The resin diluted with A-350 (trimethacrylate of trimethylol propane) was observed to give inferior strength performance. The study indicated that the amount of diluent was critical to strength performance. The ADM polyester, Aropol 7200 MC, was used as the polyester polymer portion of the resin system. Two methods were evaluated as curing mechanisms for vapor catalyzed cross-linked polyesters.

a. Vaporization Of A Chemical Accelerator

It is well established that polyester resins can be cured by free radical catalysts at ambient conditions if a chemical accelerator is present in the system. Commonly, the accelerator is present in the resin system as stored and the catalyst is added at the time of application. The gassing of a catalyzed resin by an accelerator represents a reversal of common practice.

Tertiary aromatic amines (dimethyl aniline, dimethyl-p-toluidine) are commonly used to accelerate peroxide catalyzed resin systems and should have moderate volatility at room temperatures and 10^{-5} to 10^{-6} mm Hg. It was found that gassing polyester impregnated structures with these amines produced a very small degree of cure. Gassing catalyzed resins with mercaptans, another accelerating agent for peroxide containing resin, likewise did not yield satisfactory cure. The following disadvantages are apparent in this approach:

The level of accelerator is critical, too much being as harmful as too little, and this approach does not allow control of accelerator level;

Resins containing useful levels of peroxide catalysts do not have sufficient shelf-life.

Use of secondary accelerators is prohibited because of storage life requirements.

TABLE 7

FLEXURAL STRENGTHS OF POLYESTER LAMINATES

Polyester	Diluent	% Diluent	Flex Strength [A]
7200 MC	Styrene	40	47,390 psi
7200 MC	A-206	75	17,440
7200 MC	A-209	75	34,130
7200 MC	A-305	75	22,600
7200 MC	A-206	60	37,450
7200 MC	A-209	60	47,340
7200 MC	A-305	60	15,350

A = Average of five tests

A-206 ethylene glycol dimethacrylate

A-209 tetraethylene glycol dimethacrylate

A-305 trimethacrylate of trimethylol propane

The hydrolysis of thio acetals to mercaptans was evaluated as a method of generating an accelerator in situ. In this approach the polyester resin could be charged with a catalyst and hopefully have sufficient shelf life prior to accelerator generation (Reaction A). Since this reaction is sluggish, the more reactive thioxalane was synthesized for ultimate hydrolysis (Reaction B). Incorporation of a mercaptan precursor in a polyester laminate would afford accurate control of the amount of accelerator used.

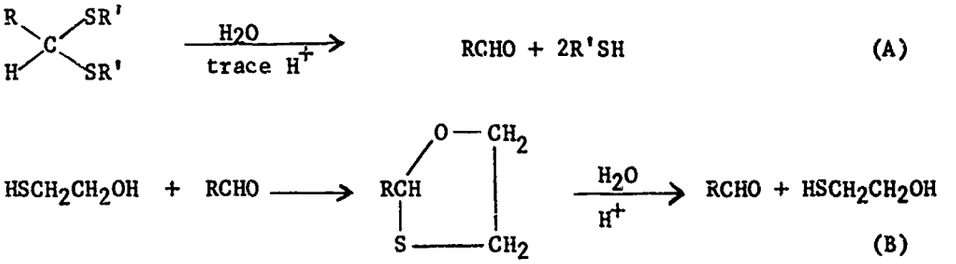

This approach was only a partial success as, apparently, the thioxalane was not hydrolyzed sufficiently under the reaction conditions. As a result only a partial cure was observed. Resins including the peroxide and mercaptoethanol were found to gel in 25 minutes in bulk without appreciable exotherm.

b. Vaporization Of A Chemical Catalyst

The disadvantages outlined in the previous approach can be overcome by gassing an accelerated resin system with a peroxide catalyst. The level of catalyst is not as critical as is the level of accelerator in obtaining a cured polyester. Although a large excess of catalyst could adversely affect physical properties, the work indicates excess peroxide is not present in the gassed resin. The polyester resins containing only accelerators have been found to have good shelf-life at a variety of accelerator levels and combination of accelerators. It has been found that combinations of several accelerators give the fastest curing systems.

The volatile catalyst employed has been methyl ethyl ketone peroxide. This is commonly supplied at 60 percent active material in an aromatic ester plasticizer and is available in faster reacting versions. The "fast" types were used in this work. This catalyst volatilizes moderately well at room temperature and 10^{-5} to 10^{-6} mm Hg.

A number of accelerator combinations have been examined and it was found that a mixture of aromatic amines and a cobalt salt gave the fastest cures. The addition of very low levels of copper salts, originally intended as a shelf-life extender, also has a marked accelerating effect on the peroxide curing of these resin systems.

Table 8 shows the curing times of polyester resins containing the indicated accelerators and which have been catalyzed with 1 percent peroxide addition to a ten gram sample in a shallow dish at ambient conditions of temperature and pressure. Small structures, impregnated with the resins, were rigidized in 30 minutes when gassed with peroxide vapors in a high vacuum. The rigid structures continued to harden over a 24 hour period, probably via the absorbed peroxide which promoted a type of post curing.

TABLE 8

CURE TIMES OF ACCELERATED POLYESTERS (1)

Polyester (2)	Accelerators (3) (%)	% Co	Catalyst (3)	Peak Exotherm (°F)	Gel Time (min)	Cure Time (min)
1	0.3 DMA, 0.3 DMT	0.06	DDM	-	11	20
1	0.3 DMA, 0.3 DMT	0.12	DDM	-	8	11
1	0.3 DMA, 0.3 DMT, 0.01 Cu	0.12	DDM	-	3	4
1	0.3 DMA, 0.3 DMT	0.06	X	315	5	8
1	0.3 DMA, 0.3 DMT, 0.01 Cu	0.06	X	340	2	4
2	0.3 DMA, 0.3 DMT, 0.01 Cu	0.06	X		1.4	2.0
2	0.4 DMA, 0.4 DMT, 0.01 Cu	0.06	X	310	0.5	1.0
2	0.3 DMA, 0.3 DMT, 0.01 Cu 4.0 TPP	0.06	X	235	0.9	1.3
2	0.3 HEA, 0.3 DMT, 0.01 Cu	0.06	X	-	1.2	1.6
2	0.4 HEA, 0.4 DMT, 0.01 Cu	0.06	X	304	0.5	0.75
2	0.3 HEA, 0.3 DMT, 0.01 Cu 4.0 TPP	0.06	X	236	1.0	1.3

(1) Gel time and cure time recorded with 10 g resin in 6 cm aluminum dish. Gel time recorded when smooth flow stopped, cure time when dish became too hot to hold in hand.

(2) Polyester 1 contained 54.5% dimethacrylate ester of tetraethylene glycol, 36.3% Aropol 7200 MC, 9.1% styrene, 100 ppm hydroquinone. Polyester 2 contained 54.5% trimethacrylate of trimethyiol propane, 36.3% Aropol 7200 MC, 9.1% styrene and 100 ppm hydroquinone.

(3) DMA = N,N-dimethylaniline, DMT = N,N-dimethyl-p-toluidine, HEA = N-hydroxyethyl aniline, Cu = copper (as napthenate), Co = cobalt (as napthenate), TPP = triphenylphosphite, DDM = Lupersol DDM, X = Lupersol-Delta X.

5. Imino Polyesters

The addition of ethylene imine to the double bond contained in unsaturated polyesters results in the formation of an imino substituted polyester. This material can be cross-linked via ring opening polymerization catalyzed by Lewis acids. The reaction and curing mechanism is as follows:

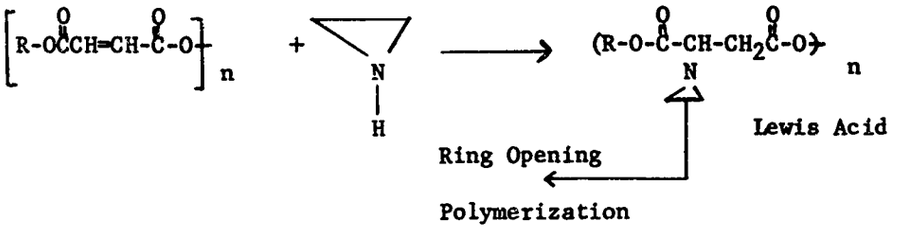

The imino polyester was readily cured in bulk by dialkyl sulfates and Lewis acids. When impregnated onto glass and gassed with boron trifluoride etherate, resin gelation occurred but the laminate was not sufficiently rigid. This, no doubt, was due to the low degree of polymerization.

6. Epoxy Resin

Previous work has shown the feasibility of using epoxy resins for gas phase rigidization of honeycomb reinforcing fabric. This work involved volatilizing low molecular weight amine compounds which behave as polymerization catalyst and co-reactant.

The research conducted under this study had as an objective the improvement in cure time and in cured resin strength properties. To accomplish these objectives, the following tasks were undertaken:

a. synthesis and evaluation of reactive and non-reactive diluents,

b. evaluation of commercial epoxide resins, and

c. the synthesis of reactive epoxide monomer.

a. Synthesis and Evaluation Of Reactive And Non-Reactive Diluents

The primary function of the diluent is to reduce the viscosity of the resin. It has been shown that reactive diluents can also add beneficially to the strength properties in some instances. The purpose of this task was to determine the affect of the diluents on cure rates and strength.

The inert diluents evaluated were varied according to polarity and boiling point. The polarity of the diluent affects the viscosity whereas the boiling point is a measure of the rate of evaporation under hard vacuum. Previous studies have shown that the rate of plasticizer boil-off is important in the curing process. Table 9 shows the affect of solvents on reducing viscosity. The lower molecular weight solvents are more effective at reducing viscosity. Dow DEN 438 (Epoxy Novolac Resin) was diluted with a variety of reactive diluents specifically prepared for evaluation. A wide range of viscosities was observed and are recorded in Table 10.

TABLE 9

VISCOSITIES OF DOW DEN 438 EPOXY NOVOLAC DILUTED WITH SOLVENTS

Solvent (1)	Type	Boiling Point	Viscosity (2)
Methyl Isobutyl Ketone	Ketone	114°C	4.7
Pentoxone	Ketone	160	21.2
Xylene	Aromatic	140	8.9
Cymene	Aromatic	180	incompatible
Cellosolve Acetate	Ester	150	10.3
Butyl Cellosolve Acetate	Ester	190	17.9
Ansul E 121	Ether	85	2.5

(1) 20% of total weight

(2) Gardner-Holdt seconds at 25°C

TABLE 10

VISCOSITIES OF DOW DEN 438 EPOXY NOVOLAC DILUTED WITH EPOXY MONOMERS

Monomer	%	Type	Viscosity(1)
Furfuryl Glycidyl Ether	20	Mono epoxide	40.1
Tetrahydrofurfuryl Glycidyl Ether	20	Mono epoxide	54.1
Phenyl Glycidyl Ether	20	Mono epoxide	102.9
Unox 206	20	Diepoxide	125.0
Butadiene Dioxide	20	Diepoxide	18.1
Glycidyl Acrylate	20	Acrylic Mono epoxide	20.4
Glycidyl Acrylate	10	Acrylic Mono epoxide	166.5
Allyl Glycidyl Ether	20	Unsat Mono epoxide	18.6
Allyl Glycidyl Ether	10	Unsat Mono epoxide	239.6

(1) Gardner-Holdt seconds at 25°C

Several of the diluents were difunctional and enhanced the physical properties of the cured epoxy. Synthesized glycidyl ethers were most effective at lowering viscosity and gave the best combination of properties with the Dow DEN 438 resin. The glycidyl methacrylate diluted resin increased in viscosity upon aging. This viscosity build up was no doubt due to a free radical induced homopolymerization of the acrylate.

b. Evaluation of Commercial Epoxide Resins

The continued evaluation of commercial resins led to an improvement in epoxy cure rate. Honeycomb fabric structures impregnated with Kopoxite 159, a glycidyl ether based on resorcinol, and gassed with propylene diamine at 10^{-2} mm Hg, have been cured and sufficiently rigidified in six hours. This is a substantial improvement over the Dow DEN 438 system.

c. The Synthesis of Reactive Epoxide Monomer

A room temperature, anhydride cured monomer was synthesized and considered for this program. Preliminary data indicated some potential in this system. Copolymers of glycidyl methacrylate have been synthesized which include the following:

a 2:1 methyl methacrylate: glycidyl methacrylate copolymer,
a 1:1 styrene: glycidyl methacrylate copolymer, and
a homopolymer of glycidyl methacrylate.

These polymers cure at about the same rate as Novolac type epoxies. This type of epoxy has the advantage of yielding a non-tacky glass laminate before cure. The polymers were prepared in a 50 percent non-volatile solution and applied to the glass substrate. Evaporation of the solvent at room conditions left a non-tacky, flexible laminate. These were rigidified by aliphatic diamine catalysts.

Polymerization of epoxides by Lewis acids is a cationic polymerization which is catalytic. The epoxide resins examined during this contract period were screened with several select Lewis acids. Usually excellent results were obtained when polymerizations were carried out in bulk as can be observed from Table 11. The gassing of resin impregnated structures with Lewis acids under hard vacuum gave very little rigidization. A controlled release of catalyst may be necessary to achieve sufficient polymerization.

TABLE 11

REACTIVITY OF EPOXIDES TO LEWIS ACIDS AT ROOM TEMPERATURE

Epoxide	Acid	Result
Butadiene Diepoxide	$SnCl_4$ and $BF_3 \cdot Et_2O$	Very rapid, exothermic reaction
(80% DEN 438 - 20% Butadiene Diepoxide)	$SnCl_4$	Thickened to soft gel rapidly
1:1 Styrene-Glycidyl Methacrylate copolymer 50% in Xylene-MIBK	$SnCl_4$	Thickened to hard gel rapidly
Unox 201	$SnCl_4$	Slow reaction - gel
Unox 269	$SnCl_4$	Very rapid, no hardening
Furfuryl Glycidyl Ether (FGE)	$SnCl_4$	Explosively - high exothermic (1)
80% DEN 438 20% FGE	$SnCl_4$	Hardened to brittle solid rapidly

(1) Furan ring also polymerizes under these conditions.

SECTION 4

SOLAR COLLECTORS

A. Background Information

The design, fabrication, and rigidization of an expandable solar energy concentrator using completely flexible, sandwich type structural materials were shown feasible under Contract No. AF33(657)-10409. Efforts of this portion of the present program were directed toward refining the fabrication and rigidization techniques and optimizing the basic structural and rigidizing materials. These optimum techniques and materials were then to be used to construct two and ten foot diameter collectors.

B. Solar Collector Design and Fabrication

The final design and fabrication procedures developed for the solar collectors are summarized below. A more detailed description follows in subsequent sections. Figure 6 presents an illustration of the main features of the solar collector structure.

1. Reflective Surface

The reflective surface consisted of a 1 mil (.001 inch) aluminized Mylar film tailored with gores to produce a paraboloid with a 60^{o} rim angle.

2. Assembly Fixture

A set of rings was used as an assembly fixture for the two foot experimental models. The film of assembled Mylar gores was clamped between the rings and inflated by pressurizing between the film and a cover plate. This fixture also mechanically lowered a pressurized fabric backing onto the Mylar film in order to remove wrinkles from the fabric.

3. Flexible Bonding Layer

A bonding layer was sprayed onto the pressurized Mylar. The bonding layer consisted of a flexible two component epoxy resin formulated for spray application.

4. Structural Material

The structural material selected for the end items was a three dimensional fabric woven from nylon with two faces separated by drop threads located in a random (overall) pattern. The separation of the faces was one inch and the material weighed about 13 oz/yd^2.

5. Resin Impregnation

The rigidizing resin was uniformly vacuum impregnated onto the structural material.

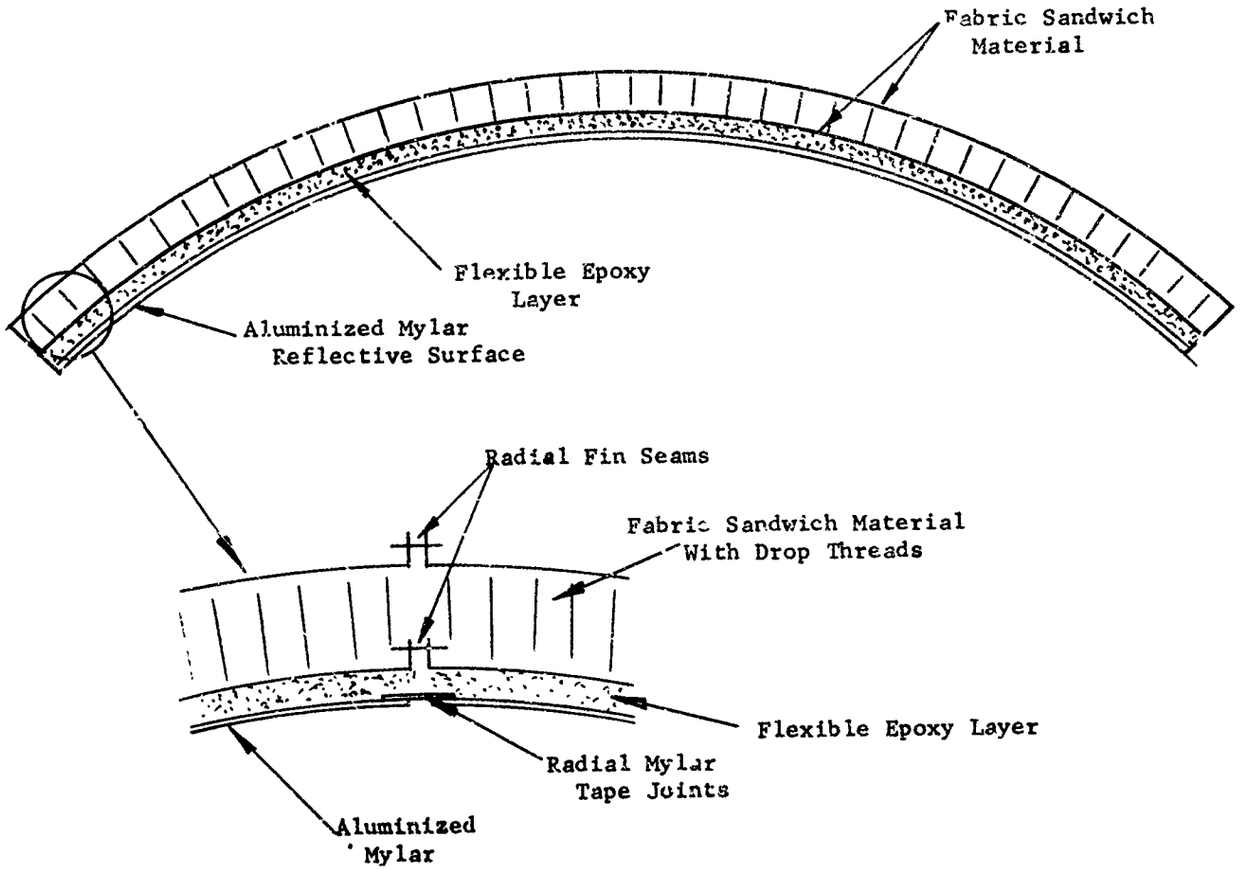

Figure 6 - Details Of Solar Collector

6. Catalyst Distribution

The rigidizing vapors were introduced through a flexible manifold which became an integral part of the cured structure.

C. End Items

Three - two foot diameter solar collector composites were prepared at Viron and rigidized at Wright Patterson Air Force Base during the week of September 28, 1964.

A ten foot diameter composite was delivered and rigidized during the week of November 29, 1964, on corporate funds. The procedures and results of these collectors are discussed in detail in this section.

D. Development of The Design, Materials, And Fabrication Techniques

1. Reflective Surface

a. Material

The Mylar reflective surface used for the effort of Contract AF33(657)-10409, and in the very early stages of this contract, was pre-formed by holding a film in place with metal rings and creating a pressure differential across the film. These films were essentially all 3 mil aluminized Mylar to aid in eliminating the show-through. It became apparent, that larger diameter collectors would require films made in sections and the stringent weight and packaging requirements would make it necessary to use thinner films. Therefore, 1 mil aluminized Mylar was selected for the reflective surface and gore patterns were designed.

The task of laying out a gore pattern was basically one of representing the curved three dimensional figure on a two dimensional plane. First, a series of arc lengths (points 1, 2, 3, and 4 of Figure 7) for a 24 inch diameter parabolic surface with a 60° rim angle were calculated starting from the apex. This gave a number of dimensions in one direction of the gore pattern. The second set of dimensions for each gore was obtained by dividing the circumference of the paraboloid at the various arc lengths (points 1, 2, 3, and 4) by the number of gores in the total paraboloid (distances a, b, and c).

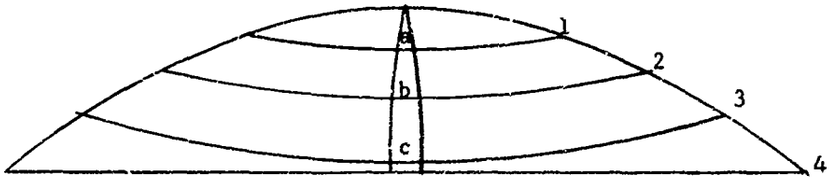

Figure 7 - Gore Pattern Layout Approach

The 1 mil aluminized Mylar gored films used in making the two foot collectors in this program were made from patterns calculated as discussed above. An excess in the length of each gore was provided to clamp the film in the assembly fixtures.

b. Methods of Joining The Mylar Gores

(1) The first gore joining method investigated used clear thermosetting tape on the Mylar side of the film. After the unit was fabricated, it was noted that any gap between the gores resulted in show-through of the tape on the reflective side. Also, slight heat marks in the form of wrinkles were evident on each side of the tape due to shrinkage of the Mylar. Later attempts used an aluminized thermosetting tape with similar results.

(2) The second method was to apply a metallized thermosetting tape on the metallized side of the polyester film which eliminated the gap show-through on the reflective side. However, heat marks on each side of the tapes were still evident.

(3) A third method was to apply a metallized pressure sensitive tape to the metallized side of the Mylar film. This eliminated the gap between the gores and also eliminated the heat marks as seen in the two previous methods since no heat was required to attach this tape.

When these reflective surfaces were used to fabricate solar collectors, it was decided that method 3 was most satisfactory. Method 2 was eliminated because of the pronounced surface effect from the edges of the tape and Method 3 was eliminated because of a lack of seam strength.

2. Screening For The Flexible Bonding Layer

a. Flexible Epoxies

Numerous epoxy resin systems were screened early in the program for the following properties:

(1) Cured flexibility
(2) Adhesion to Mylar
(3) Uniformity, i.e. no fish eyes or bubbles
(4) Cure time
(5) Low shrinkage

Considerable discussion of this component will follow in later sections.

b. Other Candidate Bonding Layers

Other materials which were examined as possible flexible bonding layers were: neoprene foams, urethane elastomers, vinyl foams, and unsaturated polyester. The results of these tests will also be discussed in a later section.

3. Structural Material

a. Design and Manufacture of The Structural Material

The solar collector structural material was a woven nylon or dacron fabric sandwich material with a nominal weight of 13 oz/yd^2. It had two facings connected with drop threads (pile). The threads of the pile were of the same material as those in the skins which provided an integrally woven three dimensional structure. Several variations in the weave of this fabric were designed. Two series of materials were utilized. The first had a face separation of 3/4 inch and the pile was arranged in parallel rows 1/2 inch apart. The other series had a face separation of about 1 inch with the pile scattered at random. Materials were woven from various types of yarns which included nylon and dacron. In each case, monofilament and spun yarns were incorporated into the experimental sample series. Variations were also made so that the filling diameter of one face would be different from the filling diameter of the other in an attempt to provide one degree of curvature. Table 12 describes the materials in detail. It was found that the fabrics of Series 1 resulted in a better reflective surface then those of Series 2. Figure 8 compares two cured collectors fabricated from a sample of each series. The collector at the left utilized material with the random scatter pile and is characterized by the obvious absence of flute lines.

b. Seaming of The Structural Material Gore Patterns

In the early phases of this program, 8 inch and 24 inch collectors were fabricated from one piece of material. The nylon used was pre-formed by wetting it with water and placing it together with a Mylar film in a set of rings and pressurizing to the desired height. Heat was then applied to remove the moisture and to provide the material with a permanent set.

This approach was replaced by tailoring the backing from fabric gores the same shape as the pattern designed for the reflective surface. Extra material was allowed on each gore for sewing the segments together. When joining sections of three dimensional materials, both the top and bottom skins must be fastened together. It was found that the material with the parallel rows of drop threads could be satisfactorily joined by cutting away a row or two of threads from the edge of the faces and machine sewing the bottom faces together by means of a lap seam and the top faces by means of a fine seam. Later, it was found that a fin seam in both skins eliminated the ridge from overlapped material along the gore line.

c. Bonding The Structural Material

In the feasibility study, the structural material was manually lowered onto the bonding layer. This procedure often resulted in the fabric being off-center from the Mylar. Wrinkles and folds were usually present in the lower face because the material could not be uniformly stretched. This situation was corrected through the design and use of an assembly fixture with a lowering ring. The gored structural material was draped to the lowering ring and applied to the tacky bonding layer without wrinkles by applying a uniform pressure over the fabric as it was being lowered. The uniform pressure was achieved by pressurizing an envelope of clear plastic film over the structural material. Figure 9 shows the pressurized structural material being lowered onto the tacky resin for bonding.

TABLE 12

SOLAR COLLECTOR STRUCTURAL MATERIAL

Series 1

Connecting yarns in an over-all pattern (random scatter). Face separation of 1 inch.

Sample 1 - All filament nylon
Pile = Chemstrand Nylon 70-34-10½ semi-dull
Ground = Dupont Nylon 140-68-10½ semi-dull
Filling = Chemstrand Nylon 70-34-10½ Picks = 80

Sample 2 - All filament nylon. The filling on one face smaller in diameter than the filling on the other face.
Pile = Chemstrand Nylon 70-34-10½ semi-dull
Ground = Dupont Nylon 140-68-10½ semi-dull
Filling = Bottom = Chemstrand Nylon 70-34-10½ Picks = 72

Sample 3 - All nylon-filament ground and filament pile, spun filling. Filling on one face smaller in diameter than the filling on the other.
Pile = Chemstrand Nylon 70-34-10½ semi-dull
Ground = Dupont Nylon 140-68-10½ semi-dull
Top = Spun Nylon 50/1
Filling = Bottom - Spun Nylon 60/1 Picks = 76

Sample 4 - All nylon-spun ground yarn, filament pile yarn, spun filling yarn. The filling on one face smaller in diameter than the filling on the other.
Pile = Chemstrand Nylon 70-34-10½ semi-dull
Ground = Spun Nylon 60/2
Top = Spun Nylon 50/1
Filling = Bottom = Spun Nylon 60/1 Picks = 68

Sample 5 - All filament dacron.
Pile = Dupont Dacron 100-34-10 - Bright
Ground = Dupont Dacron 100-34-10 - Bright
Filling = Dupont Dacron 100-34-10 - Picks = 88

Sample 6 - All dacron-filament ground, filament pile spun filling with the filling on one face smaller in diameter than the filling on the other.
Pile = Dupont Dacron 100-34-10 - Bright
Ground = Dupont Dacron 100-34-10 - Bright
Top = Spun Dacron 40/1
Filling = Bottom = Spun Dacron 50/1 Picks = 80

Sample 7 - All dacron-spun ground, filament pile and spun filling, filling on one face smaller in diameter than the filling on the other.
Pile = Dupont Dacron 100-34-10 - Bright
Ground = Spun Dacron 50/2
Top = 40/1 Spun Dacron
Filling = Bottom = 50/1 Spun Dacron Picks = 50

TABLE 12 (Cont'd)

SOLAR COLLECTOR STRUCTURAL MATERIAL

Series 2

Connecting yarns in rows, one-half inch apart. Face separation of three quarters of an inch.

Sample 1 - All filament - nylon
Pile = Dupont Nylon 140-68-10½ semi-dull
Ground = American Enka Nylon 50-13-10 semi-dull
Filling = American Enka Nylon 50-13-10 Picks = 104

Sample 2 - All nylon-filament ground filament pile, spun filling. Filling diameter on one face smaller than the filling on the other.
Pile = Dupont Nylon 140-68-10½
Ground = American Enka Nylon 50-13-10 semi-dull
Top = 50/1 spun Nylon
Filling = Bottom = 60/1 Spun Nylon Picks = 88

Sample 3 - All filament dacron.
Pile = Dupont Dacron 100-34-10 - Bright
Ground = Dupont Dacron 70-34-10
Filling = Dupont Dacron 70-34-10 Picks = 84

Sample 4 - All dacron, filament ground, filament pile, spun filling. The diameter of the filling on one face smaller than the filling on the other.
Pile = Dupont Dacron 100-34-10 - Bright
Ground = Dupont Dacron 70-34-10
Top = Dacron 40/1
Filling = Bottom = 50/1 Picks = 80

Figure 8 - A Comparison Of Fluted (Right) And Random Scattered (Left) Core Material Collectors

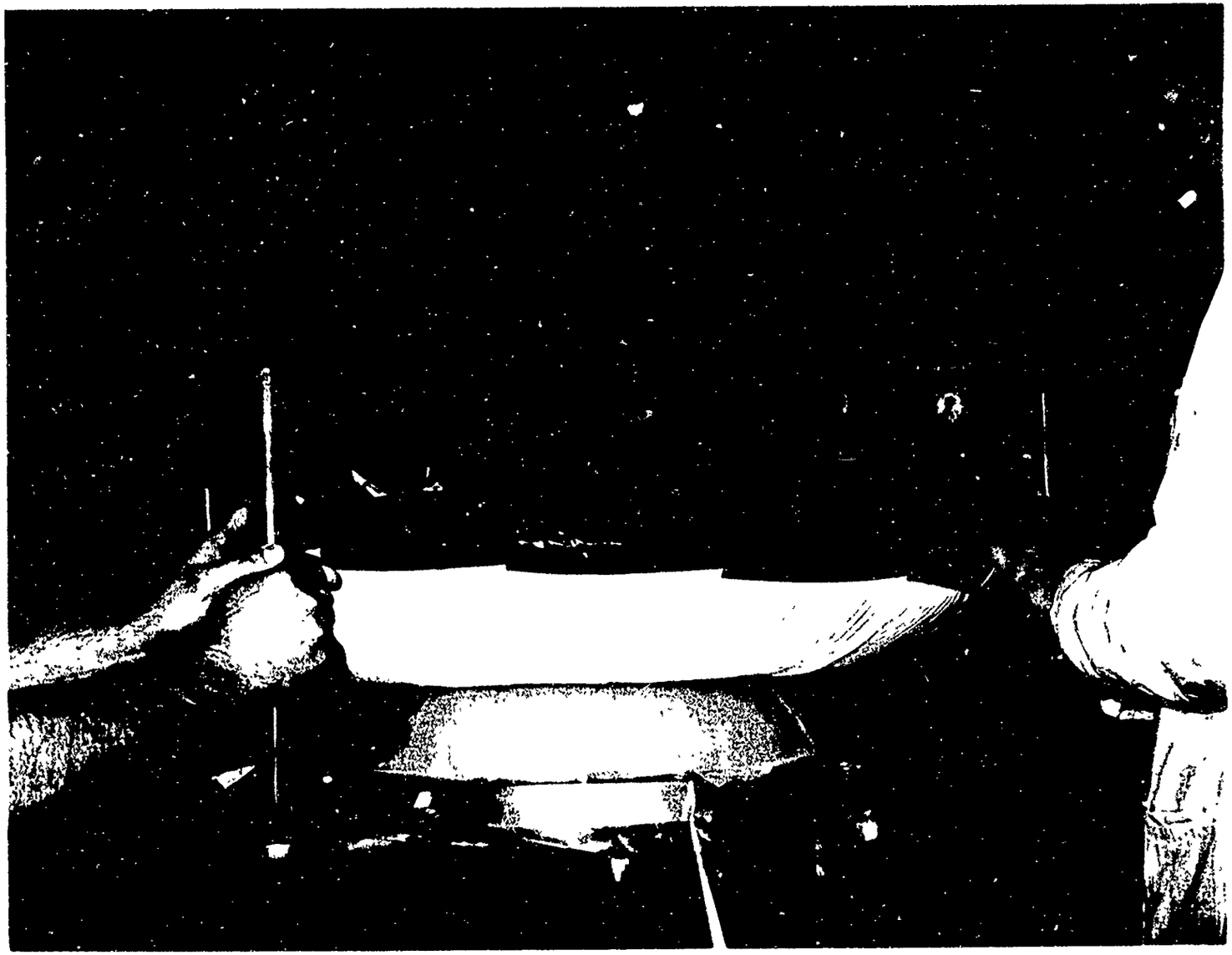

Figure 9 - Lowering Fixture Being Utilized During Assembly

Pressure build-up, as the fixture was lowered, was eliminated with a relief valve. After the material was fully lowered, Figure 10, pressure in the envelope was maintained until the resin had permanently set against the smooth lower skin. The plastic films were then removed and the structural material was ready for impregnation with the rigidizing resin.

Bonding the structural material to a 10 foot diameter solar collector was accomplished in a similar manner.

4. Resin Impregnation

The structural material was impregnated with the rigidizing resin during the feasibility study by brushing the resin onto the fabric. This method proved unsatisfactory because of uneven distribution and premature catalyzation of the resin from atmospheric moisture. It was possible to largely overcome these difficulties by vacuum impregnating the resin into the structural material.

First attempts used a clear Mylar film which was clamped over the bonded fabric with the tie down ring. Plastic valves were inserted in the top skin of the structural material for resin distribution and in the Mylar for a vacuum attachment. Figure 11 shows a typical set-up for impregnating the gored two foot collectors. One difficulty with using Mylar for the cover film was that creases and folds developed in the film, and retarded the passage of resin. This was later corrected by using a more flexible polyethylene film which was fabricated from gores to give a better fit to the contour of the collector. The flexibility of this film prevented the formation of creases and impregnation proceeded at a faster rate. The cover film prevented premature resin reaction with atmospheric moisture and was not removed until immediately before rigidization. The resin distribution valves in the structural material then served as catalyst vapor distribution points.

5. Catalyst Distribution Systems

The distribution of the catalyst was accomplished by introducing it into the core of the structural material through a series of plastic valves attached to the outer skin. These valves were connected with ordinary laboratory rubber tubing to supply flasks placed outside of the chamber during vacuum cure. The vaporization rate of the catalysts in the flask was controlled by means of ball valves placed between the flasks and the chamber inlet.

E. Experimental Work

The experimental work to develop materials and fabrication techniques was performed on 8 inch and 24 inch rings, a 28 inch assembly fixture, and a 38 inch fixture which was supplied by the government. The 8 inch rings were used primarily to find the effect of various flexible layers on surface distortion and to demonstrate feasibility of new composite systems. The 24 inch rings were used throughout the program to accelerate the experimental work. The 28 inch assembly fixture was utilized for optimizing the positioning of composite materials and the 38 inch fixture was used to fabricate collectors for surface measurements by Air Force personnel.

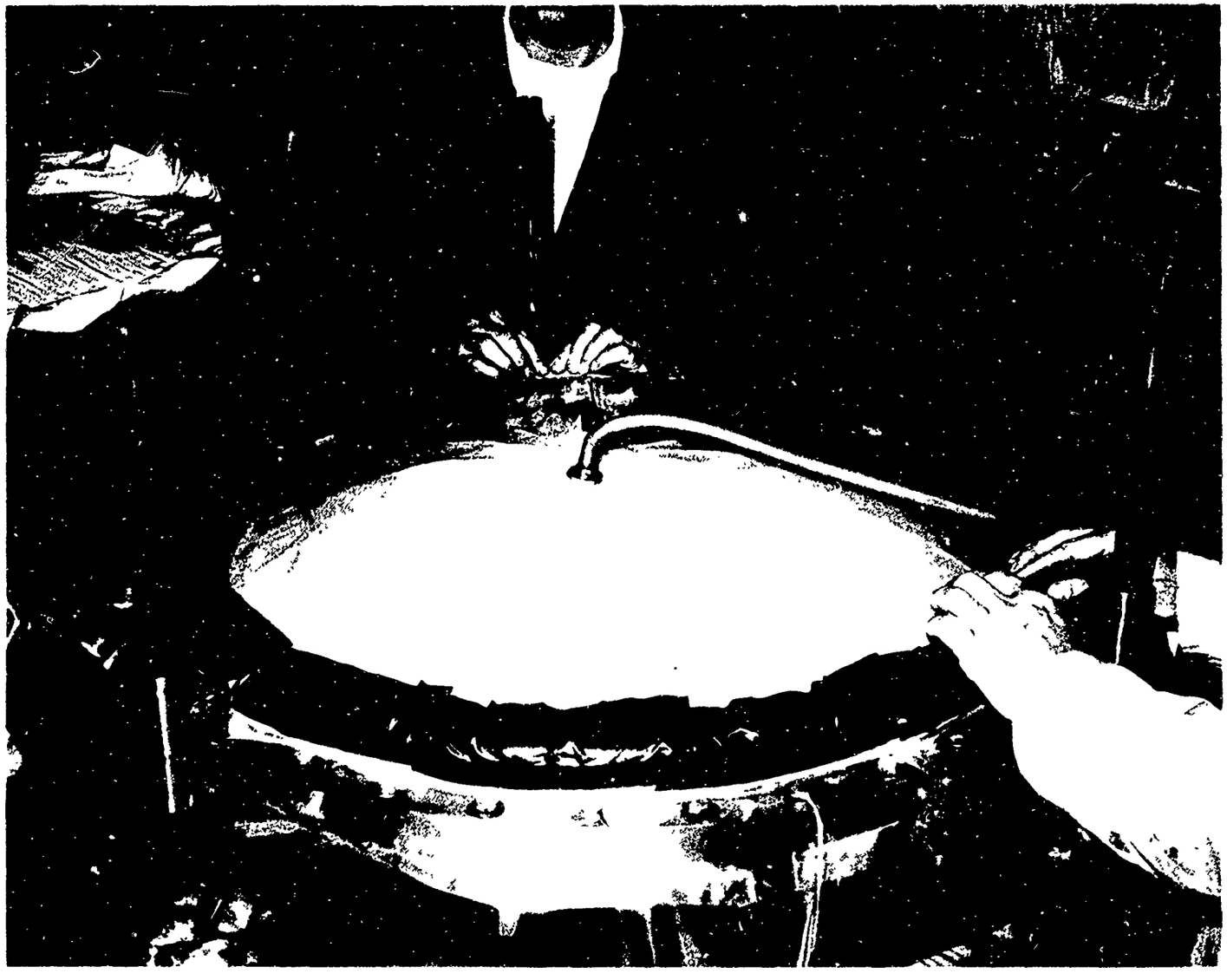

Figure 10 - Assembled Solar Collector Composite

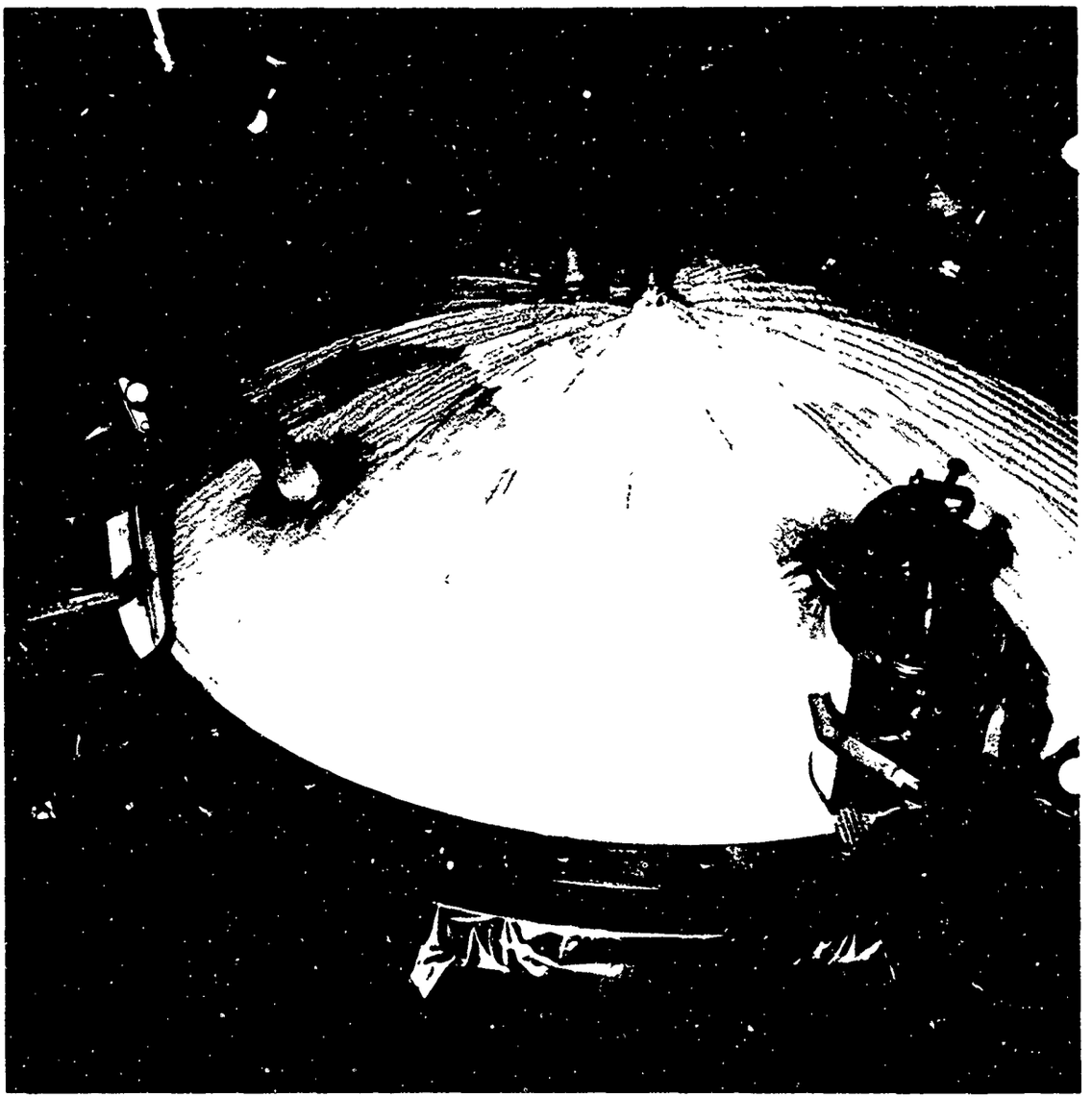

Figure 11 - Vacuum Impregnation Of Solar Collector Model

1. Screening For Flexible Epoxies

Table 13 is a summary of the epoxy resins that were screened as candidate materials for the flexible layer between the Mylar reflective surface and the fabric structural material. Each of the various epoxies were brushed on a 4 x 6 inch piece of 1 mil Mylar and allowed to air dry. The cured films were evaluated for cure time, adhesion to Mylar, and flexibility.

Table 14 describes the initial screening process which resulted in the elimination of some materials on the basis of excessive cure time, extremely high viscosity, poor flexibility, and poor adhesion. Three resin systems showed some promise. These were products manufactured by General Mills, Union Carbide, and Shell Chemical Co. Further work on these resins attempted to eliminate certain characteristics such as fish eyes and orange peel in the cured film. The Versamids possessed a high degree of flexibility and the Union Carbide resins had low viscosities as well as flexibility. The Epon products had the shortest cure time as well as very good flexibility. Another advantage of the Epon resin was that it became tack free within 24 hours whereas most of the others remained slightly tacky for several days. Table 15 compares the effect of 2% cellosolve acetate on various Union Carbide formulations. The formulations were varied in an attempt to get better flexibility. Table 16 shows additional surface active agents used in the attempt to eliminate fish eyes (small bubbles) and orange peel (dense waviness). The data from Tables 15 and 16 show that most films became brittle upon ultimate cure. No. 17 was the best film on either table, but the reason for the apparent 24 hour cure and flexibility retention is not fully understood. Table 17 describes several General Mills Epoxy formulations. Films 7b and 8 had a better appearance than did the 7a (control), however, netther film fully cured. They were brittle after two weeks. Film 18 remained flexible after two weeks and had good adhesion, as well as a good appearance, but the drawback was the extremely high viscosity.

In an effort to optimize Epon 872-X-75, Film 22, Table 14, various surfactants were added. Controls with no additive, in each case had small bubbles or fish eyes. Up to 5% of American Cyanimide Beetle 216-B was incorporated into the formulation as was Union Carbide's Sag 470. Beetle 216-B was selected because only 0.5% was required to eliminate surface distortion.

The chief objection to Epon 872-X-75 was its high viscosity (10,000 centipoises at room temperature) which made it necessary to brush it on the Mylar film. It was felt that a flexible layer could not be successfully brushed onto the large surfaces of practical sized solar collectors. For this reason, a program was started to develop a spray formulation.

The first approach was to find the effects of adding low viscosity reactive and non-reactive diluents. Table 18 shows work done utilizing Cardolite NC513 of Minnesota Mining and Manufacturing Company. The data on this table show that viscosities were decreased until an excess of diluent resulted in a prolonged cure time. Film 59 was added to the table as a control. Film 65 was prepared to determine what effect the diluent had on a rigid resin since Cardolite is also known to be a flexibilizer.

Tables 19 and 20 describe additional work on viscosity control. Formulations 73 and 76 produced the best films which were applied with conventional spray equipment. The acetone did not interfere with other properties, such as cure time or flexibility, because a large percentage of it apparently did not re[illegible]

TABLE 13

EPOXY FLEXIBLE LAYER CANDIDATES

Manufacturer	Epoxy	Hardener
1. Union Carbide	ERL-2774	22L-0822 ERL-2793 22L-0845
2. General Mills Inc.	Gen Epoxy 185 175 190 450x75 525	Versamide 140 141 250
3. Atlas Mineral Products Co.	Rezklad 3-30CN	164-087
4. Iso Chem Resins Co.	R1249 407	AEP 13
5. Thiokol Chem Corp.	Tipox E	TETA LP-3 EH-330
6. American Cyanamid Co.	BR-93A	BR-93B
7. Hysol Corp.	PC12-007	H8-3496
8. Merco Products	M-4501	Mactivator
9. Waldman Epoxy Products	2200	125
10. Ciba	Ardalite 502	Pentamed 825
11. FMC	Axiron 2000	Chlorendic Anhydride
12. Reichhold	37-135 37-151	37-611 37-614
13. Wisconsin Protective Coatings	Plastic 7118A	7118B
14. Magnolia Plastics Inc.	6061A 6063A	6061B 6063B
15. Dennis Chemical Co.	6805	EF-7
16. Dow Chemical Co.	DER 732	DER 337 DEH 14
17. Shell Chemical Co.	Epon 872-X-75 Epon 828	Agent U

TABLE 14

SCREENING FOR A FLEXIBLE EPOXY

Film No.	Resin	Hardener	Cured Film Thickness	Adhesion to Mylar	Flexibility	Cure Time
1	Bakolite ERL-2774	ZZLA-0822	13 mils	Very Good	Good	< 24 hours
2	ERL-2774	ERL-2793	20 mils	Poor	Poor	< 24 hours
3	ATLAS 3-30CN	164-087	17 mils	Very Good	Good	24-48 hours
4	ERL-2774	ZZL-0845 ZZL-0822	10 mils	Good	Fair	24-48 hours
5	General Mills 185	250	15 mils	Good	No Good	24-48 hours
6	General Mills 185	140	10 mils	Good	Fair	24 hours
7	Iso-Chem R-1249	AEP				> 5 days
8	Iso-Chem 407	13	5 mils		Good	48 hours
9	American Cyanamide BR93A	BR9313	ab.10 mils	Good		48 hours
10	Waldman 2000	X-2469	10 mils	Fair	Brittle	> 48 hours
11	Waldman 2000	125	10 mils			> 5 days
12	Thiokol Tripox E	LP-3 EH-330	5 mils		Brittle	
13	DOW DER 732	DER-331 DEH-14	12 mils		Brittle	> 5 days
14	Magnolia Part A-6061	Part B-6061	15 mils	Fair	Good	> 48 hours
15	Magnolia Part A-6063	Part B-6063	14 mils	Fair	Good	48 hours
16	Dennis 6085	EF	6 mils	Fair	Good	48 hours

TABLE 14 (Cont'd)

SCREENING FOR A FLEXIBLE EPOXY

Film No.	Resin	Hardener	Cured Film Thickness	Adhesion to Mylar	Flexibility	Cure Time
17	Reichhold Epouf 37-151	37-614	30 mils	Good	Fair	< 48 hours
18	Epotuf 37-135	37-611	20 mils	Fair	Fair	48 hours
19	FMC Oxiron 2000	Chlorendic Anhydride	20 mils			> 7 days
20	Ciba Ardalite 502	Pentamid 825				
21	Wisconsin Protective Coatings Plastite 7118A	7118B				
22	Epon 872-X-75	Agent U	20 Mils	Good	Very Good	< 24 hours

TABLE 15

UNION CARBIDE FORMULATIONS WITH 2% CELLOSOLVE ACETATE SURFACTANT

Film No.	1	2	3	4	5	6*	7*
Parts ERL 2774	100	100	100	100	100	100	100
Parts ZZL 0822	12.5	- -	10	25	- -	- -	25
Parts ZZL 0845	- -	- -	- -	- -	80	80	- -
Parts ERL 2793	12.5	25	15	- -	- -	- -	- -
Film Thickness Mils	- -	18	11	9	9	- -	- -
Cure							
24 hours	Tacky	Tacky	Tacky	Tacky	Tacky	Cured	Cured
48 hours	"	"	"	"	"		
1 week	"	"	"	"	"		
2 weeks	"	"	"	"	"		
Flexible							
24 hours	Yes	Yes	Yes	Yes	Yes		
1 week	Yes	No	No	Yes	Yes		
2 weeks	No			No	No		
Appearance	Good	Good	Good	Good	Good	Fish Eyes	Orange Peel

* Control, No surfactant

TABLE 16

EFFECT OF OTHER SURFACTANTS ON UNION CARBIDE RESINS

Film No.	11	14	15	17
Parts ERL 2774	100	100	100	100
Parts ZZ1 0822				
Parts ZZL 0845	50	80	80	80
Parts ERL 2793				
Film Thickness	7	20	12.5	20
Cure				
24 hours	Tacky	Tacky	Tacky	Cured
48 hours	"	"	"	"
1 week	"	"	"	"
2 weeks	"	"	"	"
Flexible				
24 hours	No	Yes	Yes	Yes
1 week	No	Brittle	No	Yes
2 weeks	Brittle	Brittle	No	Yes
Appearance	Large Fish Eyes	V. Good	Orange Peel	Good
% Surfactant	2% Cell.Acetate[1]	0.5% PC 1244[2]	1% SR-82[3]	0.5% AntiFoam A[4]

(1) Worum Chemical Company
(2) Monsanto Chemical Company
(3) General Electric
(4) Dow Corning

TABLE 17

GENERAL MILLS FLEXIBLE EPOXY SYSTEMS WITH VARIOUS SURFACTANTS

Film No.	7a	7b	8	9	10	18
Genepoxy No.	185 (20p)*	185 (20p)	185 (20p)	185 (20p)	185 (20p)	525 (28p)
Versamid	140 (25p)	140 (25p)	140 (25p)	140 (25p)	140 (30p)	401 (21p)
Film Thickness (mils)	6.5	9.0	10.5	10.5	20.0	18.0
Cure						
24 hours	Tacky	Tacky	Tacky	Cured	Cured	Cured
48 hours	"	"	"			
1 week	"	"	"			
Flexible						
24 hours	Yes	Yes	Yes	Yes	Yes	Yes
1 week	No	No	No	No	Yes	Yes
2 weeks	Brittle	Brittle	Brittle	Brittle	Yes	Yes
Appearance	Fish Eyes	Good	Good	Fish Eyes	Good	Good
% Surfactant	- -	0.5% PC-1244	1% SR-82	2% BuOH	.5% PC 1244	- - -

* Parts

TABLE 18

EFFECT OF CARDOLITE ON VISCOSITY OF EPON 872-X-75 FORMULATIONS

Film Number	59	60	61	62	63	64	65
Parts 872-X-75	100	100	100	100	100	100	- -
Parts 828	10	10	10	- -	- -	- -	100
Parts Agent U	7.2	7.2	7.2	4.2	4.2	4.2	25
Other							
Cardolite	- -	5.0	10.0	10	20	40	20
Viscosity, cps	35-4000	2877	2492	2450	1540	850	4550
Cure Time	24 hrs	24 hrs	24 hrs +	24 hrs +	48 hrs +	1 week +	24 hrs
Flexible	Yes	Yes	Yes				No

TABLE 19

EFFECT OF TYPICAL REACTIVE AND NON-REACTIVE DILUENTS ON EPON 872-X-75 FORMULATIONS

Film Number	70	71	74	77	73	76
Parts 872-X-75	75	75	50	100	100	100
Parts 828	25	25	50			
Parts Agent U	10	10	2.4	7.2	4.8	4.8
Parts Agent T			12			
Other		Isoflexrez[1] 10		(2) A.G.E.10	(3) 1% Sag	1% Sag
Cardolite	10	10	10	5		
Acetone			10		20	7.5
Cabosil					0.5	
Viscosity cps	1750	3990	1120	840	210	420
Cure Time	24 hrs	24 hrs	24 hrs	24 hrs +	24 hrs	24 hrs
Flexible	Yes	Yes	Yes	Yes	Yes	Yes

(1) Isochem Resins Company
(2) Allyl Glycidyl Ether
(3) Union Carbide

TABLE 20

EFFECT ON VISCOSITY OF A.G.E. AND ISOFLEXREZ ON EPON 872-X-75 FORMULATIONS

Film Number	78	79	80	82	83
Parts 872-X-75	100	100	100	100	100
Parts 828			10		
Hardener	U 7.2	T-1 7.2	U 7.2	U 4.7	T 4.7
A.G.E.	10	10			
Isoflexrez			5.0	10	10
Viscosity, cps	1120	840	3600	4530	3150
Cure Time	24 hrs +	24 hrs +	24 hrs	24 hrs	24 hrs
Flexible	Yes	Yes	Yes	Yes	Yes

the Mylar film when sprayed at a high atomization pressure. That portion of the solvent which did reach the film probably evaporated very quickly.

A formulation was then developed which contained only non-reactive diluents which are commonly used in the spraying of paints, lacquers, etc. The formula selected, which will hereafter be referred to as Z-20-2, was as follows:

		Parts By Weight
Part A:	Epon 872-X-75	100.0
	Epon 828	10.0
	Beetle	3.9
	Methyl isobutyl ketone	24.0
	Poly-Solve EE	23.6
	Xylol	23.6
	Cabosil	2.2
Part B:	Epon Agent U	8.0

The above mixture, when properly sprayed, gave clear, uniform films which were pin hole and sag free. A Binks Model 62 spray gun with a 1 quart pressure cup was used to apply flexible films to the 2 foot diameter solar collectors. While fabricating a 10 foot diameter collector, two spray guns were employed simultaneously, drawing resin from a 2 gallon pressure pot.

2. Eight Inch Solar Collector

An eight inch set of rings was used from time to time to screen flexible layers and structural material candidates. Those materials tested were:

a. Flexible Epoxies,
b. Neoprene Foams,
c. Vinyl Plastisol, and
d. Polyester Rigidizing Resins.

a. Flexible Epoxies

While screening epoxies, numerous eight inch collectors were bench cured to establish the effect of different flexible resin systems on fabric show through, flexibility, and film appearance. The collectors were made by brushing on the resin to a thickness of about 25 mils and bonding on the structural material. The urethane resin was then brushed into the fabric structural material and cured in the atmosphere with water and triethylamine vapors. Table 21 summarizes the work on four of these collectors. It was decided after this preliminary investigation to concentrate on developing the larger solar collectors to eliminate scaling effects.

b. Neoprene Foams

Several eight inch collectors were bench cured utilizing light weight neoprene foams for the flexible bonding layer. These foams, obtained from the Rubatex Corporation of Bedford, Virginia, consisted of a sponge cellular material coated with smooth outer surfaces. In one case, Goodrich's Hycar 2100 X 20 produced an excellent bond between the neoprene and the Mylar. A Swift adhesive, Z-7423 produced a good bond between the neoprene and the nylon structural material.

TABLE 21

BENCH CURED EIGHT INCH SOLAR COLLECTORS

Run No.	Cushion and Structural Backing Materials			Resin System	Resin Catalyst	Results and Remarks
	1st layer	2nd layer	3rd layer			
J-117-1	Gen Epoxy 180 1 Versamide 140 1	Same	Used as bonding layer to Nylon	ADM urethane 1988-19	Water vapor and TEA	Show through from flute lines and drop threads. Fabric was only partly inflated. 0.28 lbs/ft^2.
J-121-1	Epon 872 100 Epon 828 10 Agent U 7.6	Same	Used as bonding layer to Nylon	ADM urethane 1988-19	Water vapor and TEA	Fish eyes. Pronounced flute line show through. Very good inflation. 0.28 lbs/ft^2.
J-125-1	ERL 2774 100 ZZLA 0822 26 ZZLA 0845 7	Same	Used as bonding layer to Nylon	ADM urethane 1988-19	Water vapor and TEA	Good surface. Faint flute line show through. No show through between flutes. 0.33 lbs/ft^2.
J-128-1	BR-93 A 2 BR-93-13 4	Same	Used as bonding layer to Nylon	ADM urethane 1988-19	Water vapor and TEA	Faint flute line show through. Wrinkles between flutes. 0.32 lbs/ft^2.

After pressurizing the foam-Mylar combination to a bubble, the smooth faces became crinkled and took a permanent set when the pressure was removed. These crinkle lines were evident in the reflective surface of the cured collector and would probably have become more pronounced upon packaging. The foam, however, did completely eliminate all fabric show-through as well as effects of rigidizing resin shrinkage.

c. Vinyl Plastisol

A commercially available vinyl plastisol was brushed on an eight inch Mylar bubble and heated in an oven to 230°F. It would not yet foam at this point. More intense heat provided by a heat gun caused the resin to foam. Although the foam did not seem to cause adverse surface effects, work was not continued on this type of material because of the difficulties which would be encountered in attempting to heat large areas of film to the high temperatures required to activate the foam.

d. Polyester Rigidizing Resin

Two eight inch collectors were rigidized in a vacuum using methyl ethyl ketone peroxide vapors to cure a polyester resin thinned with a polyacrylate reactive monomer. One advantage in using this monomer was that unlike styrene, it did not volatilize at the pressures (about 1 mm Hg) used in the experiment.

The cure seemed rapid where the greatest concentration of peroxide vapors contacted the resin. These areas were rigid in 1/2 hour. Partial cure had occurred over the balance of the resin. It was also noted that the fastest cure took place where the resin mass was greatest. A temperature of about 100°F, indicated by a thermocouple buried in the top skin of the nylon, was reached in less than 10 minutes. A higher exotherm would occur in areas of greater resin mass.

The overall surface of the two collectors was good and it appeared that the method could be applied to the cure of a two foot collector.

3. Two Foot Solar Collectors

The experimental two foot solar collector work is summarized in Tables 22 through 25. Table 22 surveys the early work which was done to establish bonding and resin impregnation techniques as well as to develop an optimum spray formulation for application of the flexible layer. Except for runs 8 and 9, the structural material and the urethane resin used in these experiments were developed under Contract No. AF33(657)-10409. The fabric consisted of two nylon faces separated by parallel rows of 5/8 inch drop threads.

These experiments demonstrated that the assembly fixture and lowering ring centered the structural material evenly on the tacky bonding layer and that vacuum impregnation resulted in a very even resin distribution. Run 6 describes the first collector fabricated by spraying the flexible layer. Each coat was allowed to cure 24 hours before applying the next coat.

TABLE 22

TWO FOOT SOLAR COLLECTOR EXPERIMENTS

Run	Reference and size	Flexible Layer Material	Parts	Bonding Procedure	Fabrication Pressure	Remarks
1	R-95-1 28 inch	Epon 872-X-75 Epon 828 Agent U PC 1244 Brushed on Mylar 400 g	100 10 7 0.6	Manually	- - - - - -	Atmosphere cured with H_2O and TEA. Poor surface, numerous wrinkles, and flute lines. Final weight was 0.25 lbs/ft^2. Urethane brushed on nylon.
2	R-100-1 28 inch	Epon 872-X-75 Epon 828 Pabosil Sag 470 Agent U Mist sprayed on nylon and brushed on Mylar	100 10 .5 2.0 7.0	Lowering ring	- - - - - -	Gored nylon centered well, coated nylon had folds and wrinkles. Could not be removed by stretching. Poor skin separation. Epoxy soaked through skin and trapped drop threads. Final wt. = 0.52 lbs/ft^2. Atmosphere cured urethane brushed on nylon.
3	R-106-1 28 inch	Epon 872-X-75 Epon 828 Cabosil Sag 470 Agent U Brushed three coats of 200 g each	100 10 .5 2.0 7.0	Lowering ring with pressure envelopes	- - - - - -	Pressure envelope worked well. No wrinkles and folds from nylon. Atmosphere cured. Urethane brushed on nylon.
4	L-67-1 24 inch	Epon 872-X-75 Epon 828 Cabosil Agent U Two coats brushed on nylon	100 10 1 7	manually	- - - - - -	Nylon was coated with epoxy while held to shape by pressurized film. Resin soaked through and prevented skin separation by inflation. Experiment discontinued.
5	Z-25-1 24 inch	Epon 872-X-75 Epon 828 Acetone Cabosil Sag 470 Sprayed	100 10 1.2 .5	manually	0.75 in.Hg.	Epoxy coating ran excessivly and was uneven. Experiment discontinued.

TABLE 22 (Cont'd)

TWO FOOT SOLAR COLLECTOR EXPERIMENTS

Run	Reference and Size	Flexible Layer Material	Bonding Procedure	Fabrication Pressure	Remarks
6	Z-27-1 28 inch	Z-20-2, sprayed four coats. 400g each	Lowering ring with pressure envelopes	0.75 in. Hg.	Vacuum impregnation worked well. Much wrinkling near edges, poor inflation. 0.35 lbs/ft^2. Atmosphere cure, 24 hours.
7	Z-31-1 28 inch	Z-20-2, sprayed four coats. 400g each	Lowering ring with pressure envelopes	0.75 in. Hg.	Vacuum impregnated, vacuum cured. Used 1000g H_2O and 100g TEA. Not cured one hour at 1mm Hg. Good cure after 10 hours. Poor surface. Weight = 0.27 lbs/ft^2. Used 800g urethane.
8	Z-32-1 28 inch	Z-20-2 to about 40 mils	Lowering ring with pressure envelopes. 5/8" fluted dacron.	1/8 in. Hg.	Vacuum impregnated 800 grams resin with 5% DMLA. Vacuum cure 3 hours at 1mm Hg. Good surface but faint flute lines. Sent to Wright-Patterson Air Force Base.
9	Z-35-1 28 inch	Z-20-2 on dacron drawn to shape by vacuum. Two coats on Mylar.	Coated fabric lowered manually. Surfaces did not match. Poor bond.	3/8 in. Hg.	500 grams brushed. Atmosphere cured. No inflation as resin was poorly distributed. Good surface probably because urethane did not penetrate to the lower face.

The collectors in runs 2, 4, and 9 were attempts to coat the lower face of the structural material with a layer of flexible epoxy to prevent soak-up of the rigidizing resin. It was thought that shrinkage of the urethane during cure probably distorted the lower face of the fabric and translated through the flexible layer to the reflective surface. Applying a uniform coating to the fabric proved difficult and the results did not seem to show sufficient improvement to warrant further work.

A resin was developed which, when sprayed onto the structural material, cured rapidly and substantially reduced the porosity of the fabric. The purpose of this resin was to reduce the porosity of the fabric so the vapor pressure of the catalyst would inflate the fabric sandwich material.

In run 13, Table 23, the details of fabrication were worked out and fixed. This experiment resulted in the best overall structure to that date. The noticeable improvements were as follows:

1. A very good inflation of the structural material due to the porosity reducing resin.
2. A good overall contour.
3. Complete cure of the ADM urethane resin, 2106-49, after 2 hours.
4. Good bond between all of the composite parts.
5. Good visual reflectivity.
6. No fabric patterns between the flute lines, Figure 12.
7. A more rapid vacuum impregnation.

The first sample of the new structural materials were utilized in the experiments in Table 23. In general, the three dimensional fabrics were woven from either nylon or Dacron. The skin separation was nominally 3/4 inch and the parallel rows of drop threads were spaced 1/2 inch apart. No important improvements were apparent from these Series 2 samples.

Run 14 of Table 24 describes an experiment in which the flexible layer was modified to consist of two degrees of flexibility. A schematic illustration of this modification is shown in the sketch below.

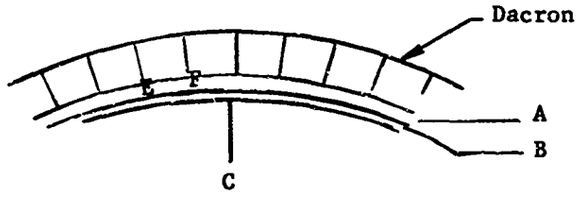

TABLE 23

DEVELOPMENT OF SOLAR COLLECTOR FABRICATING TECHNIQUES

Run	Reference and Size	Structural Material	Bonding Procedure	Fabrication Pressure	Rigidizing Resin	Remarks
10	Z-37-1 24 inch	Series 2 sample 1 nylon 2 coats porosity resin 2 coats Z-20-2	Lowered Manually	- - - - - -	ADM S-2022 Vacuum impregnated. Used 80g H_2O 8g TEA	3 hours vacuum cure at 1mm Hg. Faint flute lines. Weight = .35 lbs/ft^2.
11	Z-39-1 28 inch	Series 2 sample 3 dacron 2 coats porosity resin 4 coats Z-20-2 on dacron	Lowering ring, pressure envelopes. Bonding resin was brushed.	- - - - - -	ADM 2106-49 15% Ethyl acetate 80g H_2O 8g TEA	Resin set up fast because ethyl acetate contained H_2O. Poor inflation.
12	R-108-1 28 inch	Series 2 sample 1 nylon 2 coats porosity resin 1 coat Z-20-2	Lowering ring, Pressure envelopes.	.75" Hg.	ADM S-2022 .5% DMLA 800g resin 200g H_2O 20g TEA	2 hours vacuum cure. Good cure, fair surface. Weight = .62 lbs/ft^2. Poor inflation. Catalyst valves had clogged.
13	Z-46-1 28 inch	Series 2 sample 3 dacron Porosity resin on top skin only.	Lowering ring, pressure envelopes	1/8" Hg.	2106-49 800g 10% Ethyl acetate 100g H_2O 10g TEA	Good 2 hour cure. Weight = 0.57 lbs/ft^2. Best collector to date. Good inflation. See Figure 12.

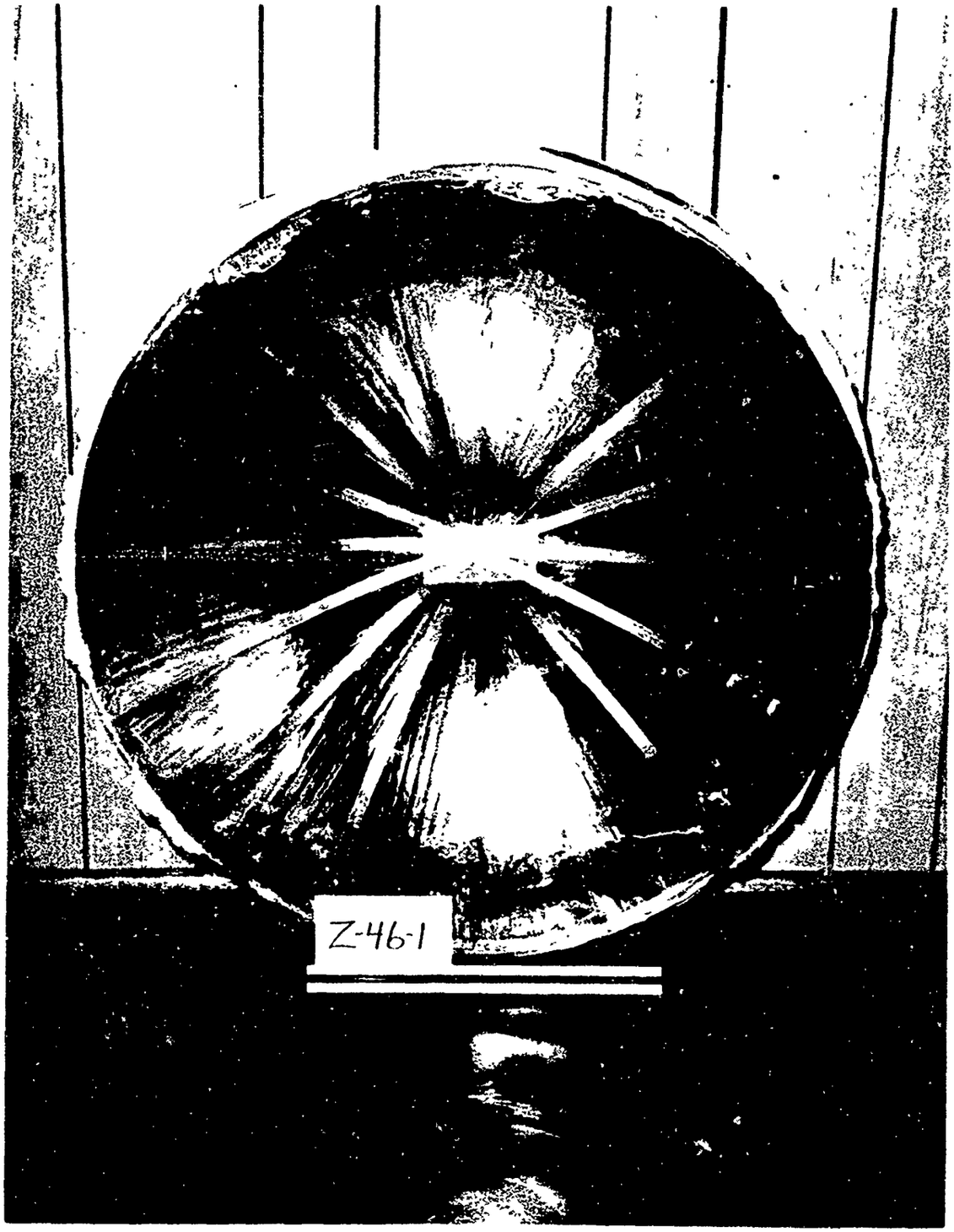

Figure 12 - Cured 28 Inch Diameter Solar Collector Model

TABLE 24

SOLAR COLLECTORS, VARIED FLEXIBLE LAYERS AND FABRICATION PRESSURES

Run	Reference and Size	Flexible Layer	Structural Material	Fabrication Pressure	Rigidizing Resin and Catalysts	Remarks
14	L-101-1 24 inch	First coat - 10 mils Z-20-2 + 20% 828. Second coat - 20 mils Z-20-2 without 828. Bonding coat - 10 mils	Dacron - Porosity resin both sides	1/8" Hg	#2106-49 + 15% ethyl acetate 1145 g	Good cure. Surface very good but worsened after three days. Poor bond between dacron and epoxy.
15	R-110-1 28 inch	Same as Run 14	Nylon - Porosity resin both sides	1/2" Hg	#2106-49 + 15% ethyl acetate	Good cure. Wrinkles in Mylar, otherwise good surface. See Figure 13.
16	Z-52-1 28 inch	Same as Run 14	Nylon - Porosity resin top skin only	1/8" Hg	#2106-49 800g 200g H_2O 20g TEA	Attempt to inflate flutes while bonding partially successful. Crease lines in Mylar. Weight = 0.58 lb/ft^2. See Figure 14.
17	Z-55-1 28 inch	Z-20-2 (See page 57)	Series 2 sample 2 Porosity resin top skin only	1/8" Hg	#2106-49 1000g 10% ethyl acetate 200g H_2O 20g TEA	Delamination of flexible layer, numerous crease lines. Weight = 0.57 lbs/ft^2. See Figure 15.
18	Z-57-1 28 inch	Same as Run 14 First 3 layers applied in 8 hrs.	Series 2 sample 3 Porosity resin top skin only	3/4" Hg	#2106-49 1150g 200g H_2O 40g TEA	Collector completed in 4 days instead of 8. Best surface to date. Weight = 0.49 lbs/ft^2. See Figure 16.

Layer C of the above sketch represents the 1 mil aluminized Mylar. Layer B consists of the spray formulation containing 20% Epon 828. Layer A is the flexible spray formulation with no rigid resin blended in. It was felt that the more flexible layer A, might absorb the waviness caused by shrinkage between points E and F. The somewhat rigid layer B would not translate the distortion. This approach, however, did not produce the desired results probably because of an insufficient difference in flexibility.

Different levels of skin stress of the Mylar film were investigated. It was found that an inflation pressure of .75 inches of Hg (maximum Mylar stress = 8000 psi) produced the best surfaces. No crease lines formed on the Mylar at this pressure such as developed on the Mylar when fabricating at lower pressures.

The collector described in Run 18, Table 24 was completed in 4 days. This was half the amount of time previously required and was accomplished by applying three coats of the flexible layer in 8 hours. A better bond between layers resulted because of the slight tack of the incompletely cured underlayer.

The experiments summarized in Table 25 were performed on a set of 24 inch rings. The Mylar and the structural fabric were not gored to a parabolic configuration. This fixture was used as a screening tool throughout the program. When the results showed promise, the experiment was repeated on the 28 inch fixture utilizing gored films and fabrics.

Runs 23 and 24, Table 25 and Figure 17, demonstrated that a filler in the flexible layer did not greatly improve the reflective surface, but considerable improvement was noted in Run 24 through the use of structural material with random scattered pile. After vacuum curing, this collector surface had areas that were nearly free from distortion. One obvious change was the absence of flutes lines brought about by replacing the rows of pile threads with a random scatter pattern. A better surface would have resulted had the 28 inch fixture with the lowering ring been utilized because that fixture would have applied the structural material more uniformly. This fact was proved in Experiment 2 described in the next section.

4. Solar Collector Experiments At Wright-Patterson Air Force Base

During the week of September 28, 1964, three solar collector composites were cured in a Wright-Patterson 4 x 5 foot vacuum chamber. Two of the collectors were fabricated and cured on the 28 inch diameter fixture. The first of these collectors utilized a Dacron fabric from Series 2 with the pile woven in parallel rows. The structural material for the second unit was Series 1, sample 1 nylon having the pile scattered at random between the faces. The third composite was fabricated over a 28 inch diameter fixture, supplied by the Air Force, which was equipped with a reflective surface contour measuring device. Series 1, sample 1 nylon was also used as the structural material for this experiment.

Thermocouples were located in various areas of the outer skin of the structural material. Heat was supplied by two infrared heat lamps. Tables 26, 27, and 28 describe the conditions of each experiment.

Figure 18 shows the arrangement of the vapor distribution system used in Experiment 1. The collector was placed vertically in the chamber so that any changes in the reflective surface during cure could be observed through a porthole. The infrared lamps which caused the two areas of delamination in the cured collector surface are also shown.

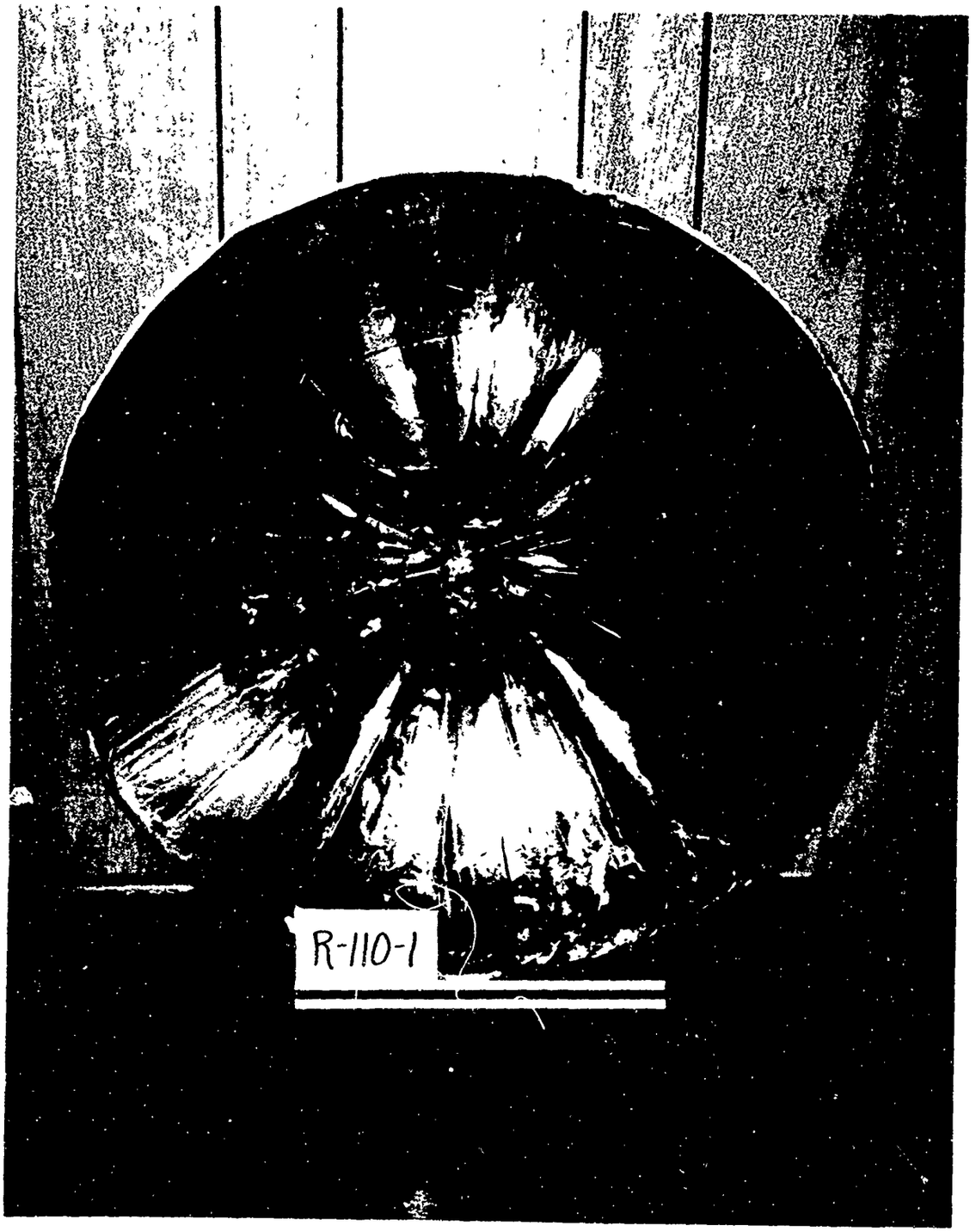

Figure 13 - Cured 28 Inch Diameter Solar Collector Model

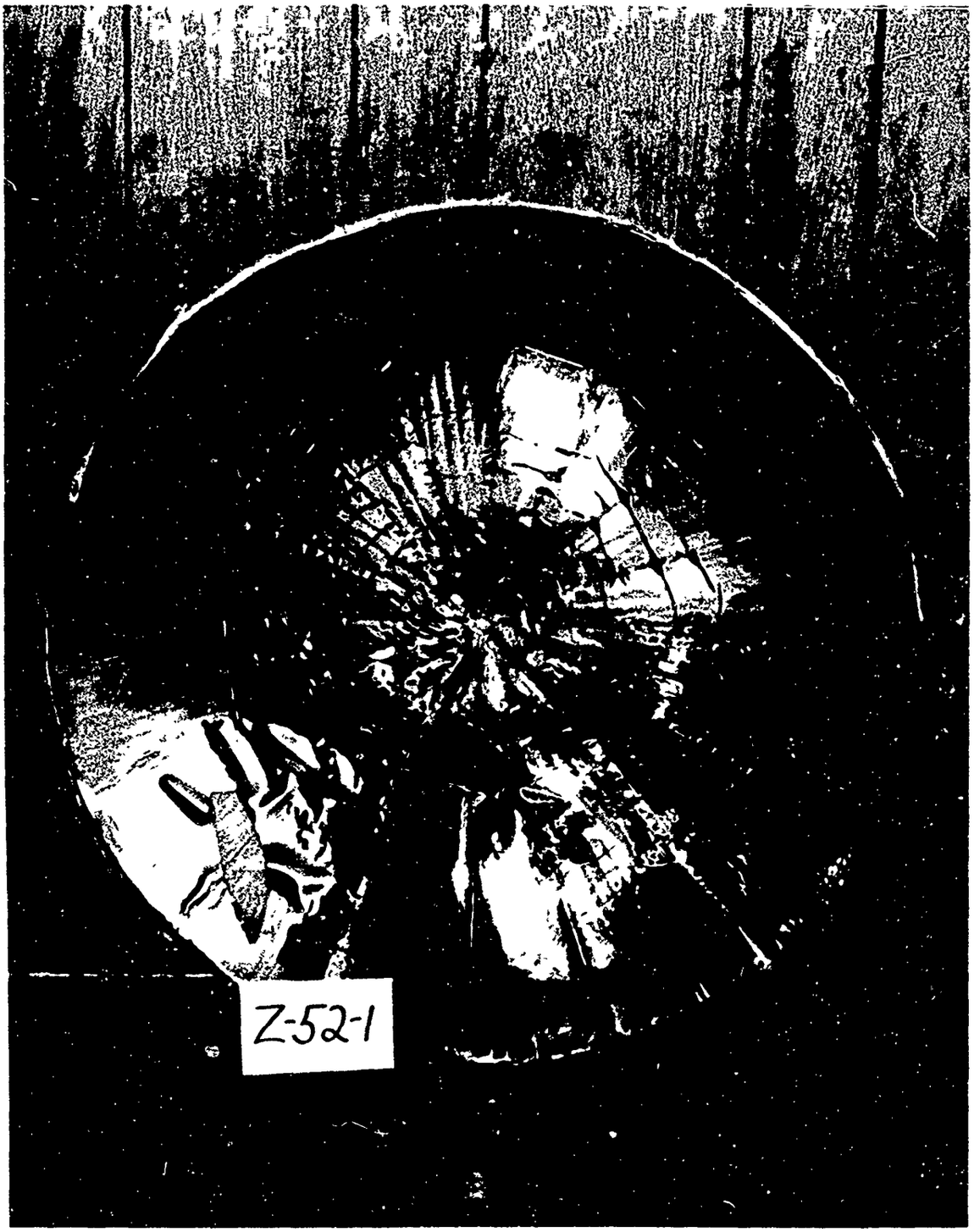

Figure 14 - Cured 28 Inch Diameter Solar Collector Model

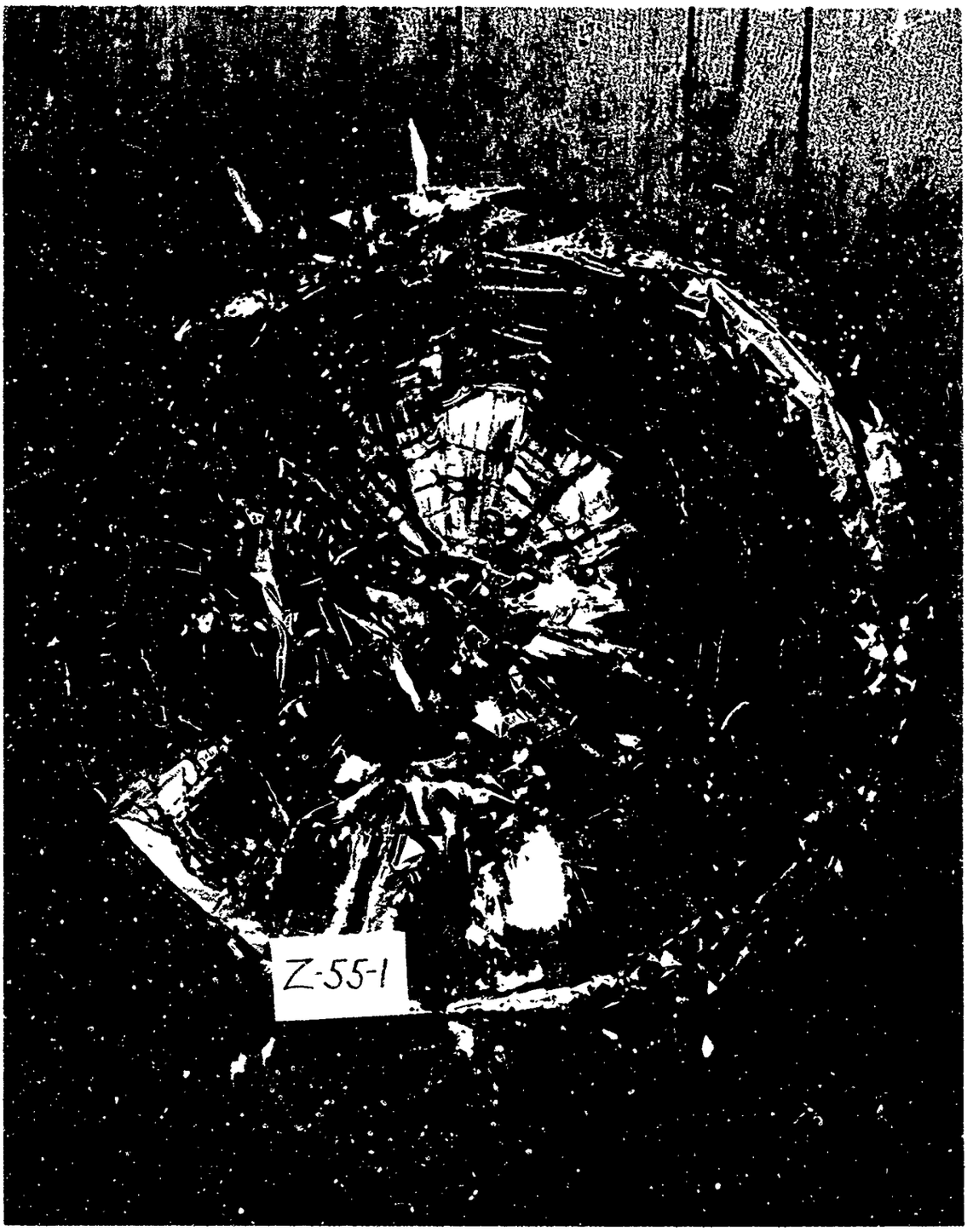

Figure 15 - 28 Inch Diameter Solar Collector Cured With Low Skin Stress

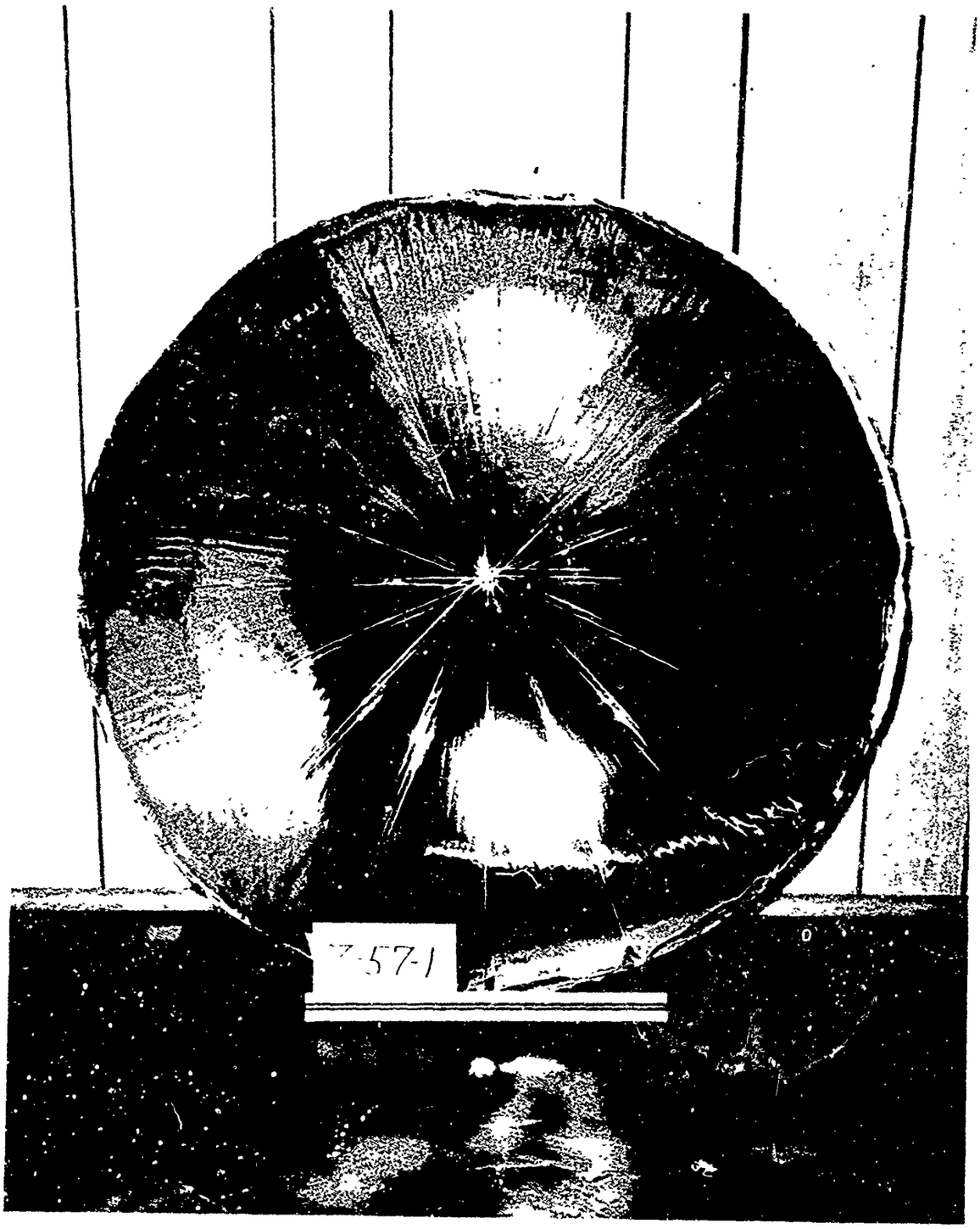

Figure 16 - 28 Inch Diameter Solar Collector Cured With High Skin Stress

TABLE 25

TWO FOOT SOLAR COLLECTORS WITH FLEXIBLE LAYER MODIFICATIONS

Run	Reference and Size	Flexible Layer	Structural Material	Fabrication Pressure	Rigidizing Resin	Remarks
19	Z-40-1 24 inch	Light coat Z-20-2 for adhesion. Three layers ADM flexible polyester.	Series 2 Sample 1 Nylon	- - - - - - -	ADM S-2022 vac. impregnate 0.5% DMLA. Vac. cured.	Polyester was under catalyzed. Only partially cured. Weight = 0.39 lbs/ft^2. Surface very distorted.
20	Z-45-1 24 inch	Light coat Z-20-2 Four coats flex. polyester filled with asbestine. 6 min. gel time.	- - - - - -	- - - - - - -	- - - - - - - - -	Discontinued. Flexible layer too thick. Surface had fine orange peel and curled up from shrinkage.
21	Z-41-1 24 inch	Same as #20 Three coats talc filled polyester.	Series 2 Sample 1 Nylon	- - - - - - -	ADM S-2022 Brushed on surface.	Atmosphere cured. Large waviness. Filler did not eliminate show through. Weight = 0.77 lbs/ft^2.
22	L-105-1 24 inch	Urethane Elastomer brushed on film. Set up in 5 min.	- - - - - -	- - - - - - -	- - - - - - - - -	After 24 hours, Mylar had excessive orange peel, bubbles and ripples. Experiment discontinued.
23	L-107-1 24 inch	Z-20-2 + 15% asbestine.	Series 2 Sample 3 Dacron Porosity resin top skin only.	.75 in. Hg. 1.0 in. during vacuum cure.	2106-49 + 15% Ethyl acetate vacuum impreg.	Filler did not eliminate all show through. Surface pattern had broad waviness. Weight = 0.61 lbs/ft^2. See Figure 17.
24	L-108-1 24 inch	Z-20-2 + 15% asbestine	Series 1 Sample 1 Nylon (random scatter)	.75 in. Hg. 1.0 in. during vacuum cure.	2106-49 + 15% Ethyl acetate Vacuum impreg.	A portion of surface was probably the best to date.

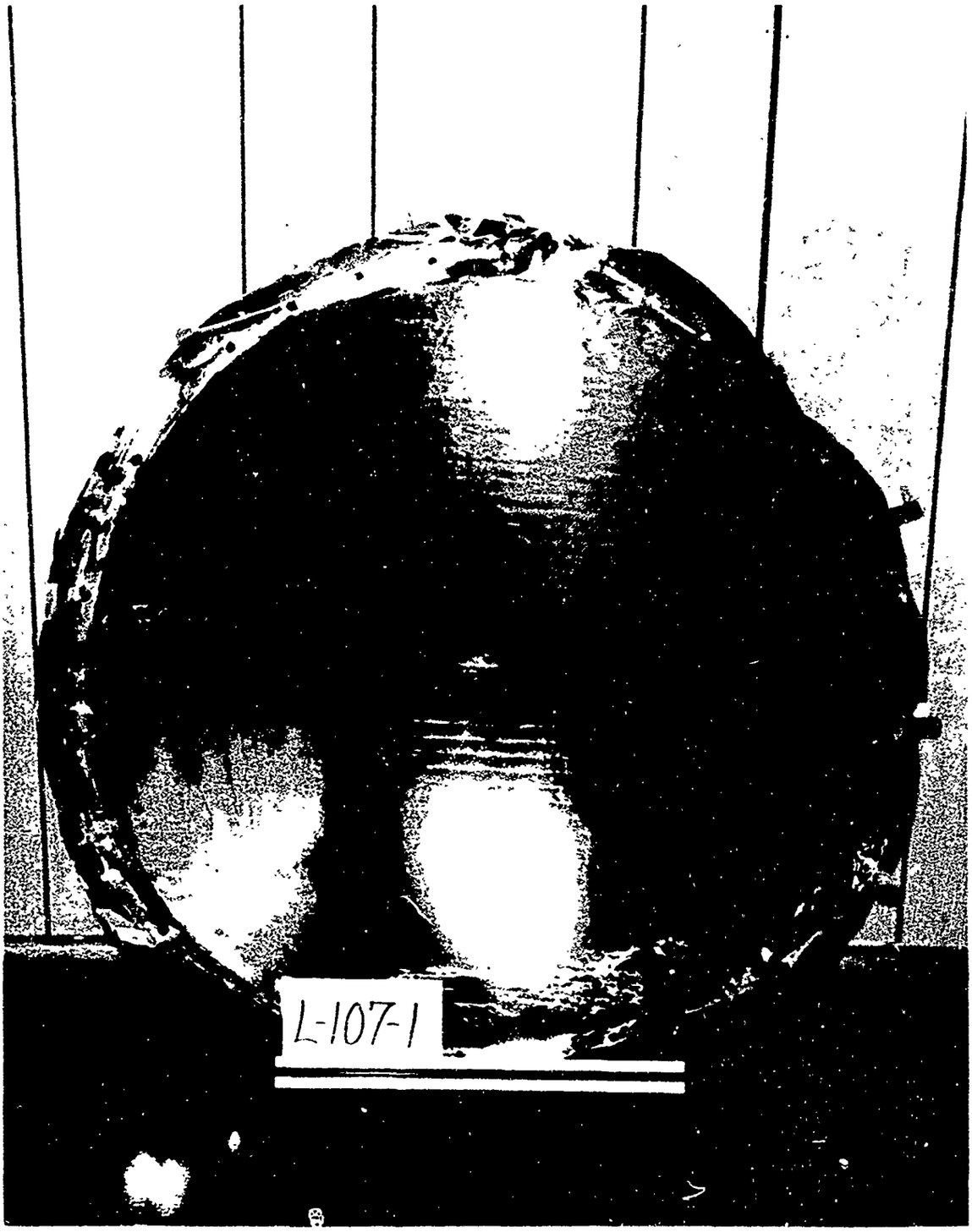

Figure 17 - Cured 24 Inch Diameter Solar Collector Model With Fillers In Flexible Layer

TABLE 26

FIRST SOLAR COLLECTOR EXPERIMENT AT WRIGHT-PATTERSON AIR FORCE BASE

Time	Chamber Pressure (Microns)	T_2 °F	T_3 °F	T_4 °F	T_5 °F	Remarks
9-30-64						
1200						Start Pump down
1215	500	20	10	45	55	
1235	1000 +	32	20	40	40	
1300	1000	40	25	40	40	
1315						Water and amine on
1320	600	40	25	37	40	
1335	1000 +	43	40	43	40	
1351						Heat lamps off and on 20-30 sec.
1354	1000 +	50	65	50	40	
1404	1000 +					Two areas of delamination.
1425		47	53	53	50	Water off

Inflation pressure kept at 1 inch Hg.

Thermocouple Positions

T_2 = In material, near cold wall

T_3 = In material, away from cold wall

T_4 = On catalyst supply pipe near cold wall

T_5 = Chamber atmosphere

TABLE 27

SECOND SOLAR COLLECTOR EXPERIMENT AT WRIGHT-PATTERSON AIR FORCE BASE

Time	Chamber Pressure	T_2 °F	T_3 °F	T_4 °F	T_5 °F	Remarks
9-30-64						
1310						Start Pump Down
1315	500 microns	25	25	42	40	
1330	750 microns	35	35	45	50	
1335						Cold wall on
1400	350 microns	35	-5	35	35	
1420		55	15		40	Wire came off surface at T_4.
1430	170 microns	60	5		40	
1440	150 microns	60	15		40	diff. pump on.
1445	7×10^{-4} mm Hg	65	15		30	
						diff. pump off.
1500	325 microns	50				A leak in collector prevented a better vacuum.
1502		60				Water and amine on
1510	360 microns	55	20		40	
1547	1000 + microns	75	45		40	
1643	1000 + microns	50	20		45	H_2O off
10-1-64						
0830	500 microns	50	50		50	

Inflation pressure kept at 1 inch Hg.

Thermocouple Positions
T_2 = In material, away from cold wall
T_3 = In material, near cold wall
T_4 = In material, near right center edge
T_5 = Chamber atmosphere

TABLE 28

THIRD SOLAR COLLECTOR EXPERIMENT AT WRIGHT-PATTERSON AIR FORCE BASE

Time	Chamber Pressure	T_2 °F	T_3 °F	T_4 °F	T_5 °F	Remarks
10-1-65 1425						Start Pump Down
1427	350 microns					(C.S. 1*)
1440	350 microns	25	25	25	50	
1442						Diff. heaters on. Cold wall on.
1453	250 microns	15	20		40	
1500	5×10^{-4} mm Hg					Diff. pump on
1505		5	35	5	40	(C.S. 2)
1537						H_2O and amine on. Heat lamps off and on.
1545	5 microns	25	60	10		
1615	1 micron	30	50	15		
1630	6×10^{-4} mm Hg	30	50	15		(C.S. 3)
1645	5×10^{-4} mm Hg					H_2O amine off
1700	4.9×10^{-4} mm Hg	30	50	0		
1730	5×10^{-4} mm Hg	30	50	0	30	(C.S. 4)
2000						(C.S. 5)
10-2-64 0800						(C.S. 6)

Inflation Pressure kept at 3/4" Hg.

Thermocouple Positions
T_2 = In material, near cold wall
T_3 = In material, away from cold wall
T_4 = In material, near right center edge
T_5 = Chamber atmosphere

* C.S. Contour Sweep

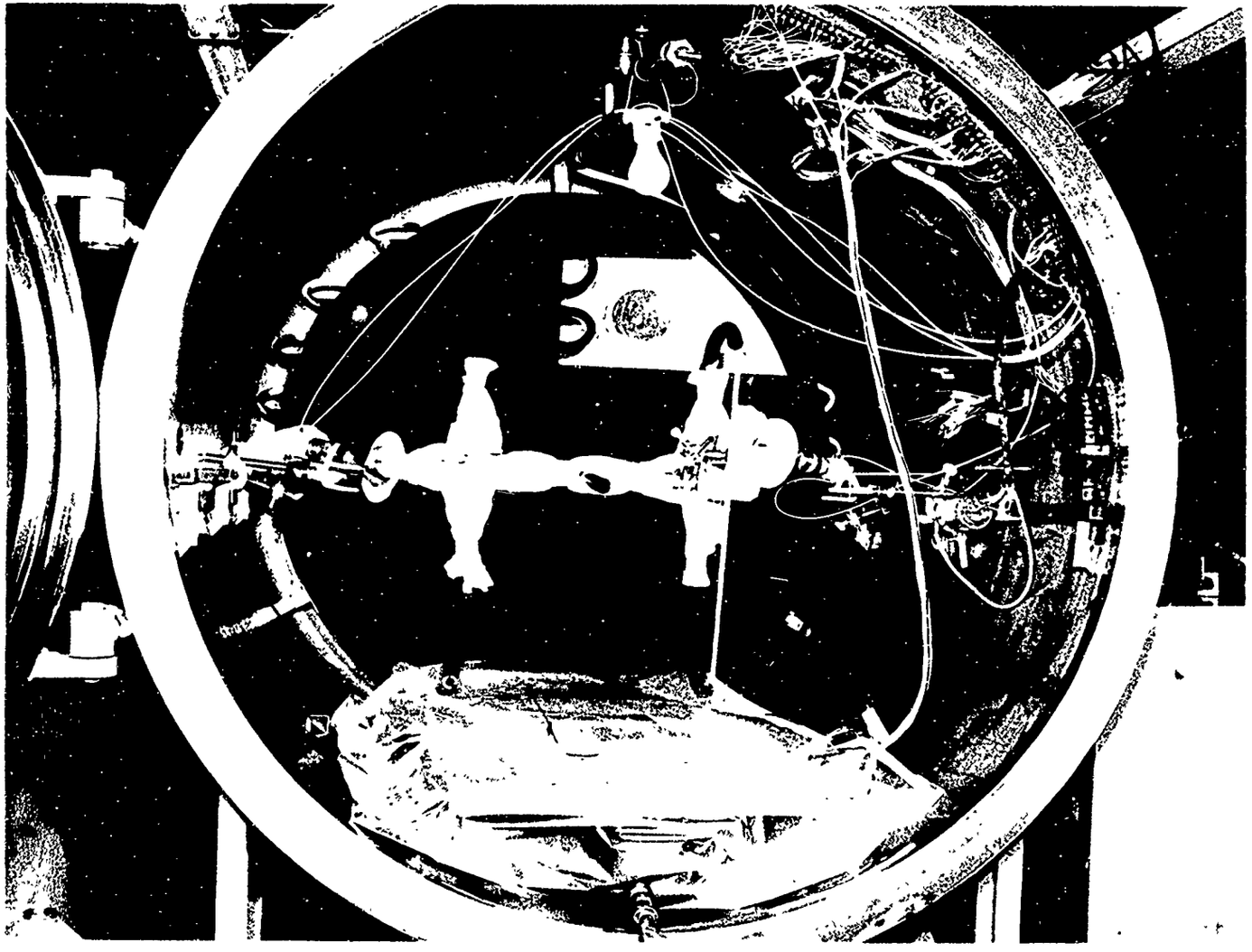

Figure 18 - Vapor Distribution System For WPAFB Experiment 1

These lamps maintained a moderate temperature on the structural material when the cold wall was in use. The quality of the reflective surface was equivalent to previous best efforts. Twenty-four hours after cure, effects of shrinkage were becoming evident. Figure 19 shows, the ability of this collector to ignite paper.

The unimpregnated composite used in Experiment 2 is shown in Figure 20. This figure demonstrates the flexibility of the structure and some of the valves used for catalyst vapor distribution. The impregnated composite, ready for cure in the chamber, is shown in Figure 21, and the reflective surface after cure is shown in Figure 22. This collector had the best reflective surface to that date. This experiment demonstrated that the structural material with the random scattered pile resulted in a better overall surface than the fabric with the parallel rows of pile.

Figure 8 gives a comparison between collectors fabricated with the two types of materials. The collector at the right is Experiment 1 (fluted core), and the one at the left is Experiment 2 (random scatter).

Figure 23 shows the 28 inch diameter collector which was assembled on the 38 inch fixture and measured for contour accuracy. The cover film is shown ready to be taped down and has valves inserted for resin distribution. The impregnated composite, Figure 24, was placed in the chamber and cured. It was then held at low vacuum for three days. Contour sweeps were made at the times shown in Table 28 and also after 3 days. Sweeps 1 through 5 showed no distortion. Sweep 6 indicated some distortion toward the outer edge of the collector. The internal pressure was released just prior to sweep number 4, indicating possible shrinkage during the interval between sweeps 5 and 6. The concentric lines on the collector surface, as seen in Figure 25, resulted from the sweeping. The creases seen on this surface are probably the result of accidently over-pressurizing while in the chamber.

5. Ten Foot Solar Collector

As previously indicated, a ten foot diameter solar collector was constructed with corporate funds. The composite was assembled at Viron utilizing a 14 foot diameter base plate and a 14 foot diameter gored aluminized Mylar film. Both of these items were government furnished.

The collector shown in Figure 26, was rigidized in a vacuum facility at Wright-Patterson Air Force Base, 4 December 1965. Rigidizing vapors were introduced through a flexible manifold which became an integral part of the cured structure.

6. Reflective Surface Effects

It has been stated in various places throughout this section, that some of the collectors had a very good reflective surface immediately after vacuum cure. Most of those surfaces, however, gradually wrinkled causing distorted reflectivity. In some cases small crease lines formed in the film and slowly increased in length.

This action can probably be attributed to residual solvent attack on the flexible layer causing separation of the reflective film. Two sources of residual solvent are apparent: (1) The flexible epoxy spray formulation containing three active solvents, and (2) The rigidizing urethane resin which contains a chlorinated solvent, 1,2-dichloroethane in addition to butyl acetate.

Figure 19 - Demonstrating The Concentration Effect Of A 28 Inch Diameter Solar Collector Model

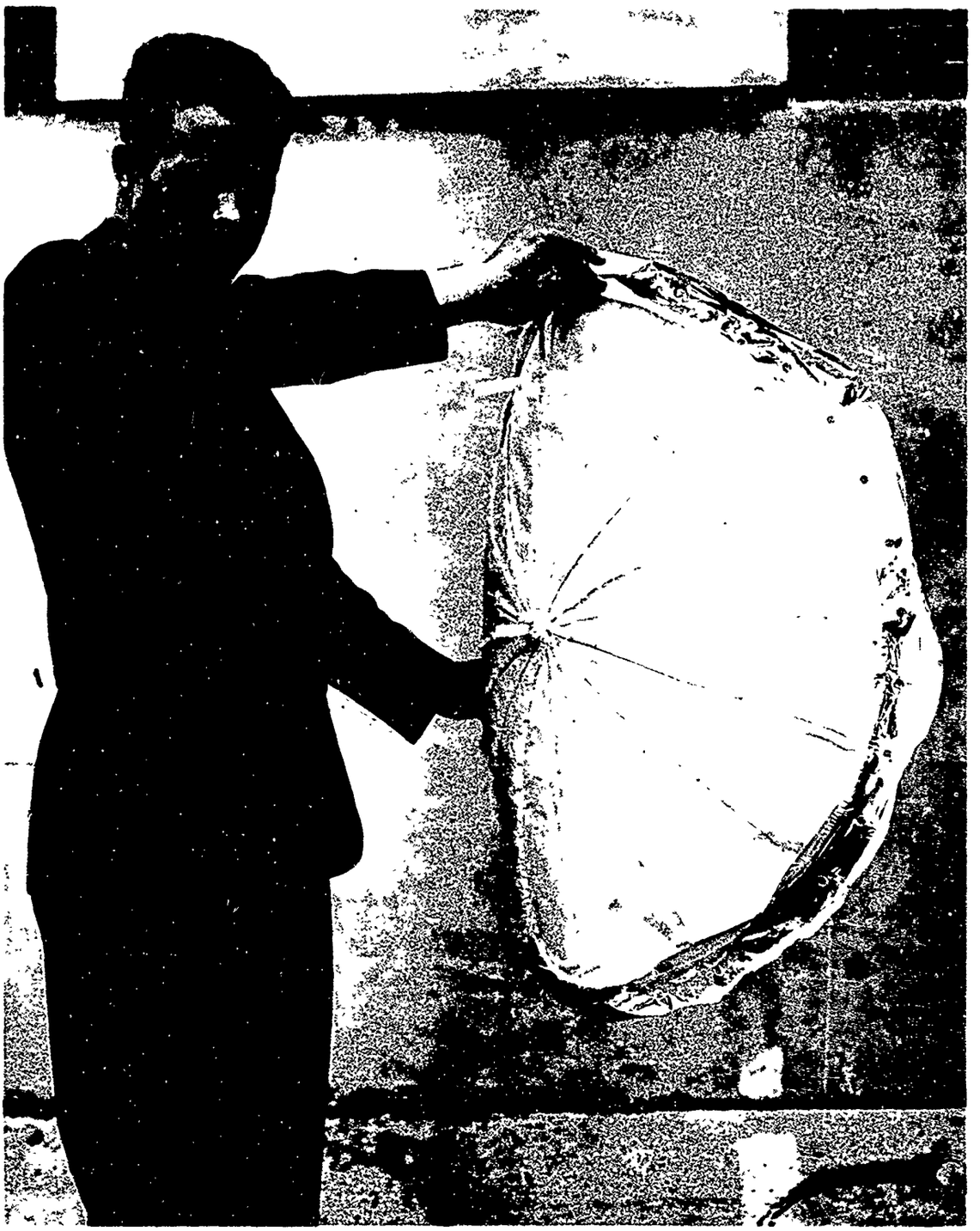

Figure 20 - 28 Inch Diameter Solar Collector Model Before Resin Impregnation

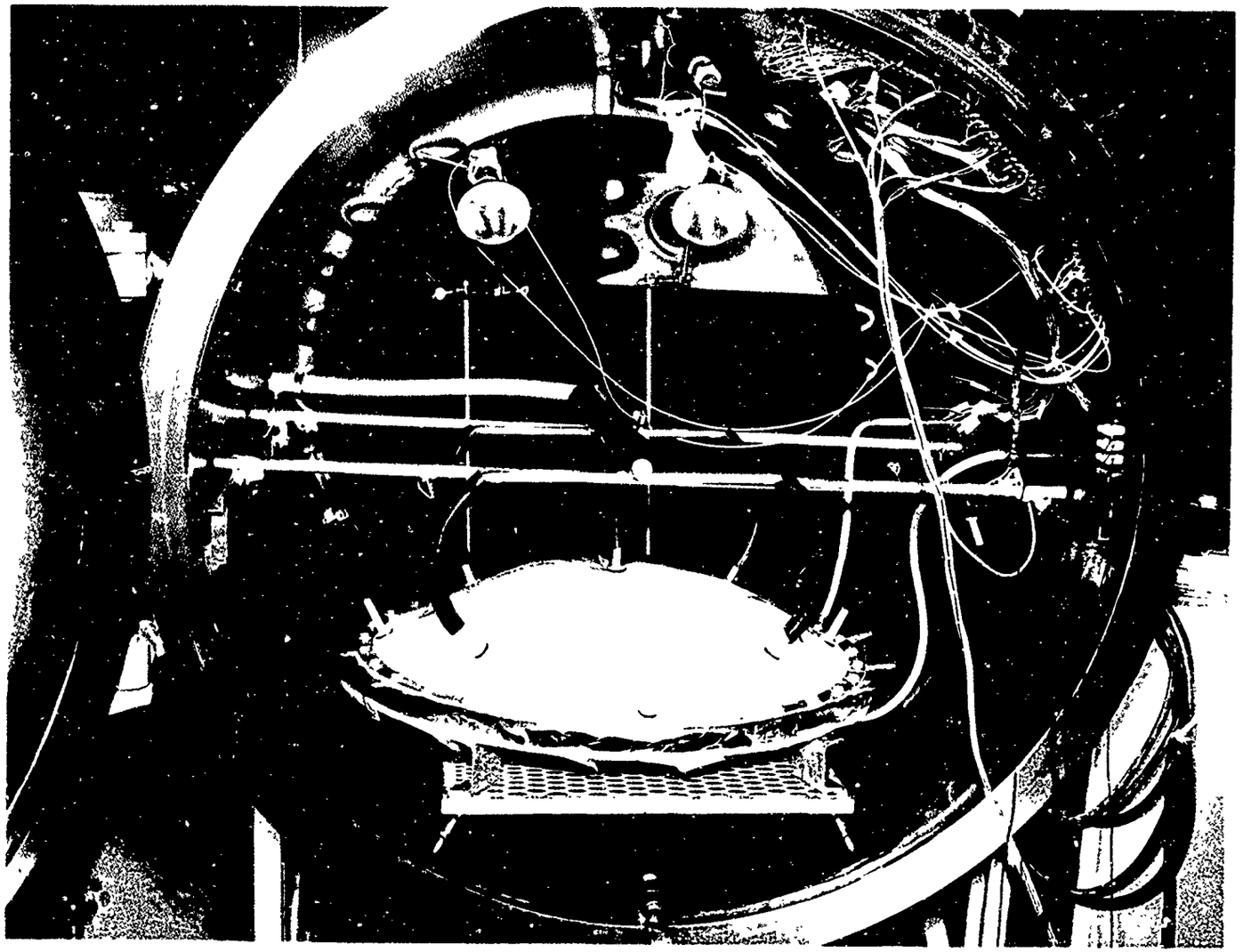

Figure 21 - 28 Inch Diameter Solar Collector Model Ready For Vacuum Cure

Figure 22 - 28 Inch Diameter Solar Collector Model After Vacuum Cure

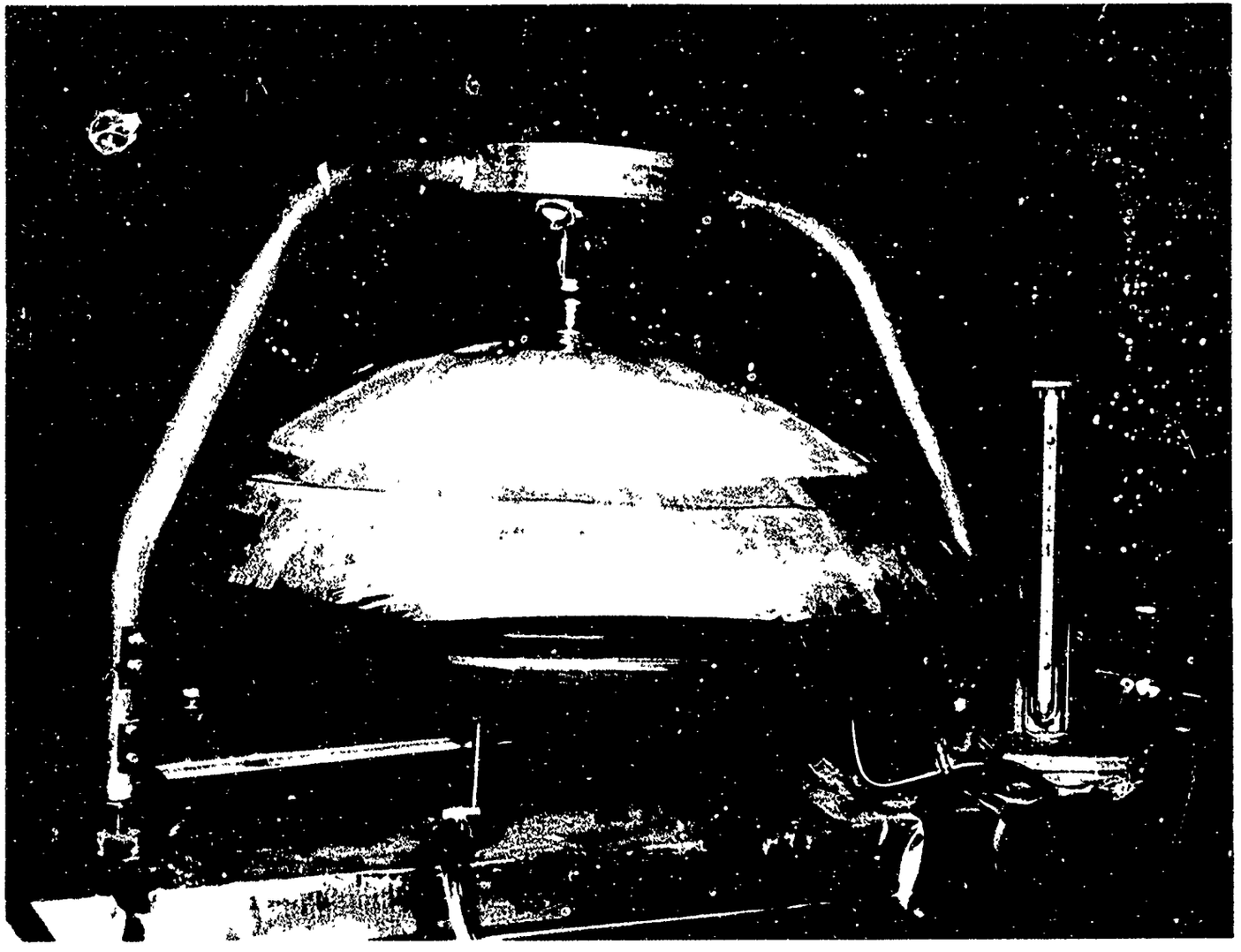

Figure 23 - 28 Inch Diameter Solar Collector Model Mounted On Contour Accuracy Measuring Fixture

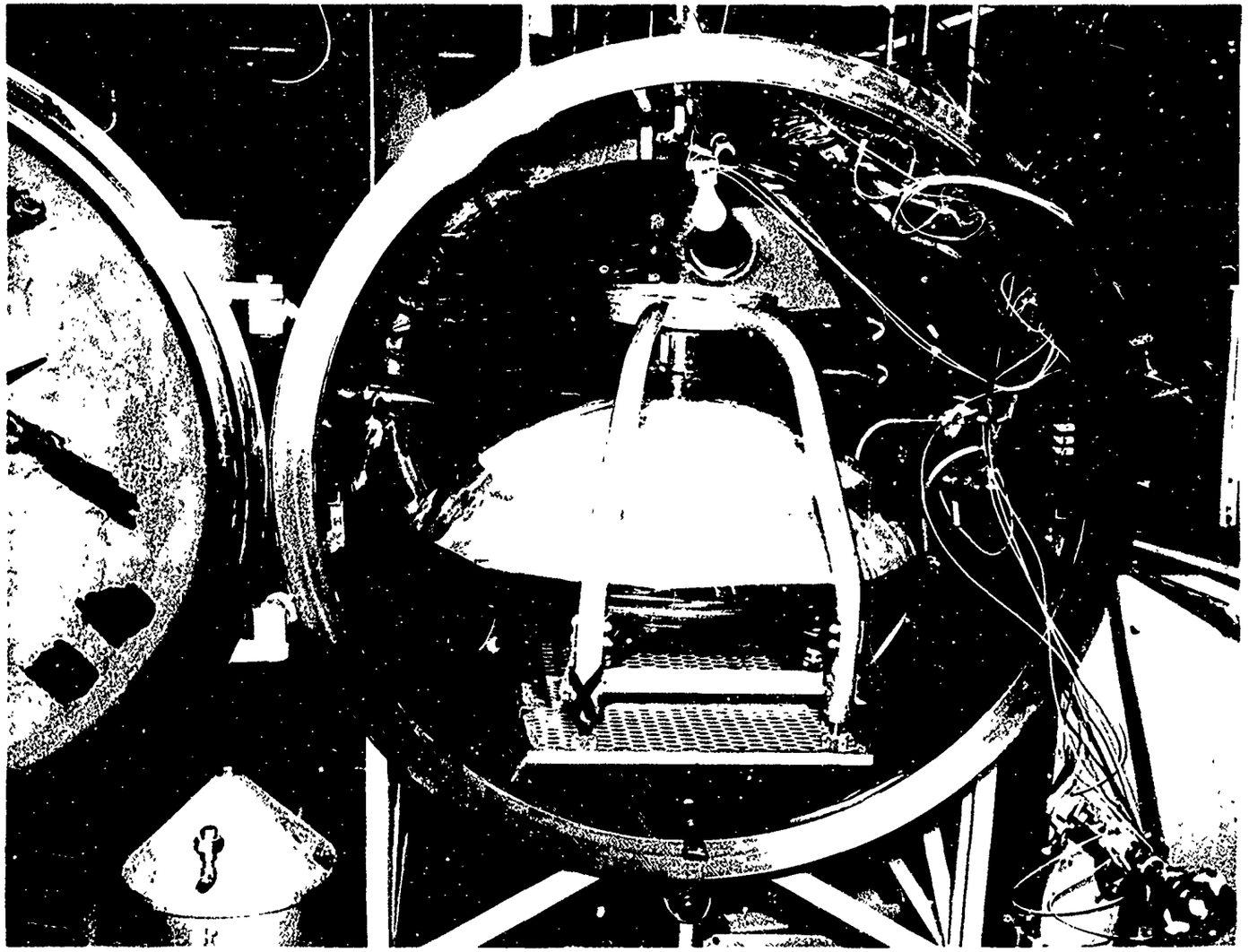

Figure 24 - 28 Inch Diameter Solar Collector Model And Contour Accuracy Measuring Fixture Installed In Vacuum Chamber

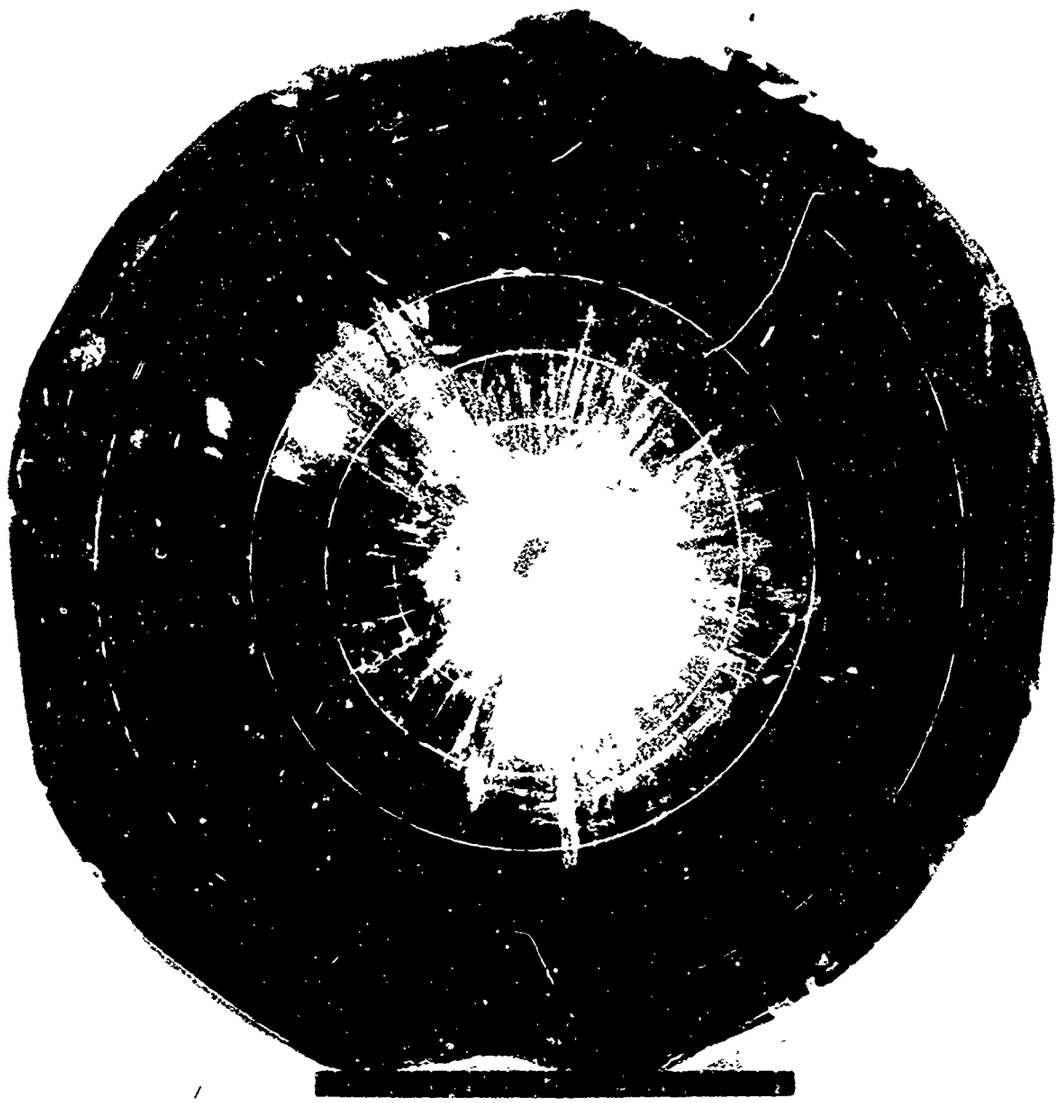

Figure 25 - 28 Inch Diameter Solar Collector Model After Vacuum Cure And Contour Measuring Sweep

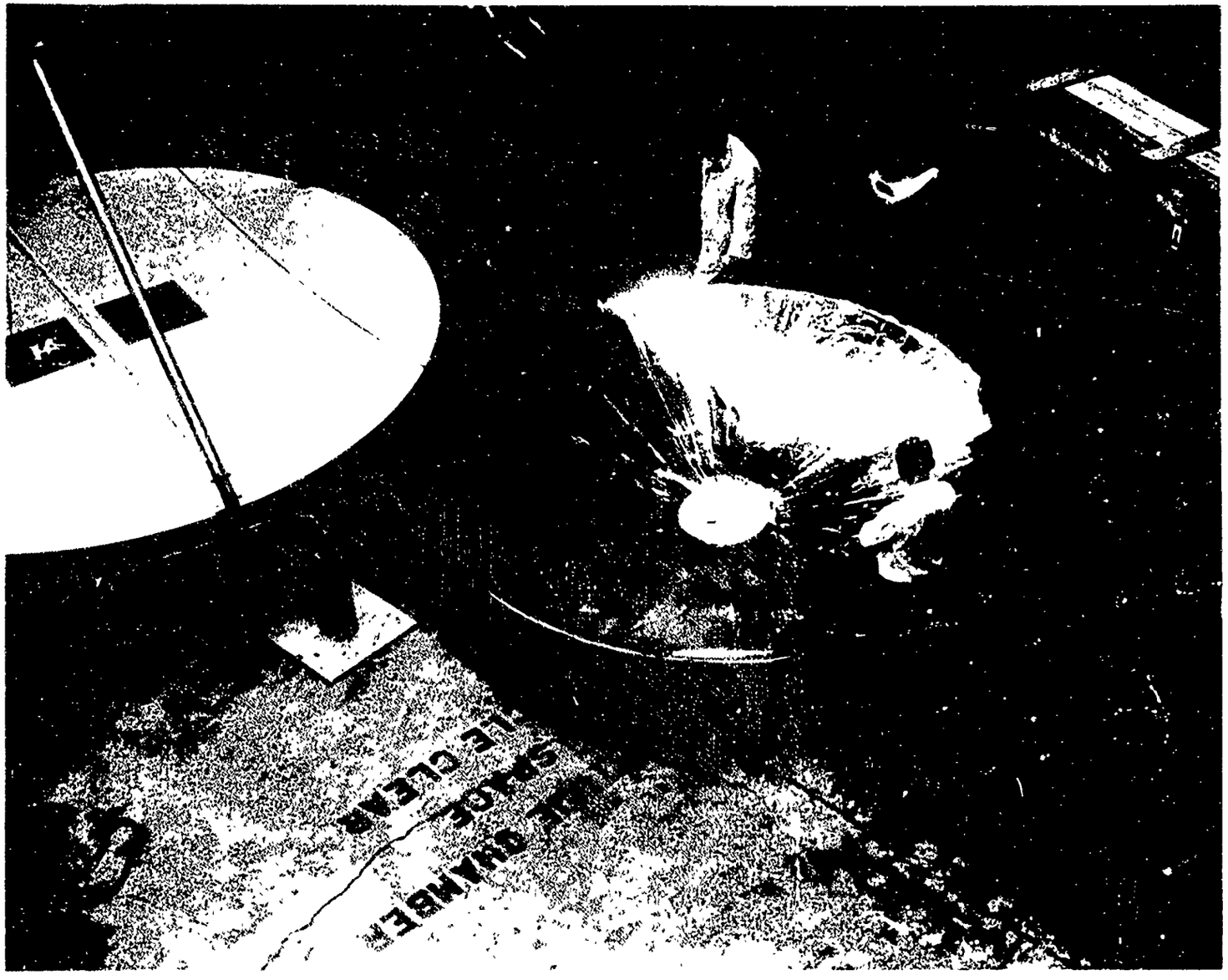

Figure 26 - Ten Foot Collector Rigidized At Wright-Patterson Air Force Base

SECTION 5

AEROSPACE MAINTENANCE DOCK

A. Concept and Description

An aerospace maintenance dock was selected as an appropriate object of a study to develop large size, inflatable, self-rigidizing, expandable structures. Such a structure could effectively be used as a shelter or repair depot in a remote region since it was to be entirely self-contained and easily deployed in a short time by two or three men. To accomplish this the total system was designed to consist of three parts:

1. The dock,
2. A portable inflation subsystem, and
3. A tie down subsystem.

The three parts were integrated into one package which could be air-lifted or otherwise transported to any destination. Thus, the deployment and rigidization of the dock could be accomplished at almost any terrestrial location.

1. The Dock

A semicylindrical configuration was selected for the dock since it was to be an inflatable structure. The half scale plan dimensions of the dock were 13 ft in diameter by 15 ft long. The floor and end walls were designed to be flat surfaces. A single door was provided in one end. This permitted a full width opening about one-half as high as the structure. A hinge across the top of the door allowed the door to be raised and lowered about this point and also to serve as a canopy.

The entire structure was fabricated from flat, woven fabric. The structure was essentially all fiberglass fabric except for a very few instances (e.g. the door hinge) in which a neoprene coated nylon fabric was used. All of the fabrics were seamed and joined by sewing. The fiberglass was fabricated into three dimensional, fluted core sandwich constructions for each of the load carrying components of the dock (the roof and end walls). Typically, the sandwich construction was characterized by continuous inside and outside facings separated by continuous webs. Generally, the webs were unidirectional thereby permitting the loads to be resolved in one direction only. This type of structural configuration gave an extremely good strength to weight ratio and was easily fabricated from the relatively inexpensive flat fabric. In addition, this type of construction readily permitted the various radii of curvature to be incorporated into the fabrication of the roof which in turn simplified the inflation of the dock.

The floor of the aerospace maintenance dock was constructed of a single layer of woven fiberglass fabric. Its primary function was to serve as an inflation pressure barrier and moisture barrier.

The dock was provided with a continuous set of catenary load tapes along the bottom edge of each side. These tapes were to be periodically attached to ground anchors and used to hold the semicylindrical shape of the dock during inflation and to resist uplift and overturning wind forces after the dock was

rigidized. See Figure 27 for front and side elevations of the dock illustrating the preceding description.

2. Portable Inflation Subsystem

The primary function of the portable inflation unit was to deploy (unfold) and hold the expanded shape of the dock until the rigidizing resin was cured. The inflation unit accomplished this by conducting large volumes of air into the dock and thereby internally pressurizing it. The other function of the portable inflation unit was to conduct heat, water vapor, and triethylamine catalysts into the dock to promote a more rapid resin cure. This was efficiently accomplished by introducing these catalysts into the intake of the inflation unit along with the air used to pressurize the dock.

The components of the inflation subsystem consisted of a gasoline engine, an axivane type blower, a blow torch heat source, a container of water and triethylamine catalyst, and miscellaneous items such as a framework on which the various items were mounted and a plenum chamber to direct the inflation vapors from the blower to the dock. All of the items selected for the subsystem were lightweight which made the total unit portable. The unit was designed to be entirely self-contained which would make it operable even in the most remote regions.

3. Tie Down Subsystem

A tie down subsystem was necessary to stabilize the dock during inflation and after rigidization. This was accomplished by tieing each valley of the catenary load tapes on both sides of the dock to a ground anchor.

The load tapes were constructed of woven nylon webbing sewn directly to the woven fiberglass fabric of the dock roof. The ground anchors were an arrowhead type anchor that could be quickly driven into soil with an auxiliary driving rod and mandrel. A tie line connected to the anchor was tied to the valleys of the nylon catenary load tape. A second line located on the ground anchor permitted the anchors to be retrieved at will.

4. Development Of The Final Design

The final design of the inflatable, self-rigidizing aerospace maintenance dock developed logically from the results of various supporting studies related to the dock. These studies were directed mainly toward optimizing the structural material and configuration of the dock and developing deployment and fabrication techniques applicable to the dock. The remaining studies were directed toward improving techniques to package, resin impregnate, and rigidize large sized structures. Most of these latter efforts were completed after the termination of the contract and are not described in this report.

The primary function of the aerospace maintenance dock is that of a load carrying structure. For this reason, a large part of the research and development effort was expended in optimizing the structural material and configuration of the various components of the dock. This was begun with a definition of the wind and gravity loads applied to the dock and the associated bending moments and end loads present throughout the dock. A study was then initiated to determine the allowable stresses to use in designing the various components of the dock.

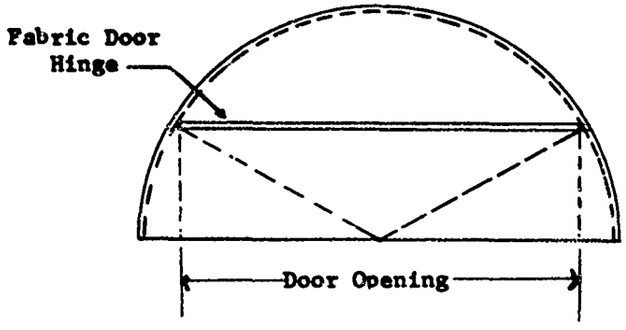

FRONT ELEVATION

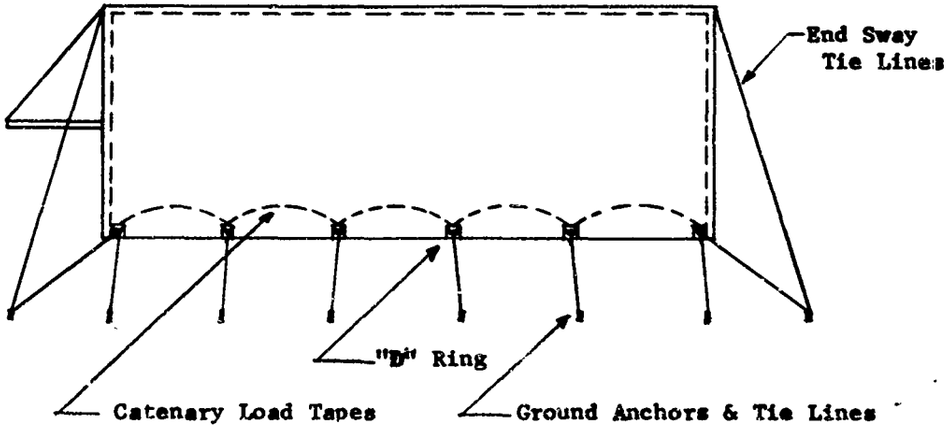

SIDE ELEVATION

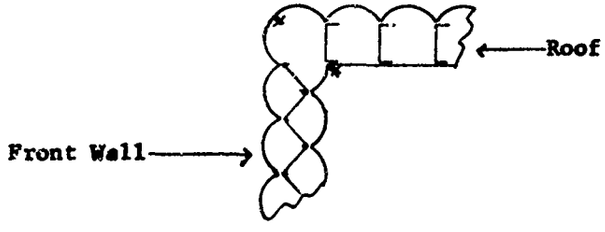

DETAIL OF SANDWICH CONSTRUCTION

DEPLOYED CONFIGURATION OF THE AEROSPACE MAINTENANCE DOCK

FIGURE 27

This study consisted of a survey of materials properties, the development of a theory of stress resolution in fiber reinforced composites, and the development of an optimized orthotropic sandwich section. With the conclusion of this study, enough background information was available to complete a stress analysis of the aerospace maintenance dock and select materials for the dock. However, as an inflatable structure, other studies were necessary to gain background information pertinent to deploying and fabricating the structure. These included a porosity study of dry and resin impregnated woven fabrics, a folding study to determine the technique that permitted a pressurized deployment of the dock, and fabrication studies which determined the handling and sewing techniques to be employed in the construction of the aerospace maintenance dock.

B. Design Loadings

1. General

The dock was designed for loads from two basic sources. These were a 100 mile per hour wind loading and a 30 lb per sq ft snow or earth load. The 30 lb per sq ft snow load nominally acts in a vertical direction only. However, for purposes of checking overall buckling instabiiity of the roof, the 30 lb per sq ft was assumed to act radially inward over the entire roof area. A safety factor of 1.5 was applied to all of the loads to give the ultimate design loads.

The above loads occur after the dock has cured. During erection and inflation of the dock, the wet seams are subjected to tensile loads created by the inflation pressures.

2. Applied Loads

a. Aerodynamic Loads

The dock was a 13 ft wide circular arch by 15 ft long, with a doorway in one of the end bulkheads. The length to diameter ratio of the dock was 15/13 = 1.15. Aerodynamic pressure coefficients taken from Ref. 1 for a length to diameter ratio of 1.0 were used as follows.

The static pressure head due to a 100 mph wind is,

$$q = \frac{V_{MPH}^2}{391} = \frac{100^2}{391} = 25.6 \text{ psf.}$$

The ultimate design static pressure is then,

$$25.6 \times 1.5 = 38.4 \text{ psf} \equiv .267 \text{ psi.}$$

A pure cross wind blowing at right angles to the cylindrical axis is angularly designated as $\alpha = 0^\circ$. A pure longitudinal wind blowing parallel to the cylindrical axis toward the door end is angularly designated as $\alpha = 90^\circ$.

As shown in Ref. 1, the external pressure coefficients over the roof area are approximately the same for wind directions of $\alpha = 0$ to $\alpha = 30^{\circ}$. However, the pressure coefficients over the end bulkheads vary considerably and the internal pressure varies with the position of the door and the amount of door air leakage. The internal pressure in the dock creates only an additional hoop tension in the roof arch. The end load stresses in the roof due to this additional tension are small compared to the bending moment stresses caused by the variance of the external pressure loads. Therefore, the roof chordwise pressure distribution plotted in Figure 28, for $\alpha = 0^{\circ}$, is only the external pressure coefficients.

The maximum lift and drag coefficients for the dock normal to the cylindrical axis, as given in Figure 15 of Ref. 1, based on the plan form area of the dock are:

$$C_L = -.42 \text{ and}$$

$$C_D = +.42.$$

The total ultimate aerodynamic lift and drag forces on the dock are then,

$$L = C_L\, q\, A = .42 \times 38.4 \times 15 \times 13 = 3140 \text{ lbs and}$$

$$D = C_D\, q\, A = .42 \times 38.4 \times 15 \times 13 = 3140 \text{ lbs.}$$

The cured dead weight of the dock was about 300 lbs.

The maximum loads on the dock tie-downs occur near the door end at the wind angle of $\alpha = 90^{\circ}$ with the door open. The longitudinal pressure coefficient distribution along the roof including an internal pressure coefficient of $C_p = +.7$ is plotted in Figure 28. By inspection the average pressure coefficient is about 1.6. The total lift force in this condition would then be,

$$L = 1.6 \times 38.4 \times 15 \times 13 = 12{,}000 \text{ lbs.}$$

The maximum net pressure on the back bulkhead occurs with the door open and $\alpha = 60^{\circ}$. From Figure 15 of Ref. 1, the net pressure coefficient is -1.1 (outward).

b. Gravity Loads

As stated in section 1 above, the snow or earth gravity design load was 30 psf. This load was taken both as a vertical load and also, as a separate condition, a uniform radial load inward.

These loads could be combined with the aerodynamic loads, but as will be shown later, this combined condition was not critical.

c. Inflation Loads

The maximum inflation pressure needed during the initial parts of the deployment was 5 inches of water. After 75 percent deployment, this pressure was reduced to 3 inches of water. The pressure was then reduced to about 1 inch of water during rigidization, which was the pressure load applied to the tie down anchors. The inflation pressure was not critical for tie down loads.

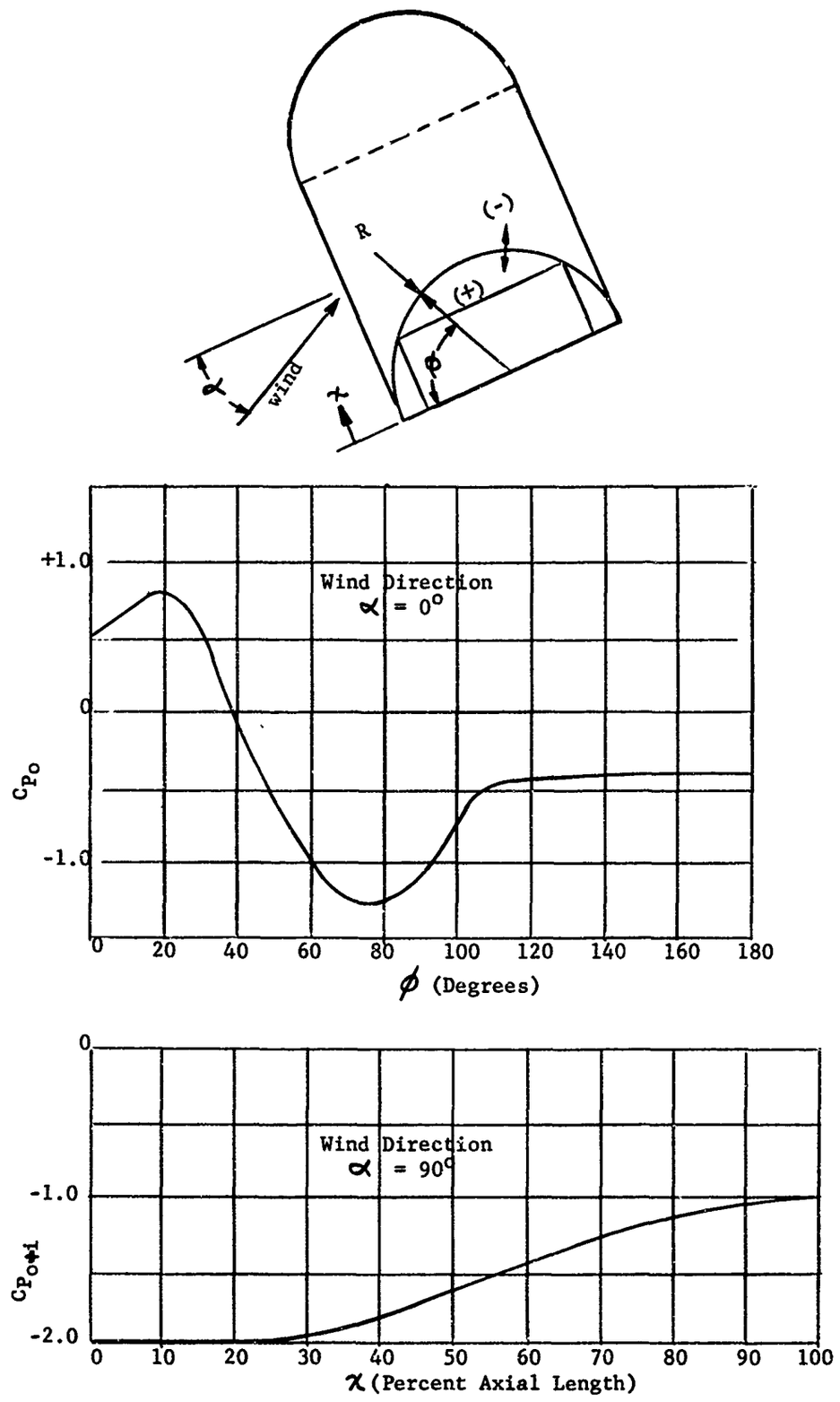

Figure 28 - Dock Roof Pressure Distribution Coefficients

3. Design Bending Moments and End Loads

The principal structural parts of the dock were the circular arch roof and the semi-circular end bulkheads. The dock was tied to ground anchors about 3 ft apart.

The aerodynamic and gravity roof loads on a quonset structure of this type would normally be partially passed out to the end bulkheads by membrane or vault action. However, the aerospace dock roof was designed as rectangularly fluted core sandwich construction with webs running only circumferentially. Therefore, while the cylindrically corrugated inflated faces of the sandwich gave good compression load carrying ability in one direction, the faces had low compressive load capacity in the other direction. The low compressive capacity in the longitudinal direction of the dock roof prevented any appreciable membrane type load transfer to the end bulkheads. Also, if the aerodynamic lifting loads were passed to the end bulkheads, they would then have to be brought back out to the tie-downs. Therefore, aerodynamic lift forces on the arch were resisted immediately by the tie-downs.

The door bulkhead was lightly loaded by any aerodynamic wind pressures due to the appreciable gap around the door edges that would develop under pressure loads. This gap allows the internal dock pressure to equalize with the external pressure in the door region. Therefore, the bulkhead aerodynamic pressures were assumed to be resisted entirely by the rear bulkhead. The rear bulkhead was an inflated, rectangularly fluted core sandwich construction similar to the roof construction. The webs ran in a vertical direction and therefore most of the bending stiffness was in this direction. The bulkhead was conservatively analyzed as a simple beam with a maximum span of 6½ ft. The two dimensional semi-circular plate action of the bulkhead was neglected as being of minor significance.

a. Aerodynamic Loads

(1) Dock Roof

The pressure loads from Figure 28 on a one inch wide section of the dock roof arch are illustrated below:

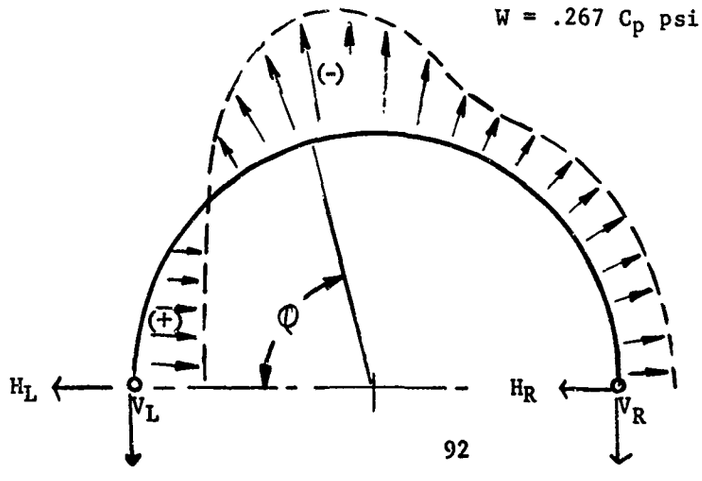

The arch was treated as a statically indeterminate structure with pin ends. The reaction loads and bending moments along the arch were found by the method of "least work". The mean radius of the arch for a 3 inch deep section was $78 + 1\frac{1}{2} = 79\frac{1}{2}$ inch. Therefore,

$H_L = +26.2$ lb/inch,

$V_L = V_R = +24.5$ lb/inch, and

$H_R = -3.6$ lb/inch.

The bending moment diagrams are plotted in Figure 29. The maximum ultimate bending moments were computed as:

B.M. = +250 inch lb/inch (Compression on outside fiber) and

B.M. = -150 inch lb/inch (Compression on inside fiber).

(2) Rear Bulkhead

The rear bulkhead was treated as a uniformly loaded beam with a span of 78 inches.

If $C_p = -1.1$ (outward):

then $w = C_p\, q = 1.1 \times .267 = .294$ psi

and Ultimate B.M. $= \frac{w L^2}{8} = \frac{.294 \times 78^2}{8} = 224$ inch lb/inch.

(3) Tie-Downs

The maximum tie-down load occurred at the second tie-down from the door end. This tie-down was the first one from the door end that was loaded by the full 3 ft tie-down spacing.

From Figure 28, for $x = \frac{3}{15} \times 100 = 20$ percent,

$C_p = -2.0$.

The ultimate load on the tie-down was then,

$L = C_p\, q\, d\, R = 2.0 \times .267 \times 36 \times 79\frac{1}{2}$

$= 1530$ lb.

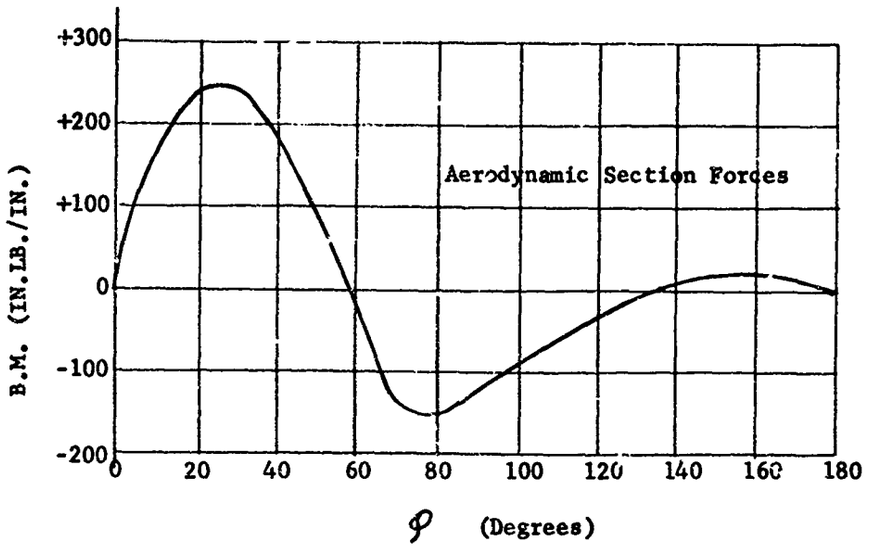

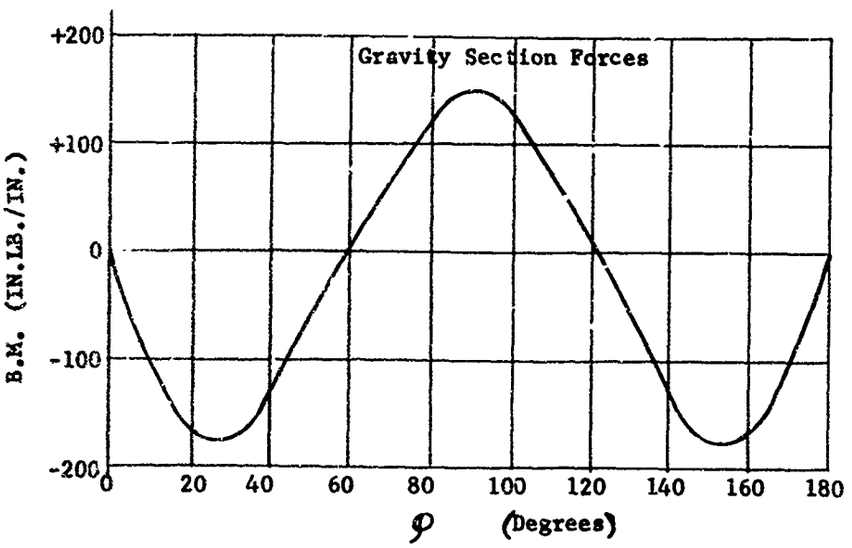

Figure 29 - Dock Roof Bending Moments Per Running Inch

b. Gravity Loads

The ultimate gravity load on a one inch wide section of the dock roof is illustrated below.

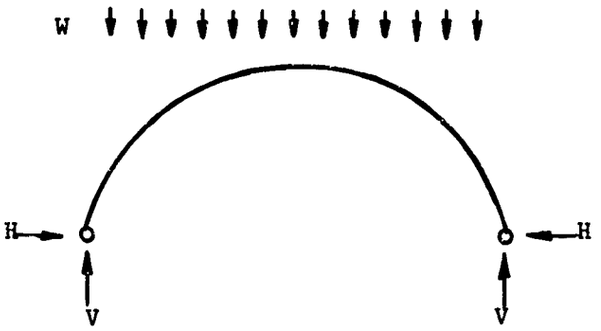

$$w = \frac{30 \times 1.5}{144} = .312 \text{ psi}$$

The arch was again treated as a statically indeterminate structure with pin ends. The ultimate reaction loads along the arch were found from a structural handbook or by use of the method of "least work" to be,

H = 10.6 lb/inch and

V = 24.8 lb/inch.

The bending moment diagram is plotted in Figure 29. The maximum ultimate bending moments were,

B.M. = +140 inch lbs/inch (Compression on outside fiber) and

B.M. = -170 inch lbs/inch (Compression on inside fiber).

C. Development of Allowable Design Stresses

1. General

a. Materials Survey

The structural sandwich elements of the aerospace maintenance dock can be classified as thin wall structures. This classification is due to the relatively large cell size used compared to the thicknesses of the facings and webs. In some areas the structural element was only one fabric layer thick.

The principal variables effecting the strength of FRP (Fiber Reinforced Plastic) structures are fiber strength, fiber orientation and crimp angle, fiber cross sectional area, resin strength, resin cross sectional area, structure configuration, and the temperature and environment in which the structure must operate. This large number of variables lends to an almost infinite number of structural possibilities.

For purposes of FRP major flight structures, the fibers used should in general only be those with a high strength to weight ratio. The resin used should be that with the greatest strength to weight ratio compatible with the environment and other conditions such as expansion and rigidization or fabrication of the structure. The fiber and resin used should also be limited by availability and cost factors.

A great deal of engineering thought, testing, and consequent technical reports has been done on the subject of FRP during the last several decades. Although much of this work concerns resins cured by pressure and heat, practically none of it is concerned with urethane resin or vapor cured resins. Data on relatively thick multi-fabric layered panels and sandwich panels was found in Refs. 2 and 3. Therefore, some engineering analysis and testing was done to develop an approximate method of analysis for the type of thin wall structure used in the dock. This approximate method of analysis allows the use of widely different fiber and resin strengths and configurations.

After surveying the field of fibers available and in light of the factors discussed above and Table 29 below, the choice of substrate fibers to be used on the dock structure was narrowed to the three with the highest yield strength/weight ratio that were available as a commercial or a special run fabric. The three candidate materials were Fortisan (H.T.), fiberglass ("E" glass), and flax (linen). Fiberglass was chosen for the dock structure because it was:

(1) Readily available in many styles of weaves and weights of fabric,
(2) Easily wetted and resin impregnated,
(3) More dense which meant that it could be more efficiently packaged, and
(4) Stable to sunlight and other terrestrial environmental conditions.

The Fortisan, H.T. would have resulted in a slightly lighter structure due to its lower density and consequently thicker structural elements. However, any great weight saving is prevented by the additional volume of resin required to wet the bulkier structure. Inflatable, self-rigidizing structures require approximately equal volumes of resin and substrate material. The flax cloth was not chosen because its strength/weight ratio was lower than the other two and it had no characteristic which bettered the other two fibers except possibly a lower cost if larger quantities were used.

The fiberglass substrate material was elected to be utilized in the form of a woven fabric. It was found that this form was the most convenient one for handling and seaming large sized structures. Also, the woven fabric provided a good means for controlling the porosity of the inflated structure.

b. Strength To Weight Survey

Since the critical stresses for the type of construction and materials used in this program are generally the compressive yield and compressive crippling stress, the usual fiber tenacity or tensile breaking strength/weight ratios are misleading. Therefore, a listing of yield strengths and corresponding modulii of elasticity was made in Table 29 for various fibers. The specific gravity and corresponding density are listed and the yield strength/weight ratio derived. Since very little compressive yield strength data was available and also since it was difficult to test fibers in compression without a matrix of resin, the tensile yield strength and modulus of elasticity were used and assumed equal in compression. This may be in error by as much as 10 percent.

TABLE 29

FABRIC STRENGTH / WEIGHT RATIOS

Material	Modulus of Elasticity (psi)	Yield Strength (psi)	Percent Permanent Set at Yield	Sp.Gr.	Density (Lb/In^3)	Yield Strength-Weight Ratio	$\frac{E}{F_{cy}}$	Ref.
Fortisan, H.T.	2,500,000	145,000	1.0	1.52	.0547	2,650,000	17	4
Fiberglass ("E" Glass)	10,000,000	210,000	.5	2.54	.0915	2,300,000	48	4
Flax (Linen)	4,600,000	115,000	.2	1.5	.054	2,100,000	40	4
Hemp and Ramie	(Similar to Flax)							
Cotton 50/1 Thread	1,700,000	73,000	1.0	1.5	.054	1,330,000	23	VIRON TEST
Steel, F_{tu} = 260,000 psi A.I.S.I. 4340	29,000,000	242,000	.2	7.86	.285	850,000	120	5
Silk (Japanese)	1,030,000	37,000	1.0	1.3	.047	790,000	28	4
Aluminum 7075-T6	10,300,000	68,000	.2	2.8	.101	670,000	151	5
Orlon	1,200,000	17,000	1.0	1.17	.042	400,000	70	4
Rene' 41	29,000,000	116,000	.2	8.3	.299	390,000	250	6
Spruce Wood	1,600,000	4,000	—	.40	.0144	280,000	400	5
Nylon	450,000	13,000	1.0	1.14	.041	350,000	30	4
Dacron (Mylar)	300,000	14,000	1.0	1.38	.05	280,000	21	4
- RESIN FILMS -								
Epoxy Resin	400,000 to 550,000	20,000 to 23,000	—	1.4	.05	460,000	22	8
Polyester Resin	600,000	22,000	—	1.4	.05	440,000	27	8
Gelatin	1,000,000@25°C 100,000 100°C	21,000	—	1.32	.0475	440,000	48	7
Urethane Resin (ADM 2106-H)	300,000	14,000	1.0	1.4	.05	300,000	22	VIRON TEST

As noted in Table 29, the yield point for fibers and resin was taken at a point corresponding to a permanent set of one percent elongation. This corresponds to commercial practice for plastics and was necessary to take care of the slight variations in the stress strain curves. While the yield point for the metals is listed at 0.2 percent permanent set, the corresponding yield point for one percent would not be much greater due to the relatively sharp knee at yield in the stress strain curves for metals.

The resin yield strengths were taken from the references cited in Table 29 and from thin film tensile tests or block compression tests.

2. Theoretical Approach

The basic principle of this method of computing allowable stresses in FRP thin wall panels and stringers is as follows. An effective solid fiber thickness, t_{tf}, for a panel or structural element is derived for elements in tension, and also another effective solid fiber thickness, t_{cf}, is derived for elements in compression. These effective solid fiber thicknesses are used with elemental end loads to get the equivalent solid fiber stress, f_{tf} and f_{cf}, or "glass stress" in the case of a fiberglass and resin matrix. Corresponding solid fiber modulii of elasticity are also derived, E_{tf} and E_{cf}, for end load purposes. Also, the equivalent solid fiber allowable tensile stress, F_{tf}, and allowable compression stress, F_{cf}, are derived.

In addition, for panels and elements critical for compressive crippling or buckling, the effective solid fiber flexure thickness, t_{bf}, is derived. This effective flexure thickness is used in conjunction with the yield strain of the element, F_{cyf}/E_{cf}, to get the allowable compressive crippling stress ratio, F_{ccf}/F_{cyf}, from suitable graphs.

Thus, in essence, effective solid fiber element thicknesses, etc., are derived and the thin wall structure treated as if it were made from homogeneous materials.

A peculiar characteristic of FRP panels that do not buckle is that the tensile strength is usually considerably greater than the compressive strength when compared to the ratio of tensile to compressive strength of metals. This is probably because the fibers are stable in tension, but are unstable in compression, and depend on the resin to support the fibers against local buckling.

a. Effective Thicknesses, t_{tf} and t_{cf}, of Resin and Fibrous Laminates

The cross sectional area of the fibers in the direction of the load must first be found. For cloth laminates, this area per inch may be found approximately by knowing the weight of the cloth, the density of the cloth fibers, and assuming that the cross sectional areas in the warp and fill direction are proportional to the ultimate cloth tensile pull strengths in the warp and fill directions. For a cloth like style #181 fiberglass, where the tensile pull strengths in the warp and fill directions are approximately equal, this results in the following formula:

$$A_f = \frac{W}{41{,}472\,\rho} \quad \text{in inches}^2 \text{ per inch} = t_{tf}$$

where,

$A_f = t_{tf}$ = equivalent solid fiber thickness in tension,

W = weight of cloth in oz per yd^2, and

ρ = density of cloth fibers, see Table 29.

For fiberglass mat, the A_f would be reduced by about 50 percent to account for the random fiber orientation. For tensile strengths of the laminate, the cross sectional area of the resin may be neglected as the resin forms hairline tension cracks under the high stresses.

For compressive strengths of the laminate however, the cross sectional area of the resin may be added to that of the cloth after being reduced by the ratio of the modulus of elasticity of the resin to that of the cloth. For the usual laminate construction, the effective compressive thickness is,

$$t_{cf} = \frac{1}{E_{cf}} \quad (A_f E_{cf} + A_r E_r)$$

where, E_{cf} is as defined below in section d,

A_r is the resin area ($in^2/in.$), and

E_r is the resin elastic modulus.

b. Tensile Yield Strength, F_{tyf}, of Laminate Fibers

In studying the initial failure points of tensile test specimens of woven fiberglass fabric and urethane resin, it was observed that stress peaks formed on the inside of the crimped fiber wherever the crimp was a maximum. Using this observation and assuming that the resin and the cross fibers supported the tensile fibers and in fact prevented them from straightening and aligning with the applied load, an equation for the tensile yield strength of the fibers in the laminate, F_{tyf}, was derived in terms of the tensile yield strength of the fiber alone, F_{tfy}. This equation is

$$F_{tyf} = C_1 F_{tfy}$$

where, C_1 is a constant related to the weave of the fabric substrate. For most fabrics C_1 is between 0.6 and 0.8. F_{tfy} is equal to 210,000 psi (from Table 29) for fiberglass.

Thus, the allowable tensile yield strength of most fiberglass laminates was analytically computed at about 150,000 psi. This, in fact, was approximately the stress at which the fibers of a number of laminates failed by actual test.

c. Compressive Yield Strength, F_{cyf}, of Laminate Fibers

From a study of cloth geometry, it was concluded that where the cloth has crimp angles and is in compression, the resin prevents the crimped fibers from buckling outward from the fabric plane. A sketch of the fabric configuration at the crimp points is shown below.

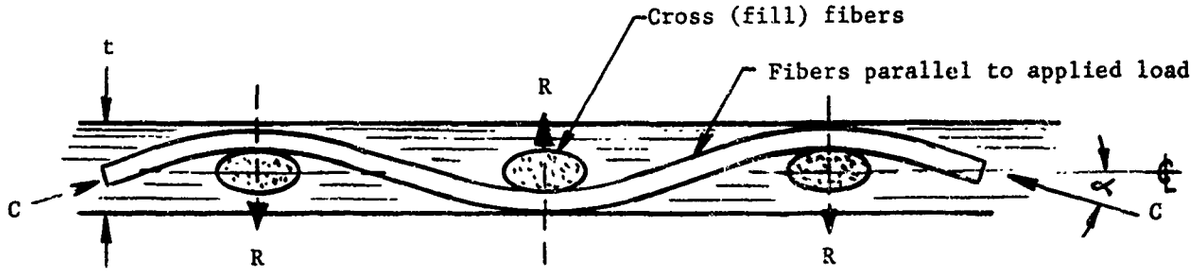

t = thickness of fiber-resin laminate
C = compressive end load in fibers
R = resultant of resin restraint at crimps of loaded fibers

Each fiber is supported radially by resin tension and by resin shear between adjacent fibers of opposite crimp directions. For multi-layer panels, there is additional support from adjacent yarns in the next layer. Again, as in the preceding section, a laminate compressive yield strength was derived from observations of tests and analytical studies. The laminate fiber compressive yield strength is,

$$F_{cyf} = C_2 F_{cyr}$$

where, C_2 is a constant related to the weave of the fabric substrate. For the fabrics of this study, C_2 is between 3 and 5. F_{cyr} is the compressive yield stress of the resin at one percent permanent set.

Thus, if from Table 29 the value of F_{cyr} is equal to 14,000 psi, the allowable compressive yield of the fibers in the laminate would be about 50,000 psi. This is the compressive yield fiber stress obtainable in a particular resin - fiber laminate. Although other factors such as compressive crippling and elastic buckling would usually preclude ever obtaining this value in a strength test; if the laminate were fully supported, a compressive crippling stess about 1.5 times the compressive yield stress can be achieved. This will be explained further in a subsequent section.

d. Modulus of Elasticity of the Fiber in Compression, E_{cf}

The modulus of elasticity of the filament fibers at the crimp was assumed to be proportional to the allowable laminate fiber stress. The modulus of elasticity of the fiber between crimps in the plain weave is the nominal filament modulus corrected by the cosine of the crimp angle, α, which is illustrated in the sketch in the preceding section. The nominal modulus of elasticity of the laminate yarns in compression is taken as the average of these two values.

$$E_{cf} = \frac{E_f}{2}\left(\frac{F_{cyf}}{F_{cfy}} + \cos \alpha\right)$$

where, E_f is the elastic modulus of the fiber (Table 29) and

F_{cfy} is the compressive yield stress of the fiber alone (Table 29).

e. Modulus of Elasticity of The Fiber in Bending or Tension, $E_{bf} = E_{tf}$

For the single layer impregnated fabric in bending, the yarns of opposite crimp angle are on opposite faces. Since only the extreme fibers are at maximum stress, the effective bending modulus of elasticity of the yarns for a single layer impregnated fabric need only be corrected by the cosine of the crimp angle.

Therefore, $E_{bf} = E_f \cos \alpha$.

The detrimental effect of the crimps on the fibers under tension loads is mainly due to the crimp angle, α . Therefore, the effective tensile modulus of elasticity of the yarns need only be corrected by the cosine of the crimp angle, or

$$E_{tf} = E_f \cos \alpha .$$

f. Effective Height of a Sandwich Section in Bending

In order to calculate the allowable elastic buckling stress or the compressive crippling stress in the compressive facing of a sandwich section, it is first necessary to convert the section to an equivalent solid section. This is done by equating the moment of inertia of the sandwich section to that of a solid section of a reduced thickness. Thus the effective height (thickness) of a sandwich section is

$$t_{bf} = \left[\frac{12}{E_{bf}}\left(E_{bf} I_f + E_r I_r\right)\right]^{1/3}$$

where, I_f is the moment of inertia of the fabric in the facings,

I_r is the moment of inertia of the resin in the facings, and

E_r is the elastic modulus of the resin (Table 29).

For a single layer plain weave impregnated fabric, the effective thickness of the fibers in bending is taken as .707 times the actual thickness of the cloth (t_c). The moment of inertia of the fabric is

$$I_f = A_f\, k^2 = A_f \quad \frac{(.707\ t_c)^2}{12} \quad (\text{inches}^4/\text{inch}).$$

The moment of inertia of the resin is

$$I_r = A_r\, k^2 = (A - A_f) \quad \frac{t_r^{\,2}}{12} \quad (\text{inches}^4/\text{inch})$$

where, A is the total area (inches^2/inch) of the laminates and = t_r the total thickness of the impregnated fabric.

For multi-layer laminates the moment of inertia of the cloth must be calculated using the A_f for each layer and its distance to the neutral axis. For laminates with markedly different properties in the warp and fill directions, the t_{bf} may be calculated for each direction and then averaged for use in the crippling graphs.

g. Allowable Compressive Crippling Stress of Flat Plate and Cylindrical Facings

The allowable compressive crippling stress, F_{cc}, for long flat plate elements of width b and with simply supported edges is found from Ref. 9 as

$$\frac{F_{cc}}{F_{cy}} = 1.42 \left[\frac{t}{b}\left(\frac{E}{F_{cy}}\right)^{\frac{1}{2}}\right]^{.85}$$

where, E is the E_{cf} of a previous section,

t is the t_{bf} derived in section f above, and

F_{cy} is the F_{cyf} of a previous section.

The critical yield strain of the panel is found for values of F_{cy}/E from the sections above.

The yield strain for the fiber is

$$\frac{F_{cyf}}{E_{cf}} .$$

The yield strain for the resin is

$$\frac{F_{cyr}}{E_r} .$$

Usually the yield strain of the fiber is less than that of the resin and is the one used in the crippling curve abscissa value.

The allowable compressive crippling stress for long flat plate elements of width b and with one edge free and one edge supported is found in Ref. 9 as

$$\frac{F_{cc}}{F_{cy}} = .6 \left[\frac{t}{b} \left(\frac{E}{F_{cy}} \right)^{\frac{1}{2}} \right]^{.85}.$$

The above two functions are plotted in Figure 30. Also plotted for reference purposes are the corresponding curves for onset of visible buckling (about 75 percent of the theoretical buckling stress).

The allowable compressive crippling stress for cylindrical elements of radius, R, is found in Ref. 10, pp. 470, 471. The formula listed there is modified somewhat to fit the median lines of the reference test data as follows:

$$\frac{F_{cc}}{.6E \frac{t}{R}} = \frac{1 - .000417 \frac{R}{t}}{1 + .003 \frac{E}{F_{cy}}}$$

$$\text{or,} \quad \frac{F_{cc}}{F_{cy}} = \frac{.6 \frac{t}{R} - .00025}{\frac{F_{cy}}{E} + .003}$$

This function is plotted in Figure 31. The abcissa function $\left(\frac{R}{t}\right)^{1.5}$ is used to extend the curves as suggested by Ref. 11. The upper F_{cc}/F_{cy} stress ratio cutoff is taken from Ref. 5. Again, $t = t_{bf}$ as derived in section f above.

It is to be noted that the E/F_{cy} ratio for fiberglass cloth and resin is usually about 60 to 100 while for metals it ranges from 150 to 1500. The compressive crippling stress for cylindrical elements, as discussed widely in reference literature, is dependent on the amount of initial surface waviness. The curves of Figure 31 are based on metallic panels of regular workmanship. For inflated sections of fiber and resin, there is relatively large surface waviness. Test results indicated that the curves of Figure 31 should be reduced 25 percent, i.e. a 25 percent margin of safety should be held on inflated sections.

The values of Figure 30, on the other hand, do not seem to be affected by surface waviness and are satisfactory for inflated sections without correction.

3. Optimization of an Orthotropic Section in Bending

In designing a structural section of the dock for a given bending moment or other loading, it was not immediately obvious what the lightest weight structural honeycomb section of a desired strength would be. After studying the types of structural cross sections that could be fabricated from cloth, resin impregnated, and inflated, it was found that a rectangularly fluted sandwich construction was one of the most satisfactory configurations. The fluted configurations were extremely efficient in resisting bending and shear stresses parallel to their webs but they possessed very little structural rigidity in a transverse direction.

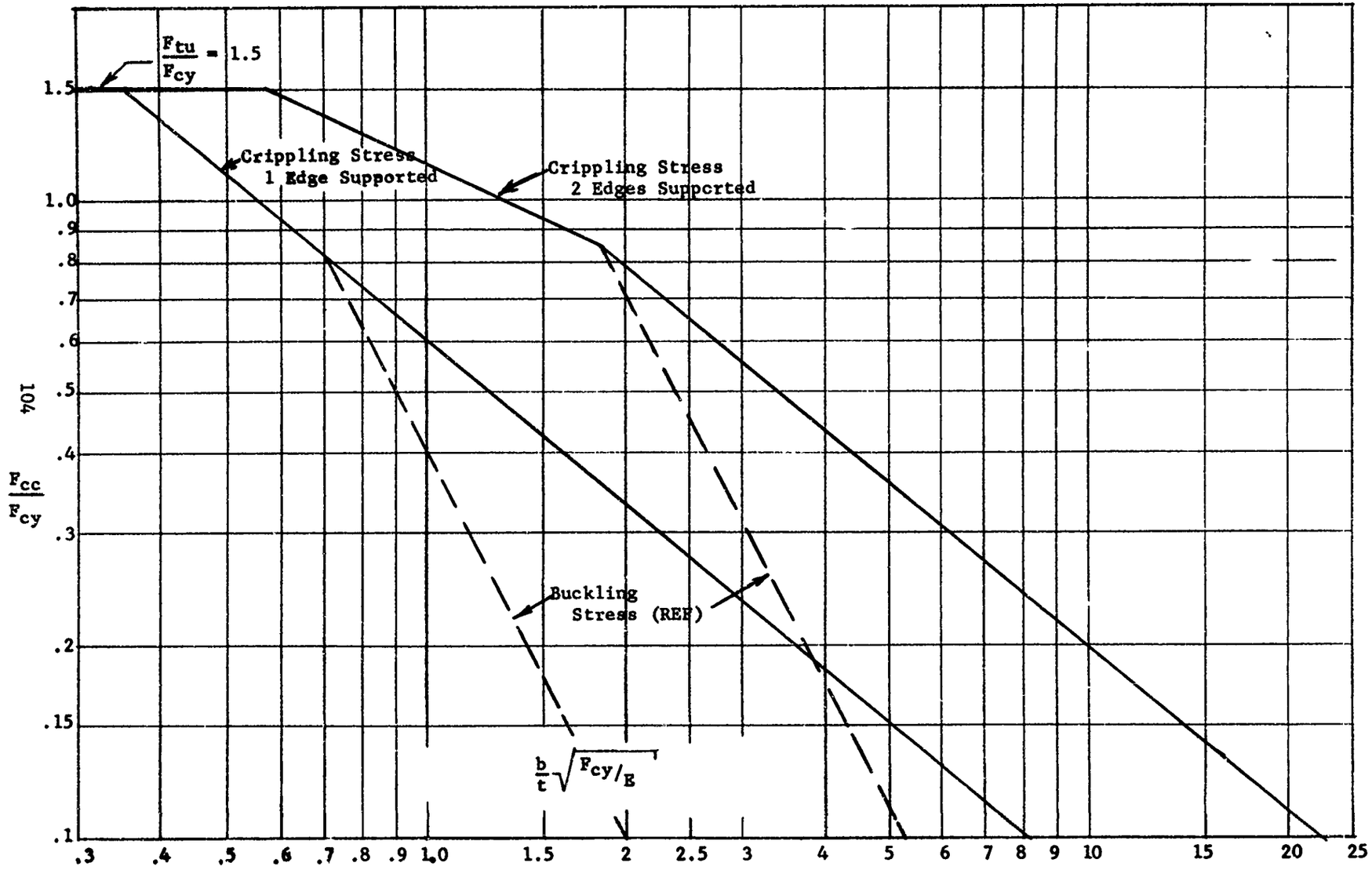

Figure 30 - Compressive Crippling Stress Ratio For Flat Panels Of Width b and thickness t

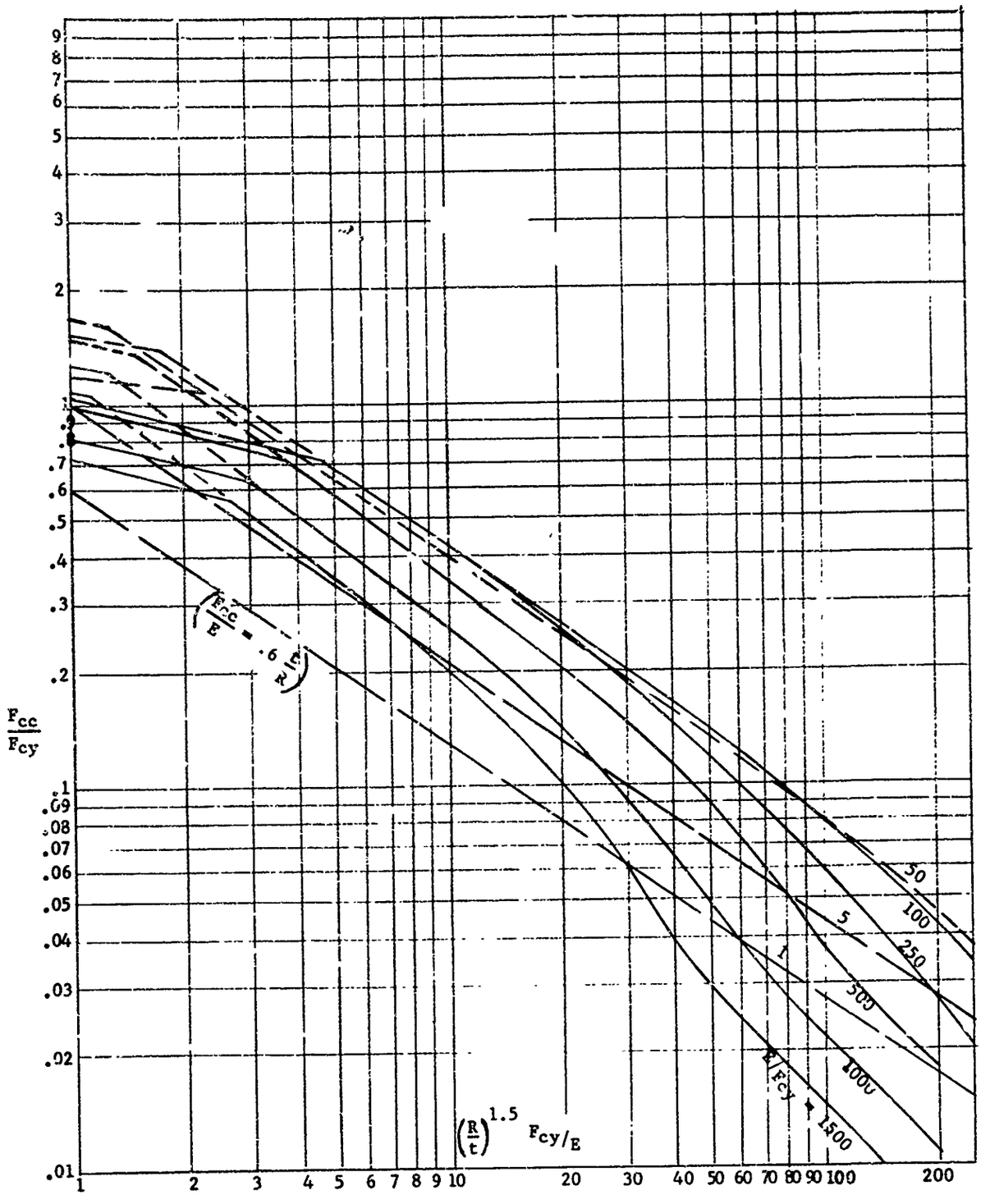

Figure 31 - Compressive Crippling Stress Ratio For Curved Panels Of Radius R and thickness t

In the following optimization study, a curved beam of rectangular fluted sandwich construction was analyzed to derive the lightest possible cross section for a given applied bending moment. A sketch of a section of the beam is shown below.

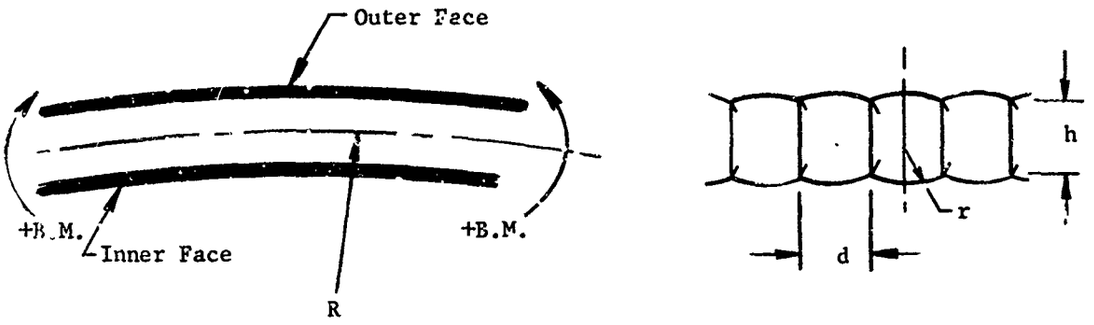

h = nominal section height
d = web spacing
r = radius of each cell facing
R = radius of overall section

The facings of the cross section were optimized for a given bending moment causing compression on the outer face. The webs were critical for radial compressive loads caused by the curved beam effect of an applied bending moment causing compression on the inside facing.

The fluted section was optimized in three parts. First, various web thicknesses were computed as a function of the web spacing, d, and the height of the section, h. Results of this study are plotted in Figure 32. The second step was to compute facing thicknesses as a function of the web spacing, d, and the height of the section. See Figure 33 for the family of curves of this study.

Finally, a cured weight of the fluted section was computed as a function of the web spacing, d, and the height of the section, h, by combining the two previous studies. This function is plotted in Figure 34. As can be seen, there is a definite optimum flute size of d = 2 inches and h = 2 inches for the particular design loads and materials of this study.

The d and h of the aerospace maintenance dock were both selected to be 3 inches. This was to increase the overall buckling stability of the dock and to facilitate fabrication. The less than optimum configuration resulted in about a 6% weight penalty to the roof.

4. Test Verifications

A considerable amount of strength testing of fiber (mostly fiberglass) and resin combinations was done during this contract. This testing included fiberglass and resin laminated samples in tension and bending under various environment and curing conditions to optimize the resin characteristics. Further testing was conducted in part to verify these optimum resin characteristics but mostly to aid in developing desirable structural components and design theory for the aerospace dock and solar collector.

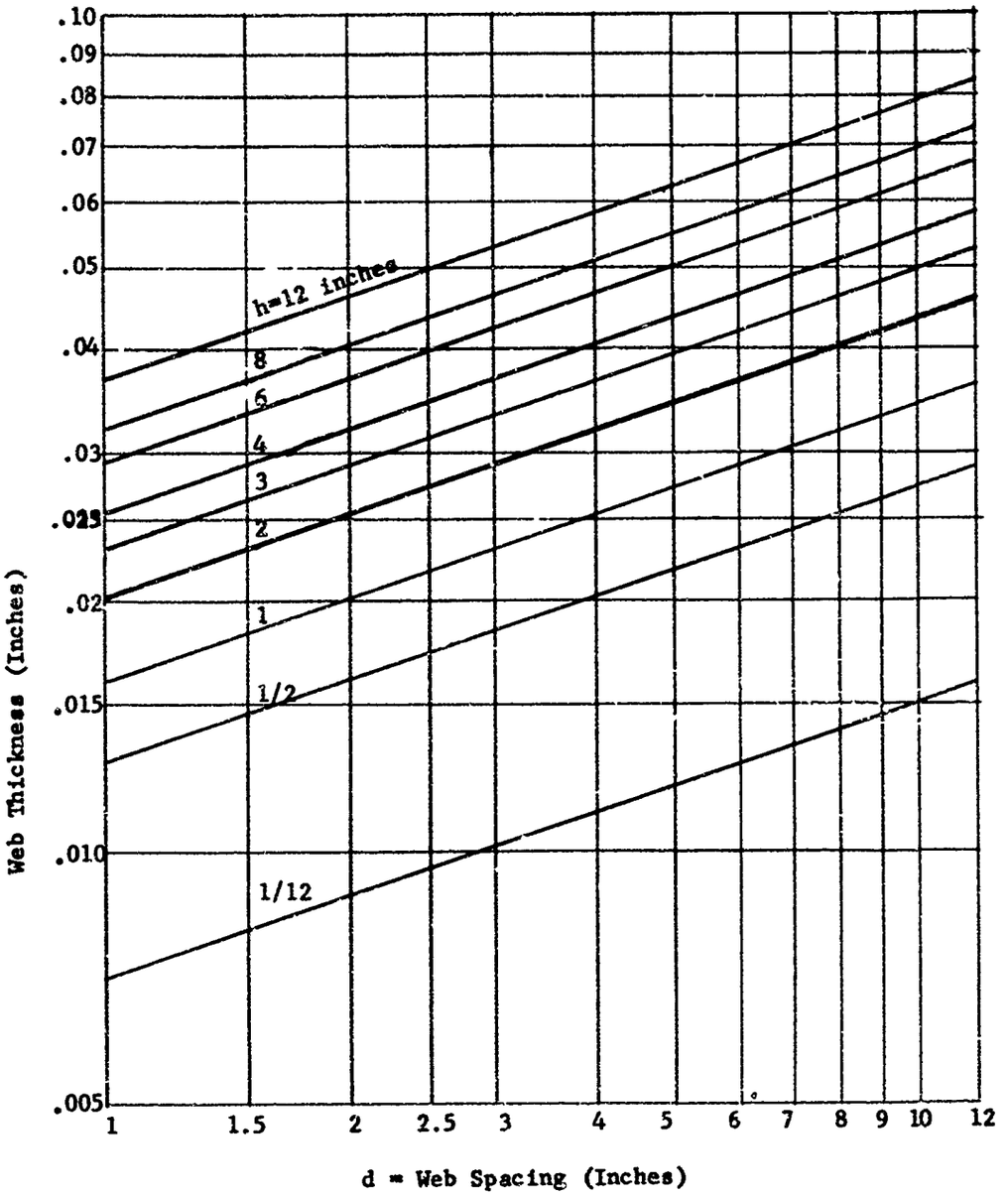

Figure 32 - Required Web Thickness

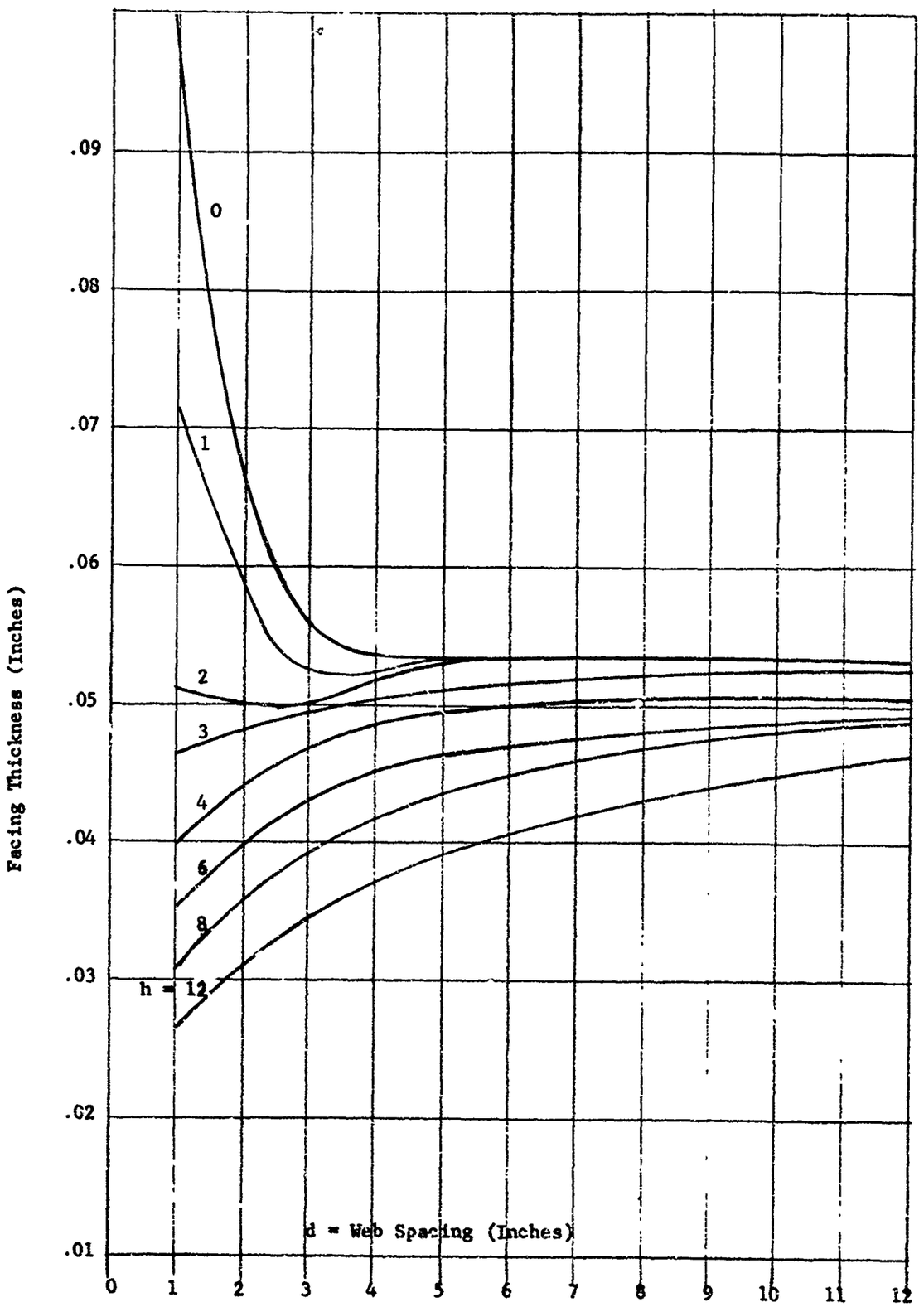

Figure 33 - Required Facing Thickness

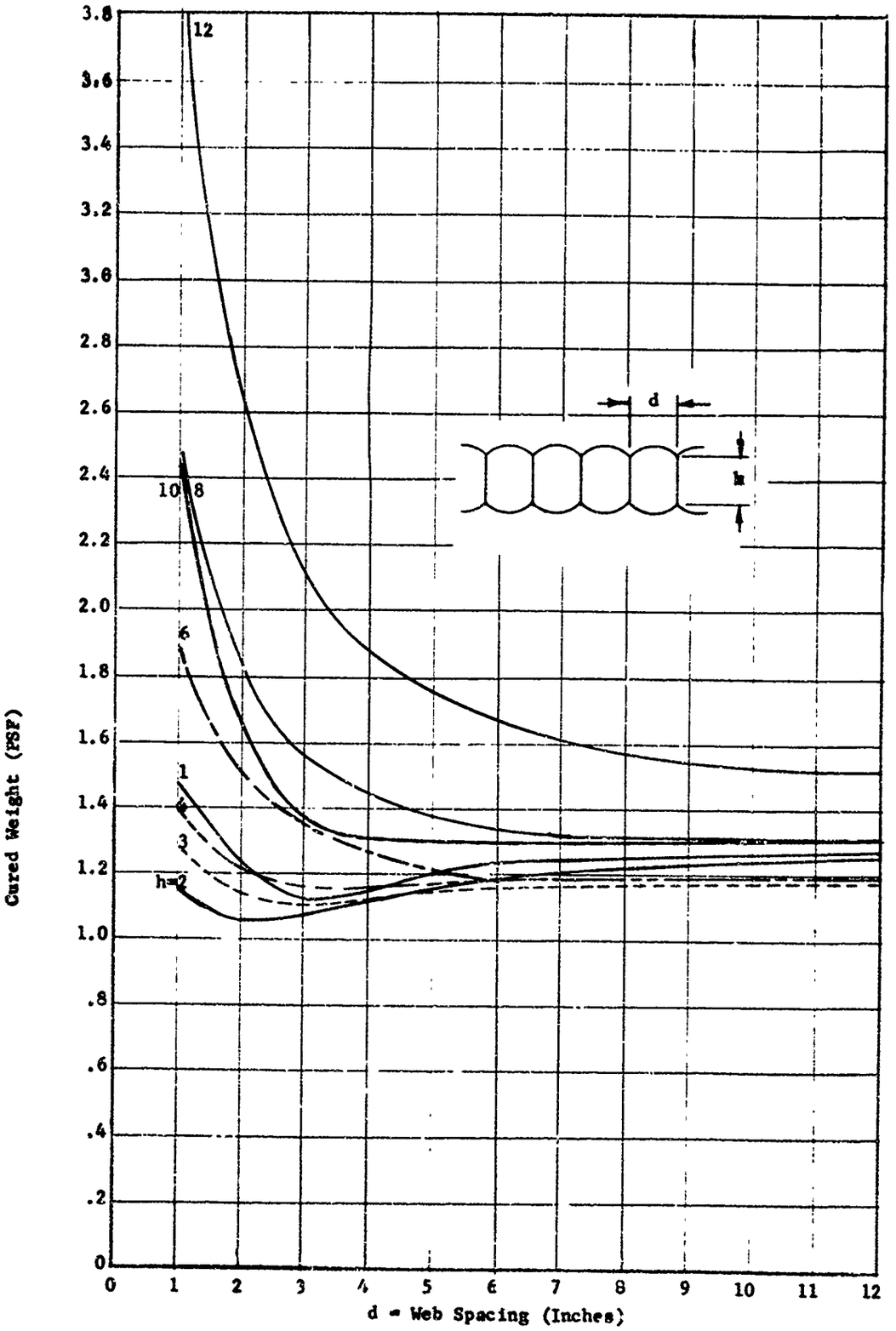

Figure 34 - Cured Weight Of Sandwich

Instron testing machines, which read out load-deflection curves for the specimens tested, were used. The regular tensile test fixtures, a compression cage, and a small bending fixture were used. In addition, a large bending fixture for specimens 6 inches wide by 16 inches long and a shearing fixture were fabricated and used. Figure 35 shows the large bending fixture in place in the Instron.

a. Single and Multi-Ply Laminates and Resin Thin Films

In testing a single layer FRP panel in tension and bending, it is often found that the maximum tension and bending stresses are about equal. If a non-buckling coupon compression test is made of the same panel, the maximum compression stress may only be two-thirds of the tensile and bending value. Since the bending test places one face of the panel in compression, there is an apparent paradox. However, this may readily be explained since bending of a solid laminate or single ply creates a modulus of rupture factor due to non-linear bending stress distribution of at least 1.5. This modulus of rupture factor would give an apparent compressive stress in bending which would be 1.5 times the actual compression stress in the outer fiber. Therefore, the approximate maximum allowable compressive stress in the compression face of an FRP sandwich panel cannot exceed that of the non-buckling coupon compression test, although this may only be two-thirds the apparent stress value of a single ply or solid laminate panel bending test.

A factor to be considered in interpreting and comparing the test results of the vapor cured urethane resin laminates developed in this contract with other types of resin and fiber panels is the manner in which the resin was cured. As a matter of practicability, the urethane resin cannot be cured with the aid of heat pressure when the structure is deployed from a relatively small package in either a space or terrestrial environment. Under heat and pressure cure conditions, the urethane resin would show approximately twice the values obtained under vapor cure conditions. The test results on single and multi-ply laminates and resin thin films are summarized in the section on resin research.

b. "Raypan" and Drop Thread Sandwich Panels

Bending tests were conducted using A.S.T.M. specification C393-57T as a guide. The specimens were loaded with two equal loads at the one-quarter points of span. A dial indicator was located at the mid-span point on some of the tests. This permitted a determination of the bending modulus of elasticity without the influence of shearing deflections. The quarter point loading also produced a long region of constant (maximum) bending moment which accentuated buckling of the compressive face if this tendency was present.

Shear tests were conducted using A.S.T.M. specification C273-58 as a guide. The shear tests were conducted by pulling the faces of the specimens in opposite directions in their respective planes by means of fixture plates glued to the sandwich faces. This placed the core material primarily in shear.

Tables 30 and 31 contain test results of #181 glass fabric, 3/8 inch thick Raypan style #302, and 3/4 inch thick nylon fluted drop thread material. The urethane resin used was that developed under contract No. AF33(657)-10409, and cured by room temperature and humidity. The improved urethane resin developed under this contract was not yet available at the time of these tests. The Raypan material weighed 34 oz/sq yd and had .010 inch thick fiberglass webs

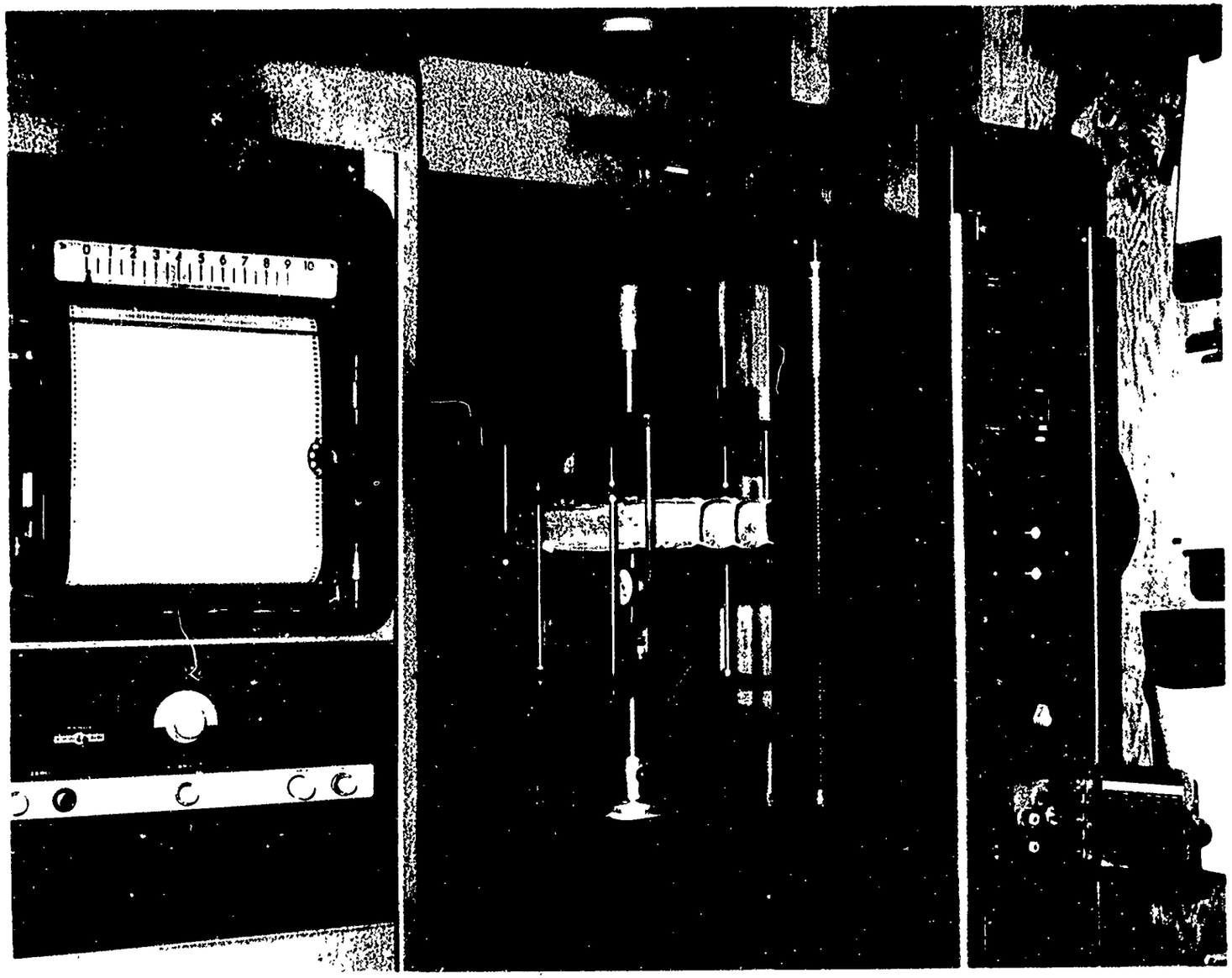

Figure 35 - Instron Testing Machine With Large Bending Fixture Installed

TABLE 30

STRENGTH TESTS OF FIBERGLASS AND RESIN COMPOSITES

Type of Test and Number	Description of Sample	Ultimate Stress (psi)	Stiffness (E) (psi)
(1) Tensile (J-138-I-#1)	#181 Glass Fabric; Urethane Resin; Cure Time About 11 Days.	21,400	1.50×10^6
(2) Tensile (J-138-I-#3)	#181 Glass Fabric; Urethane Resin; Cure Time About 11 Days.	26,700	1.57×10^6
(3) Flexure (R-90-I-#1)	#302 "Raypan" Fabric; Urethane Resin; Cure Time 25 Days. 6"x16" specimen	5,100	1.53×10^6
(4) Shear (R-90-I-#6)	#302 "Raypan" Fabric; Urethane Resin; Cure Time 42 Days. 5"x3" specimen	2,000	
(5) Flexure (R-103-I-#1)	#302 "Raypan" Fabric; Urethane Resin; Cure Time 10 Days. 6"x16" specimen	4,500	1.68×10^6
(6) Shear (R-103-I-#2)	#302 "Raypan" Fabric; Urethane Resin; Cure Time 10 Days. 5"x3" specimen	1,660	
(7) Shear (R-103-I-#5)	#302 "Raypan" Fabric; Urethane Resin; Cure Time 15 Days. 5"x3" specimen	1,440	

NOTE: Stresses calculated on gross area of glass and resin.

TABLE 31

FLEXURAL STRENGTHS OF VARIOUS SANDWICH MATERIALS

	Description of Sample	Urethane Resin Impregnation and Cure	Ultimate Flexural Stress
1.	#302 Raypan 3/8" high. Flexural stresses oriented parallel to flutes. Cured 3 weeks.	Pressure impregnated and vapor cured.	4900 psi
2.	#302 Raypan 3/8" high. Flexural stresses oriented perpendicular to flutes. Cured 1 week.	Vacuum impregnated and vapor cured.	360 psi
3.	3/4" high, fluted nylon drop thread material. Flexural stresses oriented parallel to flutes. Cured 1 week.	Vacuum impregnated and vapor cured.	380 psi

and faces, a 60 degree truss core web, and a plain weave fabric of 24 ends and 26 picks per inch. It was 3/8 inch between faces. The cured facing thicknesses of the Raypan specimens in Table 30 and 31 was between .013 inch and .018 inch. The facing distance between web connections was .45 inch.

A theoretical calculation of the crippling stress of the faces for the flexure test (3) in Table 30 is made below and compared to the test stress of 5,100 psi.

It is known that

$W/4$ = weight of glass fibers in one facing of "Raypan" (oz/yd^2) = 34/4,

$E_f = 10^7$ psi, basic for "E" fiberglass,

E_{tfy} = 210,000 psi, basic for "E" fiberglass,

E_r = 400,000 psi, basic for the urethane resin used in the test,

F_{cyr} = 10,000 psi for the urethane resin used in the test,

$\alpha = 30^o$ crimp angle for the plain weave, and

t_f = .016" (avg. of .013" and .018").

Then

$$A_f = \frac{W/4}{41{,}472\rho} = \frac{34/4}{41{,}472 \times .0915} = .00225 \text{ sq inches/inch},$$

$$F_{cyf} = 5.2\, F_{cyr} = 52{,}000 \text{ psi},$$

$$E_{cf} = \frac{E_f}{2}\left(\frac{F_{cyf}}{F_{cfy}} + \cos\alpha\right) = \frac{10^7}{2}\left(\frac{52{,}000}{210{,}000} + \cos 30^o\right) = 5{,}570{,}000 \text{psi},$$

$$\frac{E_{cf}}{F_{cyf}} = \frac{5{,}570{,}000}{52{,}000} = 107,$$

$$E_{tf} = E_f \cos\alpha = 10^7 \cos 30^o = 8{,}660{,}000 \text{ psi},$$

$$t_{cf} = \frac{1}{E_{cf}}\left(A_f E_{cf} + A_r E_r\right)$$

$$= \frac{1}{5{,}570{,}000}\left[.00225 \times 5{,}570{,}000 + (.016-.00225)\, 400{,}000\right]$$

$$= .0032 \text{ inch}.$$

$$I_f = A_f \frac{(.707\, t_c)^2}{12} = .00225\, \frac{(.707 \times .010)^2}{12} = .0094 \times 10^{-6},$$

$$I_r = A_r \frac{t_r^2}{12} = (.016-.00225)\, \frac{.016^2}{12} = .294 \times 10^{-6},$$

$$t_{bf} = \left[\frac{12}{E_{bf}} (E_{bf} I_f + E_r I_r)\right]^{1/3}$$

$$= \left[\frac{12}{8,660,000} (8,660,000 \times .0094 \times 10^{-6} + 400,000 \times .294 \times 10^{-6}\right]^{1/3}$$

$$= .0065 \text{ inch, and}$$

$$\frac{b}{t}\sqrt{\frac{F_{cy}}{E}} = \frac{.45}{.0065} \Big/ \sqrt{107} = 6.7 .$$

From Figure 30.

$$\frac{F_{cc}}{F_{cy}} = .28 .$$

Then

F_{cc} (theoretical "glass stress") = .28 x 52,000 = 14,000 psi

At each web connection there was a fully supported width of facing = .06 inches.

F_{tu} = 1.5 x 52,000 = 78,000 psi.

The average theoretical allowable "glass stress" is then,

$$F_{cc} \text{ (ave.)} = \frac{14,600 \times .45 + 78,000 \times .06}{.45 + .06}$$

$$= 22,100 \text{ psi.}$$

This theoretical "glass stress" must be converted to the gross stress to compare with the test stress,

$$F_{cc} \text{ (.016 thick facing)} = \frac{.0032}{.016} \times 22,100 = 4,420 \text{ psi.}$$

The test stress of 5100 psi was computed using the section properties of the facings only. If the section properties of the webs were added, the 5100 psi stress would be reduced to 4500 psi and would compare more closely to the 4,420 psi theoretical stress.

The 3/4 inch thick fluted nylon drop thread material of Table 31, had a flute spacing of 0.6 inch before inflation, a weight of 13 oz/sq yd, a facing thickness of .008 inch uncured and .012 inch cured, and was about 1/3 drop thread material. On this test sample, as the compression facing began to buckle, the drop threads crushed and further allowed the facings to buckle with little increase in test load.

c. Square Tube and Round Tube Specimens in Axial Compression

In order to verify the theoretical method of stress analysis and the use of Figures 30 and 31, tests were made of flat walled and cylindrically curved wall specimens. These specimens were made from fiberglass cloth impregnated with urethane and polyester resins. The specimens (three of each configuration) were about 2½ inches long with the ends potted in epoxy resin. The specimens were

tested in the compression cage of the Instron testing machine. At the same time, some thin film tensile tests were made of the resins to get the tensile yield stress and modulus of elasticity of the resin. Data on the tests are listed in Table 32.

When the theoretical compressive crippling load was calculated for these test specimens and the specimens of the next section, agreement with the actual test value was quite good except in the case of axial compression of the higher range of $\frac{R}{t}$ values of the cylinders. A margin of safety of 25 percent should be held when calculating allowable compression in cylindrical panels to account for the initial waviness of this type of FRP structure. This conclusion was based more on the results of the tests described in the next section than on the tests on this section where the specimens were of low initial waviness.

d. Bending Tests of Larger Sections

In addition to bending test sections similar to that shown in Figure 35, two bending test specimens were cut from the square fluted roof panel (upper panel) of Figure 36. The specimens were 4 inches wide, including two webs, and 16 inches long. The cross section was 3 x 3 inches (web spacing x height). The outer face was a layer of style #184 fiberglass cloth with an excess of one inch of cloth at each flange. The cloth was doubled over and sewn to the faces about 3/16 inch from the doubled edge. This gave additional flange material of two layers of #184 cloth, 3/16 inch wide at the outer and inner faces. In addition, the free edge of the web on the inner face curled over, as shown in Figure 36, to give additional effective flange material. This effect was caused by the panel forming to a radius.

The test specimens were tested in the Instron testing machine using the fixtures shown in Figure 35. The specimen with bending compression on the outside skin carried 3000 inch lb ultimate bending moment. The specimen with bending compression on the inside skin carried 2460 inch lb ultimate bending moment.

D. Supporting Systems and Techniques

1. General

In order to successfully deploy and rigidize a large, inflatable, self-rigidizing expandable structure, a number of techniques and subsystems and techniques can be broadly grouped into two main categories: Those necessary to resin impregnate and package the structure, and those necessary to inflate and deploy (including rigidize) the structure. As mentioned previously, many similar techniques were developed during an earlier study, but were necessarily modified to apply to the larger structures of this study.

TABLE 32

COMPRESSION TESTING

Size of Mandrel	Cloth	Resin	Average Resin Thickness Inches	Maximum Test Load Lbs Compression
1" sq with 1/16" radius corners	Plain weave fiberglass 9.5 oz/sq yd .012" thick	Urethane	.018	200
1" sq with 1/16" radius corners	Plain weave fiberglass 9.5 oz/sq yd .012" thick	Polyester	.018	95
1" diameter	Style #181 fiberglass 8.9 oz/sq yd .009" thick	Urethane	.016	240
1" diameter	2 layers of #181 fiberglass	Urethane	.030	1000(4)
2" diameter	Single layer #181 fiberglass	Urethane	.020	275
1" diameter	Single layer #181 fiberglass	Polyester	.030	1000(4)
2" diameter	Single layer #181 fiberglass	Polyester	.020	300

NOTE: 1. Urethane resin had F_{cyr} = 9,200 psi, E_r = 300,000 psi
2. Polyester resin had F_{cyr} = 5,500 psi, E_r = 375,000 psi
3. Crimp angles of fabrics α = 30° approximately
4. Failure was telescoping type shear failure at approximately 45° to the axis.

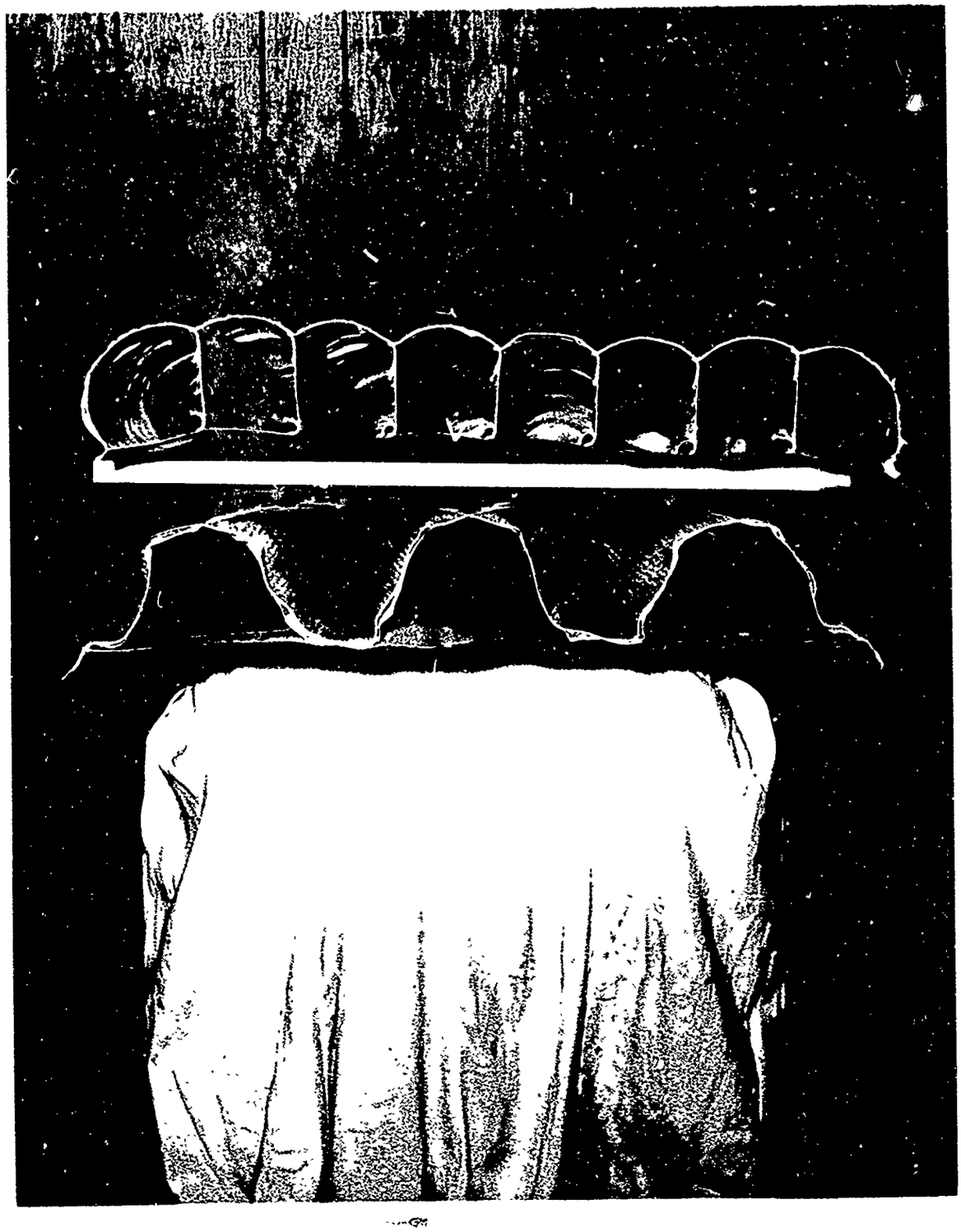

Figure 36 - Candidate Fluted Roof Sections For The Aerospace Maintenance Dock

2. Impregnation and Packaging

a. Outgassing Techniques

The rigidizing resin selected for this study was a water vapor catalyzed urethane. The substrate material selected for the aerospace dock was woven fiberglass fabric which normally retains adsorbed water on the fibers. Thus, in order to achieve a prolonged shelf life of the resin impregnated glass fabric, it was necessary to first remove the entrapped moisture from the substrate fabric. This was most efficiently achieved by outgassing the fabric in a vacuum oven for two or three days prior to resin impregnation. The vacuum oven was a normal hard vacuum facility equipped with infrared heat lamps.

A large piece of fiberglass fabric was outgassed in the preceding manner prior to resin impregnation for a shelf life study sample. There was no observable rigidization of the resin for nearly two weeks. Then, the lightly impregnated areas began to change color indicating that the resin in these areas had started to cure. In about another week, most of the resin was rigid. It is believed that some of the instability of this sample was due to faulty seaming in the package.

After carefully outgassing the substrate material, care was exercised in handling it to prevent it from re-adsorbing moisture. This was accomplished by breaking the seal on the vacuum oven with an atmosphere of dry nitrogen and immediately packaging and sealing the substrate material in an impermeable envelope.

A 4½ mil laminate of Mylar and polyethylene was found to make an effective envelope material. The Mylar layer was turned outward because of its abrasion and puncture resistance. The polyethylene was an effective liner because of its non-adhesive properties and because it was easily heat-sealable. Minnesota Mining and Manufacturing Company distributes this laminate under the brand name of "Scotch-Pak". The impermeable envelope becomes an important part of the vacuum impregnation technique which follows.

b. Vacuum Impregnation

The principle of vacuum impregnation is to use atmospheric pressure to aid in the wetting of the substrate material with resin. The most effective structural properties of fiber reinforced composites are achieved when the substrate is thoroughly wetted with an optimum amount of resin. Vacuum impregnation is the best method of achieving this.

As mentioned earlier, after outgassing, the substrate material was sealed within an impermeable envelope. The envelope was equipped with ports through which resin was introduced to the substrate and a vacuum was applied to the interior of the envelope. The atmospheric pressure differential across the envelope acted like a press to force the envelope tightly against the substrate material and to force the resin uniformly and thoroughly into the substrate fabric.

When vacuum impregnating smaller structures, the vacuum was also used to siphon resin into the envelope. Thus, this type vacuum impregnation process started with a dry substrate and slowly pulled resin into and through the substrate material. However, this process proved to be much too slow for larger structures. Also small leaks at the resin ports allowed moist air to be drawn

into the envelope which catalyzed and rigidized the resin before the structure was deployed. In order to impregnate the larger structures more quickly and to avoid premature catalyzation of the resin, the preceding vacuum impregnation technique was modified.

c. Packaging

The impermeable envelope that was used to seal and impregnate the outgassed substrate fabric becomes an important part of the overall package. It is this part of the package that seals the rigidizing resin against ever present moisture and permits the impregnated structure to be stored prior to utilization. The other part of the overall package is a stiff outer shell that protects the inner envelope during storage and transportation.

There was no need to construct the outer package moisture tight. For this study, the outer package was designed to be constructed of wood - similar to a heavy packing crate. Its primary function was to support the hydraulic pressure of the resin within the impermeable envelope. This pressure was enough to seriously distort the impermeable envelope without the side support of the outer shell.

3. Inflation and Deployment

a. Porosity Study

An understanding of the factors that influence the porosity of fabrics was essential to the inflation of a large expandable structure. To determine these factors, a comprehensive porosity study was conducted. This study provided good background information on the mechanics of porosity, the factors affecting porosity, and the information necessary to design the inflation subsystem for the aerospace maintenance dock.

The portable inflation unit was required to pressurize the inside of the inflatable structure so that it would unfold and deploy to its expanded configuration. Pressurization was controlled by the volume rate of inflation vapors conducted into the structure. Therefore, a structure with a low porosity required a small volume rate of inflation and a small inflation unit.

Some degree of porosity was desirable in the inflatable, self-rigidizing structure. A structure with zero porosity would easily deploy but rigidization would be impaired because the catalyst would stagnate inside the structure. The urethane resin of this system is not sensitive to catalyst flooding, but rather rigidization is aided by increasing the catalyst dosage. A small degree of porosity in the structure accomplishes this by permitting a continual exchange of inflation and catalyst vapors through the structure.

Dimensionally, porosity is the velocity of the inflation vapors that permeate the inflatable structure. Porosity is measured by dividing the volume rate of inflation vapors by the area of inflated materials:

$$cfm/ft^2 = ft/min.$$

For a given vapor (air) and material (fiberglass fabric), the expression for porosity was demonstrated to be primarily dependent upon the pressure differential across the fabric. This is shown in Tables 33, 34, and 35 and Figure 37. The data for these tables was determined experimentally as follows.

A number of samples of fiber glass fabric were obtained for use in connection with a porosity tester. Samples were selected and the flow rate (ft^3/hr) of air through each was directly measured with flow meters for each of three levels of pressure - 0.10, 0.50, and 5.0 inches of water.

Figure 38 shows the porosity tester in operation. Fabrics were mounted between the clamps at the right end of the tester. The air flow was introduced through one of the three meters at the left of the tester. As the flow was increased, a pressure was built up in the larger chamber and recorded on a water manometer (shown in the foreground). A record was made of the flow rate corresponding to a given pressure (0.1, 0.5, or 5.0 inches of water).

The flow rates were converted to porosities (ft/min) by dividing by 60 and the area of the sample. Porosities of the fabrics tested are tabulated in Table 33. Figure 37 shows porosity versus pressure and is representative of most of the fabrics.

Efforts were made to select fabrics that were obviously less porous than others and also to select fabrics over a wide range of thicknesses, weights, thread count, and weave. These properties are given in Table 34. The fabrics are ranked in descending order from least to most porous. Two nylon fabrics were included with the fiberglass in order to evaluate nylon as a possible liner for the aerospace dock.

The results of this testing seemed to indicate that weight, thickness, and thread count had very little to do with the porosity of a fabric. The largest determining factor seemed to be the weave type; with the crow foot satins being the least porous, the shaft satins in the middle, and the plain weaves being the most porous (see Figure 37).

The initial testing was conducted on dry fabric so that more accurate measurements of the inflation vapors could be made. Resin impregnation considerably reduces the porosity of any fabric as shown by comparing Tables 33 and 35. The second part of the porosity study was to measure the porosities of resin impregnated fabrics. A median porosity fabric, style #181 fiberglass, was impregnated and tested as before.

In order to reduce the porosity of the #181 fabric, style #1281 nylon fabric was investigated as a liner either inside (upstream) or outside (downstream) the #181 fabric. Table 35 contains the individual impregnated porosities of these fabrics as well as the two fabrics together. As was expected, the nylon liner fabric upstream provided the greatest amount of porosity control - about 15 times that of the sample with glass fabric upstream.

Further development with this configuration (nylon lined fiberglass) showed that the tightly woven nylon fabrics would not impregnate as effectively as glass. The nylon liner was then discarded and a tightly woven fiberglass fabric (style #402) was selected.

TABLE 33

POROSITIES OF DRY FABRICS - FIBERGLASS & NYLON

Fabric No.	Mfg'r	Porosity (ft/min) at pressure indicated in inches of water 0.1 inch	0.5 inch	5.0 inch
138	(1)	8.5	29	150
143	(1)	12.2	47	178
164	(1)	56	131	377 (2.8 in.water)
181	(1)	19	75	244
182	(1)	19	75	226
183	(1)	19	66	207
184	(1)	29	94	300
401	(1)	5.6	24	122
402	(1)	4.7	20	94
600	(1)	21	94	377 (3.7 in.water)
909	(1)	27	75	377
918	(1)	9.4	38	160
1543	(1)	9.4	22	150
1581	(1)	19	66	226
1583	(1)	20	75	244
1584	(1)	23	75	244
7544	(1)	75	160	377 (2.3 in.water)
7586	(1)	47	150	377 (3.3 in.water)
7597	(1)	56	150	377 (2.2 in.water)
14719	(1)	4.7	22	113
29	(1)	11	38	225
175	(1)	5.6	19	120
HG 84	(2)	36	95	310
371	(2)	150	380	- -
#3 Roving	(3)	8	23	67 (2.2 in. water)

TABLE 33 (Cont'd)

POROSITIES OF DRY FABRIC - FIBERGLASS & NYLON

Fabric No.	Mfg'r.	Porosity (ft/min) at 0.1 inch	Pressure indicated in inches of water 0.5 inch	5.0 inch
Tricon 101	(4)	20	53	67 (0.7 inch water)
Tricon H51	(4)	15	43	67 (1.5 inch water)
Tricon 201	(4)	35	67 (0.29 in.water)	- -
1347	(5)	0.15	0.67	5.5
1281	(5)	- - -	54 (6)	- - -

NOTE:

(1) Stevens Fiber Glass Fabric
(2) Hess-Goldsmith Fiber Glass Fabric
(3) Bean Fiber Glass Fabric
(4) Wimpfheimer & Bro. Fiber Glass Fabric
(5) Burlington Industrial Nylon Fabric
(6) Mfg'rs. Porosity Value

TABLE 34

FABRIC PROPERTIES

Fabric No.	Mfg'r.*	Weight (oz/yd^2)	Thickness (Inches)	Thread Count (warp x fill)	Weave Type	Porosity (ft/min) at ½ inch water
1347(Nylon)	(5)	4.2	.0075	- - - - -	- - - - -	0.67
175	(1)	24.5	.042	5 x 4	High Modulus Roving	19
402	(1)	9.5	.010	54 x 54	Cr. Satin	20
1543	(1)	9.4	.009	49 x 30	Cr. Satin	22
14719	(1)	12.0	.010	64 x 60	Cr. Satin	22
#3 Roving	(3)	24	.042	5 x 4	Roving	23
401	(1)	9.4	.010	54 x 52	Cr. Satin	24
138	(1)	6.9	.007	64 x 60	Cr. Satin	29
918	(1)	18.2	.018	52 x 56	High Modulus	38
29	(1)	28.0	.042	6 x 4	High Modulus Roving	38
Tricon H51	(4)	43	.046	- - - -	Special Triple Layer Weave	43
143	(1)	8.8	.009	49 x 30	Cr. Satin	47
Tricon 101	(4)	67	.103	- - - -	Special Triple Layer Weave	53
1281(Nylon)	(5)	2.6	.007	102 x 76	- - - - -	54
183	(1)	16.7	.018	54 x 48	Sh. Satin	66
1581	(1)	9.0	.0085	56 x 54	Sh. Satin	66
181	(1)	8.9	.0085	57 x 54	Sh. Satin	75
182	(1)	12.4	.013	60 x 56	Sh. Satin	75
1583	(1)	16.7	.020	54 x 48	Sh. Satin	75
1584	(1)	24.5	.025	44 x 35	Sh. Satin	75
909	(1)	9.7	.010	84 x 54	High Modulus	75
184	(1)	25.9	.027	42 x 36	Sh. Satin	94
600	(1)	9.0	.010	65 x 35	3 x 1 Twill	94
Tricon 201	(4)	51	.079	- - - -	Special Triple Layer Weave	67 (0.29) (inch) (water)

TABLE 34 (Cont'd)

FABRIC PROPERTIES

Fabric No.	Mfg'r.*	Weight (oz/yd^2)	Thickness (Inches)	Thread Count (warp x fill)	Weave Type	Porosity (ft/min) at ½ inch water
HG 84	(2)	25.1	.025	42 x 35	8 Sh. Satin	95
164	(1)	12.7	.016	20 x 18	Plain	131
7586	(1)	25.8	.023	62 x 20	Sh. Satin	150
7544	(1)	19.2	.022	28 x 14	Plain	160
371	(2)	37.4	.042	30 x 30	- - - -	180

* See Table 33 for Manufacturer List

TABLE 35

POROSITIES OF RESIN IMPREGNATED FIBERGLASS AND NYLON FABRICS

Sample Description	Impregnating Resin	Porosity (Ft/Min) at pressure indicated in inches of water		
		0.1 inch	0.5 inch	5.0 inch
Single Thickness - #181 Fiberglass Fabric	Urethane	*	0.22	2,3
Single Thickness - #1281 Nylon	Urethane	.15	0.67	3.2
Two Thickness - #181 Glass Fabric & #1281 Nylon (Nylon Upstream)	Urethane	*	*	0.10 (5.57" water)
Two Thickness - #181 Glass Fabric & #1281 Nylon (Glass Upstream)	Urethane	*	*	1.5

NOTE: * Not enough air flow to make an accurate reading

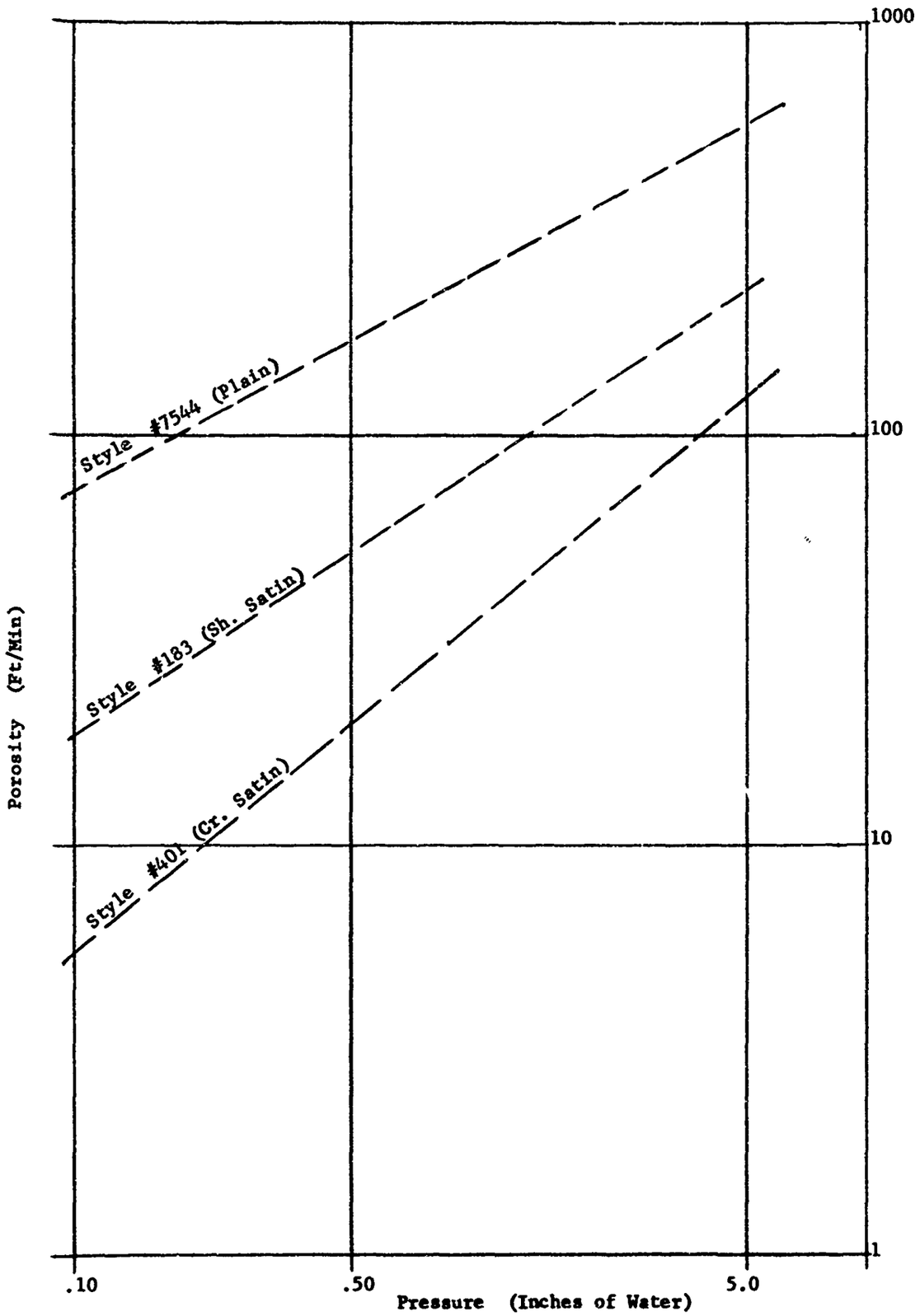

Figure 37 - Porosities Of Dry Fiber Glass Fabrics

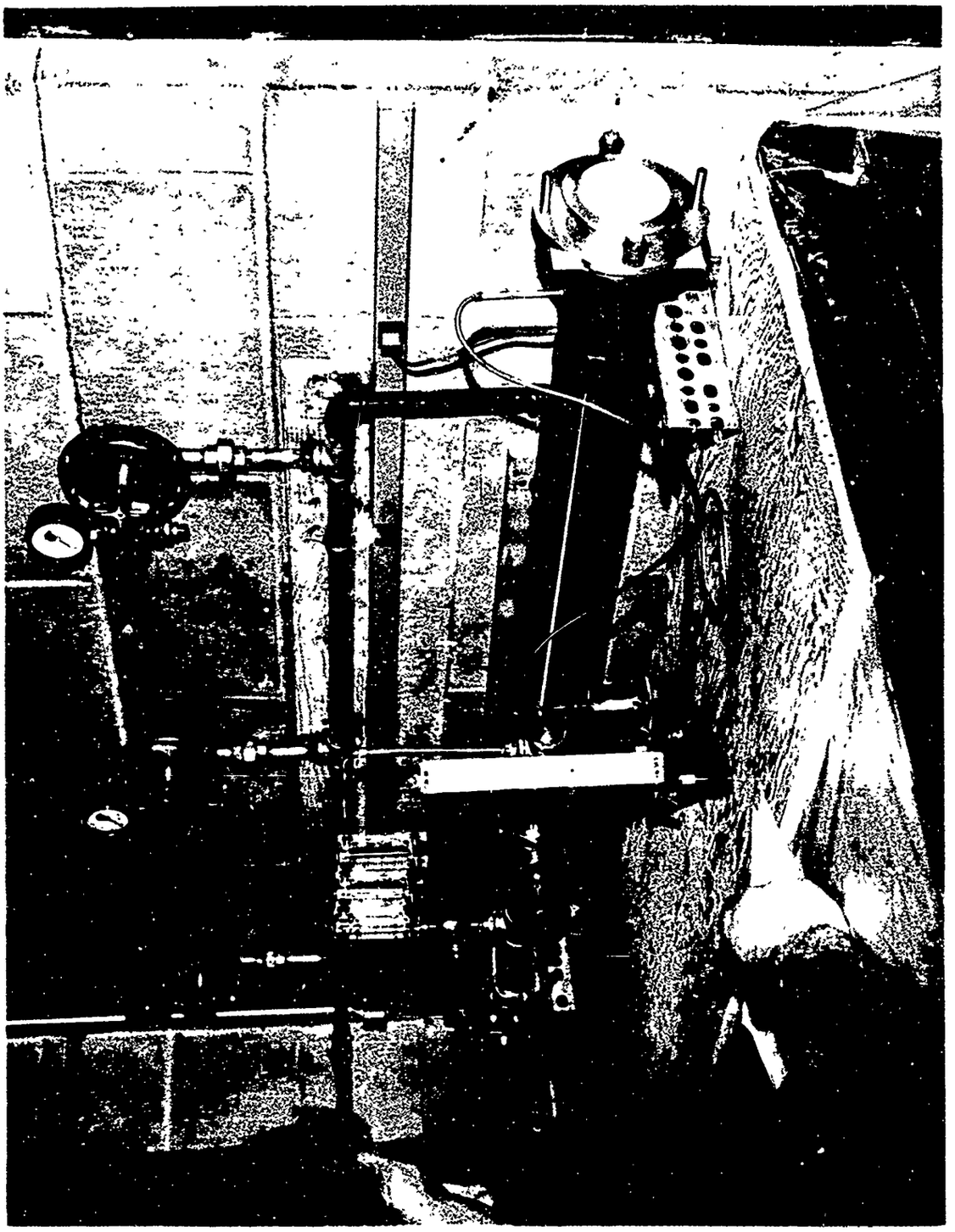

Figure 38 - Fabric Porosity Tester

The #402 fabric was very effective in reducing the porosity of the main fabric such as style #181 and was selected as the means for controlling porosity for this study. The #402 fabric by itself was not heavy or thick enough to carry the design loadings of the structure. Further investigations did not reveal a low porosity fabric that was strong enough to be used by itself in this study.

The style #181 glass fabric was later selected as the substrate material for the roof and end walls of the aerospace maintenance dock. From the above studies, it was decided to line the upstream face of the #181 fabric with #402 fabric throughout. A single layer of #402 fabric was selected for the floor of the aerospace maintenance dock.

The impregnated porosities of all of the above fabrics and combinations of fabrics present in the aerospace maintenance dock were retested in order to check the capacity required of the portable inflation system. The porosities of these double and single layer constructions are shown in Table 36. These porosities have the dimensional units of ft/min. The surface areas are based on a 13 by 15 ft semicylindrical aerospace dock. Thus, for a given internal pressure, the required volume rate of inflation vapor was computed by multiplying a component porosity by its surface area and summing these volume rates for the entire dock. For example, at an extreme condition of an inflation pressure of 8.0 inches of water, the required volume rate of inflation was calculated to be:

$$(320)(0.15) + (143)(0.15) + (202)(0.4) = 48 + 22 + 81 = 151 \text{ or } 150 \text{ cfm.}$$

Thus, a 1000 cfm blower for the portable inflation system was able to operate with a wide margin of safety.

b. Manifolding Study

The manifolding study was an analytical approach to the problem of inflating the aerospace maintenance dock. This study provided the means by which the best method of directing the inflation pressures through the dock was selected. Primarily, the inflation pressures were to expand the dock into the general overall configuration and separate the two faces of the sandwich components. Because the roof and end walls of the dock were designed as sandwich constructions, one method of inflating the dock was to pressurize between the faces of the sandwich components throughout the dock. Alternatively, the dock could be inflated by manifolding directly inside of the entire structure.

Manifolding between the faces of the sandwich constructions presented one immediate advantage. It assured that these components would deploy to their full depth of section. An obvious disadvantage, however, was the fact that this method of manifolding required relatively large inflation pressures. In addition, it required an extremely complicated system of conducting the inflation pressures to all sections of the dock.

The manifolding scheme of pressurizing the interior of the entire structure had the apparent advantage of requiring a very low inflation pressure. It was also a better method of deploying the dock from a folded configuration since there were fewer constrictions to inhibit the flow of the inflation vapors. The main disadvantage to this manifolding scheme was the apparent inability to separate the faces of the sandwich components.

TABLE 36

POROSITIES OF THE IMPREGNATED AEROSPACE MAINTENANCE DOCK

Component	Construction	Surface Area	Porosity (ft/min) at pressure indicated in inches of water				
			0.5"	3.0"	5.0"	8.0"	10.0"
Roof	#181/#402	320 ft^2	*	.07	0.1	0.15	0.2
End Walls	#181/#402	143 ft^2	*	.07	0.1	0.15	0.2
Floor	#402	202 ft^2	.03	0.2	0.3	0.4	0.5

* Not measurable

After considering the advantages of each scheme and evaluating the solutions to the disadvantages of each, it was decided to manifold into the interior of the entire dock. The one main disadvantage - that of separating the faces of the sandwich constructions - remained to be solved.

A method of separating the facings of the semicircular roof arch was not difficult to devise. Due to its circular configuration, it was necessary only to make the inside facing shorter than the outside facing. Internally pressurizing the structure would deploy the roof into a circular configuration and in turn separate the inside and outside facings. This was to be achieved by securing the inside facing at the bottom of both sides and allowing the outside facing to float free. Thus, the pressure differential across the roof would cause the inside facing to be stressed into a semicircular arch by hoop tension and the outside facing to separate away from the inside facing by an amount equal to the thickness of the roof section.

The facings of the end walls were to be separated in a similar manner. Tie lines were provided to secure the inside facing of the front wall to the inside facing of the rear wall. Thus, the pressure differential across the end walls would be directed into the internal ties and the pressure differential across the outside facing of the end walls would cause this facing to separate by an amount equal to the wall thickness.

The inside facing of the roof was to be secured by reinforcing it with a series of catenary load tapes along the bottom edge of both sides and joining these to ground anchors.

The inside facing of the end walls was secured to the tie lines through another series of catenary load tapes. Besides providing a means for separating the facings of the end walls, these load tapes and tie lines would aid in holding the flat end walls from distorting into spherical sections during the inflation of the dock. The end wall load tapes were located in three continuous horizontal rows. The middle row of load tapes was located at the door hinge to hold it from distorting during the inflation of the dock. The other rows of load tapes were equally spaced above and below the middle row. A web of neoprene-coated nylon fabric connected each of the end wall catenary load tapes to the inside facing of the end wall.

All of the load tapes were catenary shaped in order to distribute the concentrated reactions of the ground anchors and tie lines into the facings of the structure as uniform reactions. In this manner, distortions and stress concentrations in the inflated structure would be minimized.

c. Folding Study

A keystone in the successful deployment of a large inflatable structure is unfolding it from the packaged configuration. The intent of this effort was to unfold the structure with the same inflation unit that would be used to expand it. It was reasoned that a pressurized deployment of the aerospace maintenance dock would be the simplest to employ and it would not require additional equipment. However, in striving to unfold the dock with inflation pressures only, a number of problems were encountered.

The problem of folding the dock was studied first by analytical means. However, the inconclusiveness of this study led to the development of an experimental study. The principal instrument of that study was a 1/10 scale model of the aerospace maintenance dock. The purpose of the model was to provide a means for evaluating possible folding techniques.

The 1/10 scale model was repeatedly folded by one of a number of proposed techniques and then internally pressurized in a manner that could be applied to the full size aerospace maintenance dock. The effectiveness of the subsequent deployment was noted before proceeding to the next folding technique. In this manner, a number of semisuccessful techniques were evaluated and an optimum folded configuration was developed.

In order to simulate the scale thickness of a large structure, the 1/10 size inflation model was made from a single layer of style #402 fiberglass cloth. This single layer of cloth was only slightly out of scale in thickness. However, the unit weight of this material was about 1/10 the unit weight of the large structure. This meant that the pressures used to inflate the model must be 1/10 that of the pressures necessary to inflate the full size structure. The model was soaked with water to simulate the reduction in porosity due to the urethane resin in the full sized dock.

The optimized folding technique is illustrated in Figures 39, 40, 41, and 42. The subject of these figures is the 1/10 size inflation model, however, except for size, the aerospace maintenance dock was to be folded into an identical configuration. In Figure 39, the model has been layed flat (roof and end walls flat against the floor) and accordian pleated into a strip measuring 1/10 the length of the dock by the lay flat width. In Figure 40, this strip is folded twice upon itself. The last fold to the structure is shown in Figure 41. The completely folded dock with an inflation fitting located in each corner of the rear end wall is shown in Figure 42.

A maximum inflation pressure of 1/2 inch of water was necessary to unfold and deploy the 1/10 scale model from the above folded configuration. This was extrapolated to the full size aerospace maintenance dock as a maximum inflation pressure of 5 inches of water and was used in designing the portable inflation unit.

d. Portable Inflation Subsystem

The results of the porosity, manifolding, and folding studies provided the initial design information for the portable inflation unit. The porosity study indicated that a 13 by 15 ft semicylindrical structure would require a 1000 cfm inflation unit to support the structure until it had rigidized. The folding study indicated that an inflation unit capable of developing a pressure differential of about 5 inches of water was necessary to unfold the packaged structure. The manifolding study recommended that an elaborate system to distribute the inflation pressures was not necessary. Rather, a concept as simple as pressurizing the interior of the entire structure was preferred. From the folding study again, it was obvious that two inflation fittings to the interior of the structure would be superior to a single fitting.

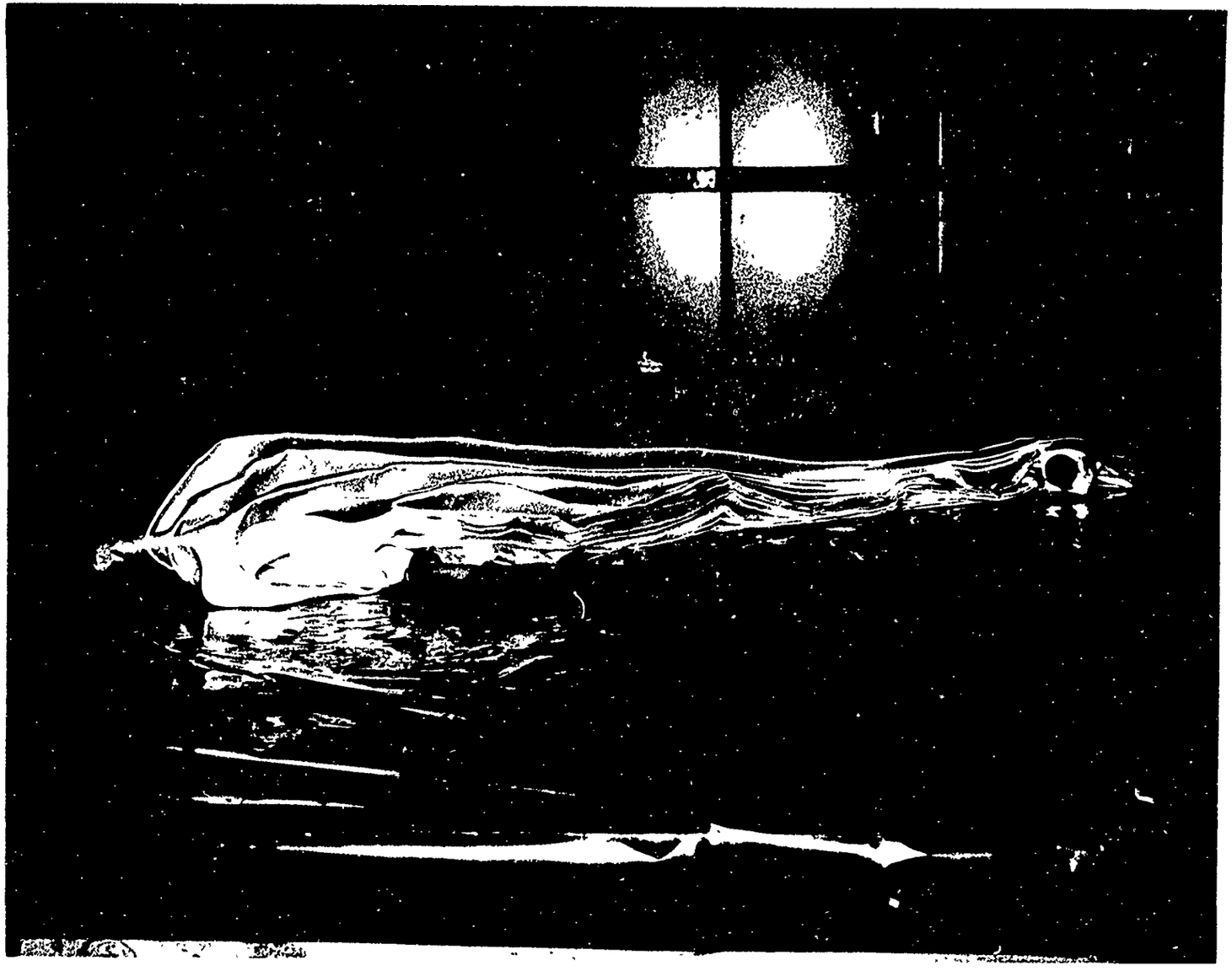

Figure 39 - First Step In Folding The Aerospace Maintenance Dock

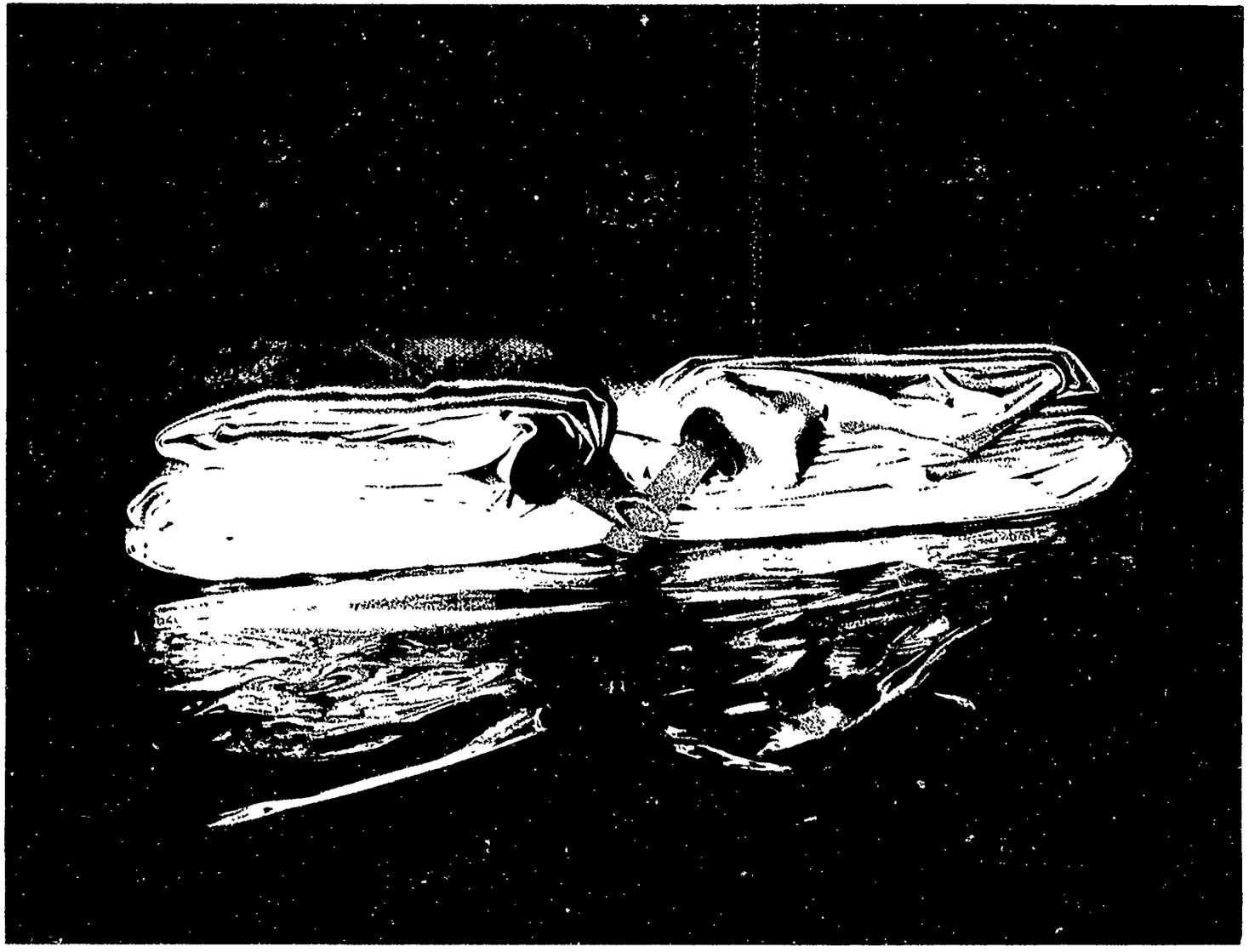

Figure 40 - Second Step In Folding The Aerospace Maintenance Dock

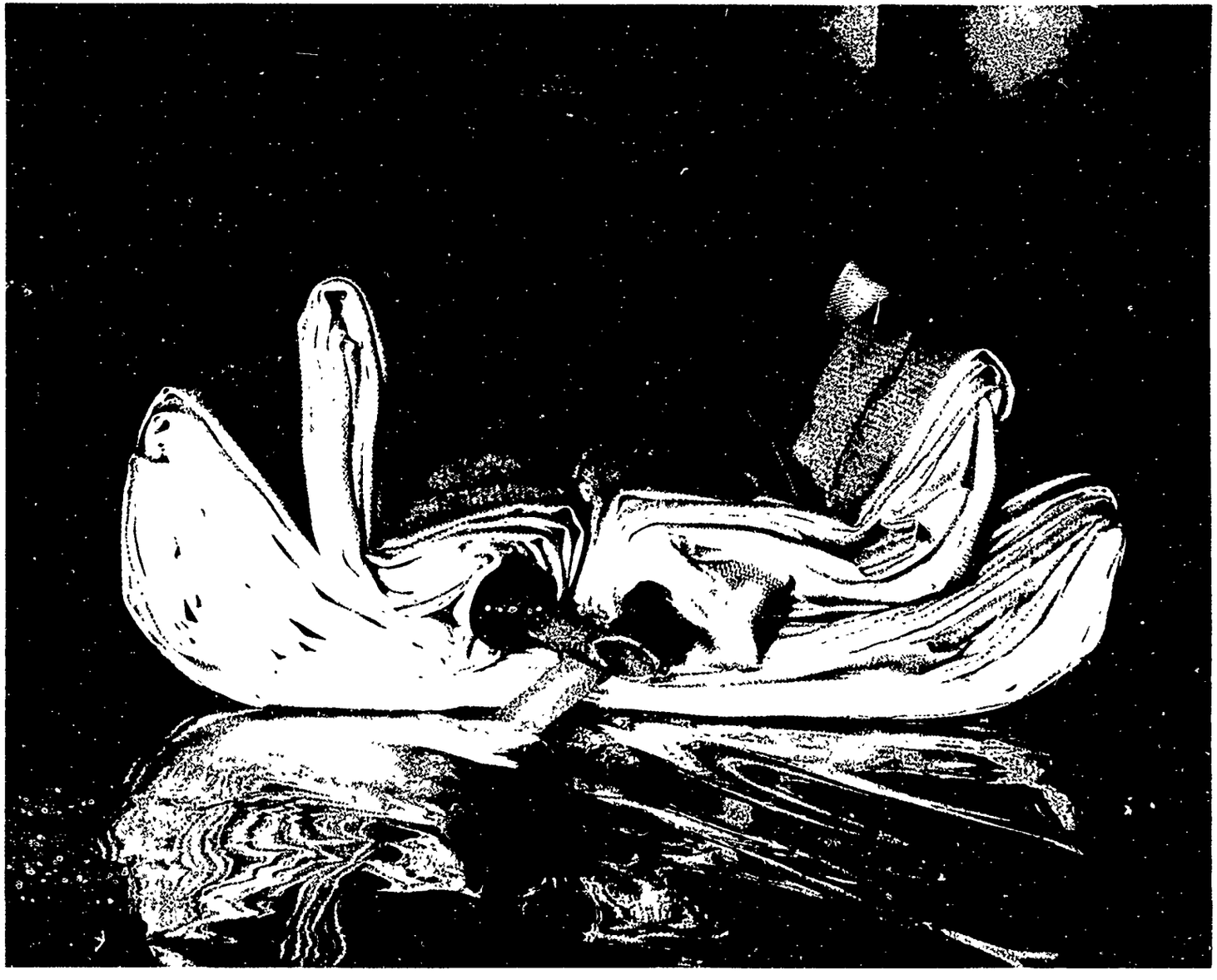

Figure 41 - Third Step In Folding The Aerospace Maintenance Dock

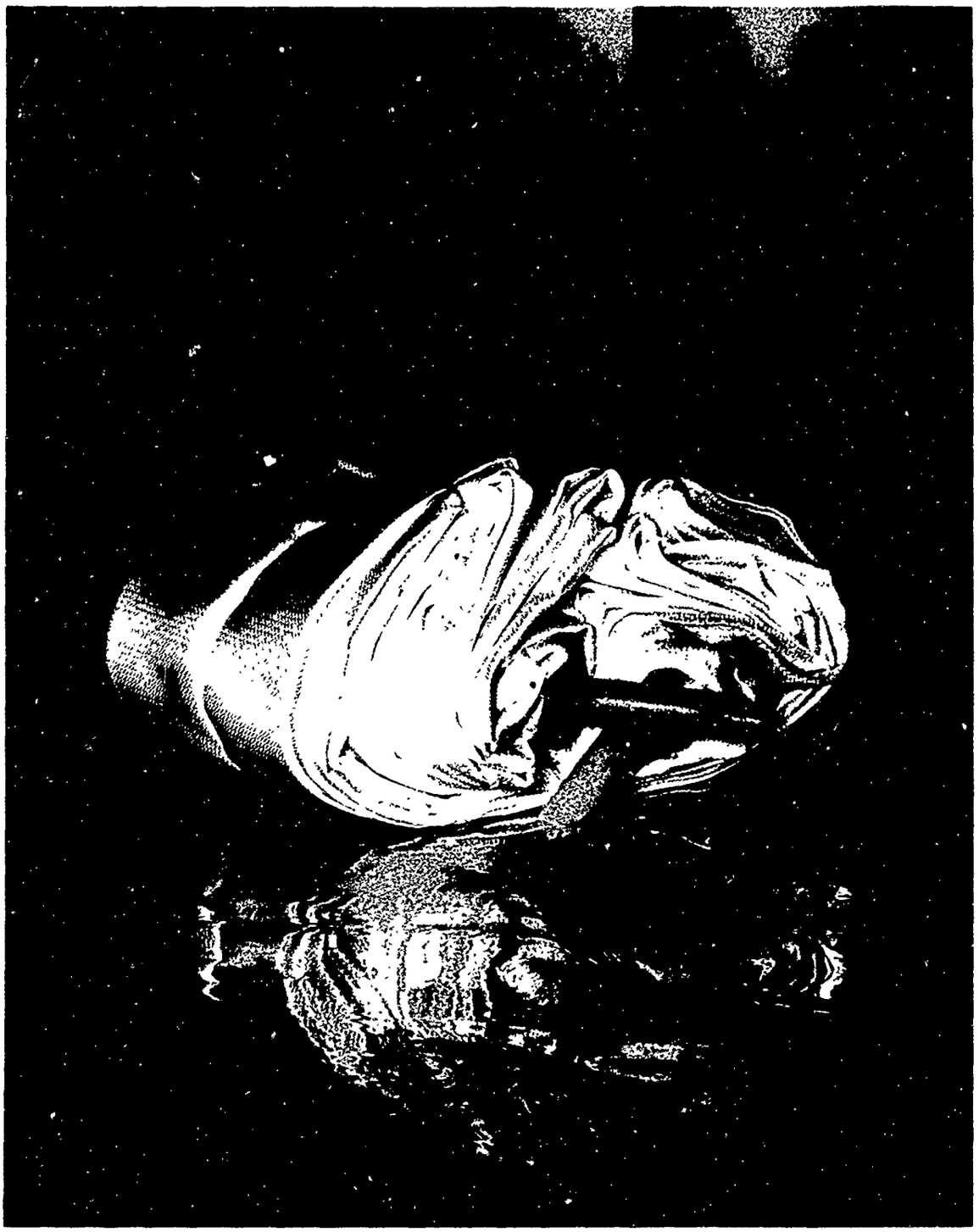

Figure 42 - Fourth Step In Folding The Aerospace Maintenance Dock

Because the aerospace maintenance dock was to function primarily in remote areas, the inflation unit for the dock was designed to be self-contained. Two alternate methods for this unit were considered: A supply of bottled gas (catalyst and air) or a motor driven blower. Although the first method was the simpler of the two, it was shown to be less efficient. Using the 1000 cfm requirement and assuming a cure time of about two hours the weight of bottled gas (at .073 lb/ft^3) was shown to be:

$$(1000)(60)(2)(.073) = 8750 \text{ pounds.}$$

Obviously a portable blower could be designed to weigh much less than this.

A complete, self-contained portable inflation unit was preliminarily designed to contain a gasoline engine, a blower, a source of catalyst vapors, and a framework to contain all of the above equipment. Since this unit could be reused many times, it was designed to inflate a much larger structure. Thus, the final design of the portable inflation system contained the following items:

1) A 14 inch diameter axivane fan with 5500 cfm air capacity at 3 inches of water pressure. This fan was capable of delivering the inflation vapors at a pressure of 8 inches of water. It was supplied by the Joy Manufacturing Company of Pittsburg, Pa.

2) A 6 hp gasoline engine connected to the axifan blower by "V" belts. It was manufactured by the Briggs and Stratton Company.

3) An air plenum chamber mounted on the axivane fan with two 10 inch diameter duct fittings and two 25 ft lengths of 10 inch diameter collapsible ducting. The ducts were compressible and designed to store under the plenum chamber. Quick connection clamps joined the ducting to the plenum chamber fitting and the dock fittings prior to inflating the dock.

4) A manifold pressure gage measuring 0 to 10 inches of water pressure. It was supplied by the Marshalltown Gage Company, Marshalltown, Ia.

5) A 3-1/2 gallon pressure sprayer to spray water and triethylamine catalyst into the intake area of the axivane fan.

6) A kerosene blow-torch of approximately 75,000 B.T.U. per hour capacity to raise the temperature of the inflation vapors to facilitate a quick cure of the dock.

7) A seamless steel tube framework to support all of the above items. This framework was designed with wheels and handles to make it maneuverable.

e. Tie Down Subsystem

A tie-down arrangement was dictated by the semicylindrical shape of the aerospace maintenance dock. Without a means to restrain the edges of the dock, a slight overpressurization of the dock would distort its semi-cylindrical shape toward cylindrical. Also, after rigidization of the dock, it was necessary to provide a means to restrain it from overturning or sliding under the action of wind loads. An efficient peripherial tie-down arrangement was the solution to both of these problems.

A system involving the use of conventional ground anchors was preliminarily selected to anchor the structure. There were two reasons for this selection. First, the majority of the sites in which the dock would be deployed would permit the use of an ordinary type ground anchor. Secondly, the tie-down subsystem was considered a minor part of the total system and did not warrant a special effort to develop an anchor that could be used in any type of terrain (e.g. rock or permafrost).

Preliminary calculations indicated that substantial tie-down reactions would be required to resist the wind and overpressurization forces. The largest reactions resulted from the wind forces and were about 1500 pounds.

An initial survey indicated that an arrowhead type ground anchor would develop the above reaction. Further, in response to our inquiry, the U.S. Army Natick Laboratories at Natick, Massachusetts endorsed the arrowhead anchor over other types of conventional ground anchors.

Twenty arrowhead type, 6 inch, aluminum ground anchors were ordered from the Laconia Malleable Iron Company of Laconia, New Hampshire. In addition, an impact driving tool and a standard four foot long drive rod were ordered from the same company. This comprised all of the equipment to enable one man to drive the anchors necessary to secure the aerospace maintenance dock. Nylon lines were to be fastened to each anchor and in turn tied to the catenary load tapes at each side of the dock.

E. Fabrication Techniques

1. General

After a complete survey of candidate substrate materials, woven fiberglass fabric was selected for the aerospace maintenance dock. This material is superior to other substrate fabrics in strength to weight and resin compatibility. However, it is a difficult material from which to fabricate, especially to seam and join.

Initially, a fiberglass sandwich material with integrally woven faces and core was considered for the aerospace maintenance dock of this study. Such a material is available in a variety of weaves and overall thicknesses from Raymond Development Industries of Huntington Park, California. It can even be obtained with a single degree of curvature (i.e., the inside facing incrementally shorter than the outside facing). However, at the time of this study the maximum length (parallel to the fluted core) of material was limited to about nine feet.

In order to orient the flutes of the integrally woven sandwich material in the circumferential direction of the 13 ft wide aerospace maintenance dock, at least two longitudinal seams would have been required. For structural reasons, these seams would have had to join the webs as well as the facings of the sandwich material. No effective method of accomplishing this was developed. Furthermore, the integrally woven fabric sandwich material could not combine a heavy load carrying facing with a low porosity facing. The successful deployment and utilization of the inflatable aerospace dock depended on the presence of both of these properties in all of the outside facings.

For the above reasons, the aerospace maintenance dock was designed to be constructed from flat, instead of three dimensional, woven fiberglass fabric. Working with flat fabrics allowed a greater freedom in the design of the configuration of the structure as well as permitting a feasible method of seaming and a good control of the porosity.

On the other hand, working from flat fabrics increased the amount of labor necessary to fabricate the structure. This did not appreciably effect the cost of the structure since it was offset by reduced materials costs.

The development of the fabrication of the actual 13 by 15 ft semicylindrical aerospace maintenance dock was directed into three main areas:

1) Model studies which evaluated design configurations, material handling techniques, and seaming techniques,

2) A seam strength study which evaluated the strength of various seaming configurations, and

3) The fabrication of the aerospace maintenance dock.

1) Model Studies

a) Design Configurations

A number of sandwich core configurations were available for use in this study. A true biaxial honeycomb core was not considered because of the difficulty in constructing such a core. Of the fluted core configurations, the rectangular, triangular, and corrugated cores were investigated.

A corrugated core was possible to achieve in the roof construction only. This was due to the curvature of the roof which permitted the various radii of curvature of the corrugated section to be attained by correctly varying their circumferences. Thus, when the model was internally pressurized, each of the circumferential elements of the corrugated core tended to assume the position of its respective radius. A number of 26 by 30 inch models of the aerospace dock roof were constructed using various corrugated sections. See Figure 43.

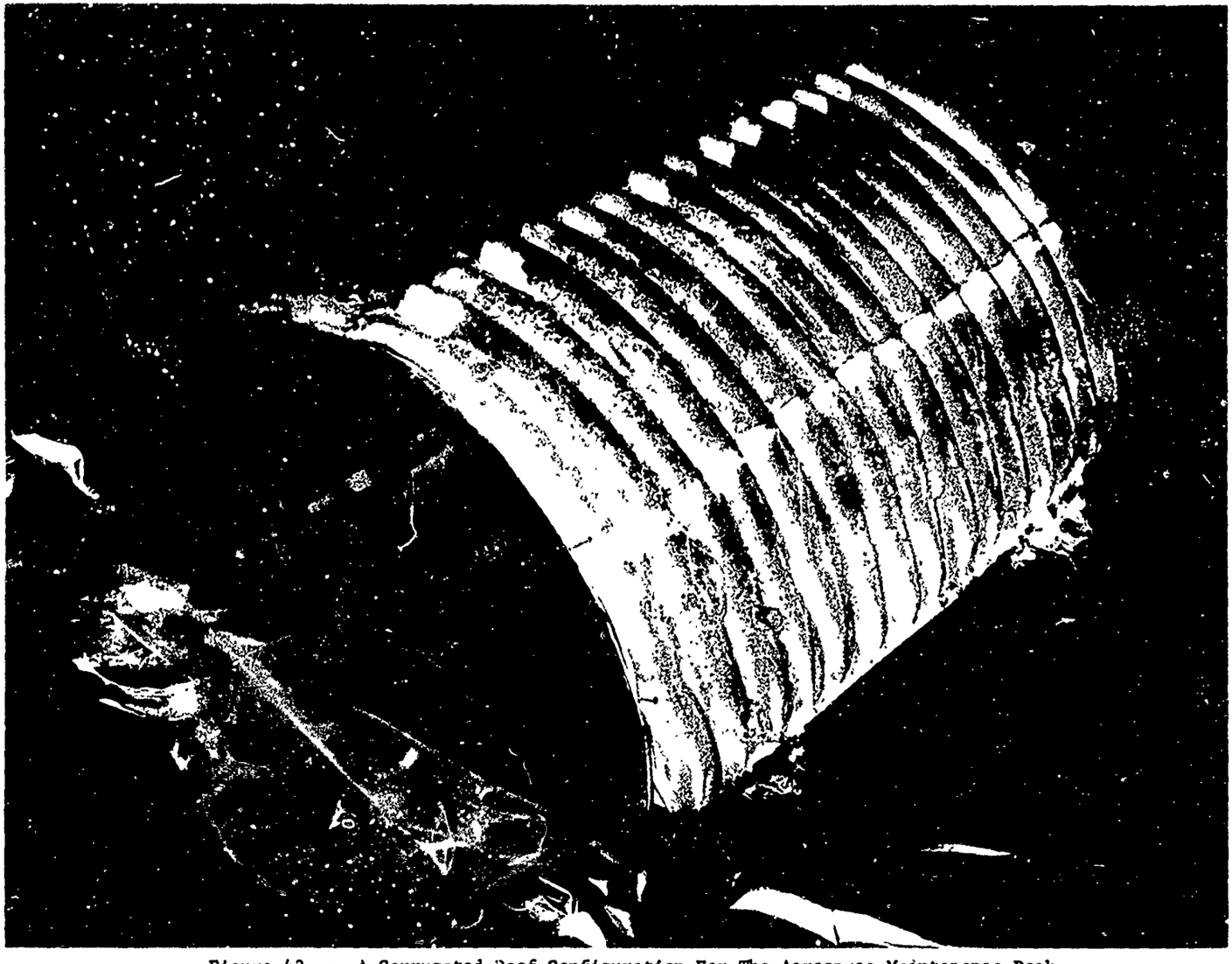

Figure 43 - A Corrugated Roof Configuration For The Aerospace Maintenance Dock

The corrugated core section was found to be very satisfactory from the standpoint of construction and deployment. However, it was difficult to join to the facing material. Also, it did not permit a satisfactory support of the facings since the minimum pitch of the corrugations was four times the height of the section. On the other hand, the rectangular and triangular core sections were no more difficult to construct and were much more effective in supporting the facings of the sandwich constructions.

A comparison of two 26 by 30 inch models is shown in Figures 44 and 45. In Figure 44, the roof section utilizes a corrugated core. In Figure 45, vertical webs are used to separate the two facings of the roof sandwich section.

The success of the rectangularly fluted models led to the development of a larger model of the aerospace dock. This model was one-third as wide as the prototype but of a foreshortened length. The completed model measured 52 inches wide by 30 inches long. The roof and rear wall were constructed of a rectangularly fluted sandwich section. The front wall was constructed of a triangularly fluted sandwich section. The cells (webs) were oriented circumferentially in the roof, vertically in the rear wall, and horizontally in the front wall. These orientations gave the most stiffness to the various components of the dock.

In this model, as in the smaller models, the structure was packaged, resin impregnated, and deployed by the techniques developed under a previous contract. As was noted in a preceding section, these techniques were not applicable to the larger structure of this contract and were accordingly modified.

In Figure 46, the roof, floor, and end walls of the model are shown prior to assembly. The folded structure is being inserted into an impermeable envelope for resin impregnation, Figure 47. In Figure 48, the model has been deployed to its desired configuration and rigidized.

A commercial, electric vacuum cleaner was used in conjuction with a "variac" transformer as an inflation unit for the model studies. This unit permitted any volume rate of inflation between 14 and 80 cfm to be selected. Thus, as models were constructed and deployed a continuous check of their porosities was recorded. A simple U-Tube water manometer measured the internal pressures necessary to deploy and stabilize each model until it became rigid.

b) Seaming Techniques

From the model studies, the most effective method of seaming and joining the fiberglass substrate material was developed. This method was sewing. Other methods were investigated and found to be entirely unsatisfactory. Adhesive seams would not withstand the folding and packaging abuse without separating, and mechanical fasteners would cause the glass fabric to ravel and separate. Even sewing was not totally satisfactory.

Many types of woven glass fabric would not hold a sewn seam. These fabrics would ravel at the sewn seams until a large unwoven area resulted. Even the fabrics that could be sewn reasonably well had very weak seams. The ability of a fabric to be successfully sewn became a primary criteria in selecting it for use in the aerospace maintenance dock. As the model studies progressed, the easily joined fiberglass fabrics became apparent.

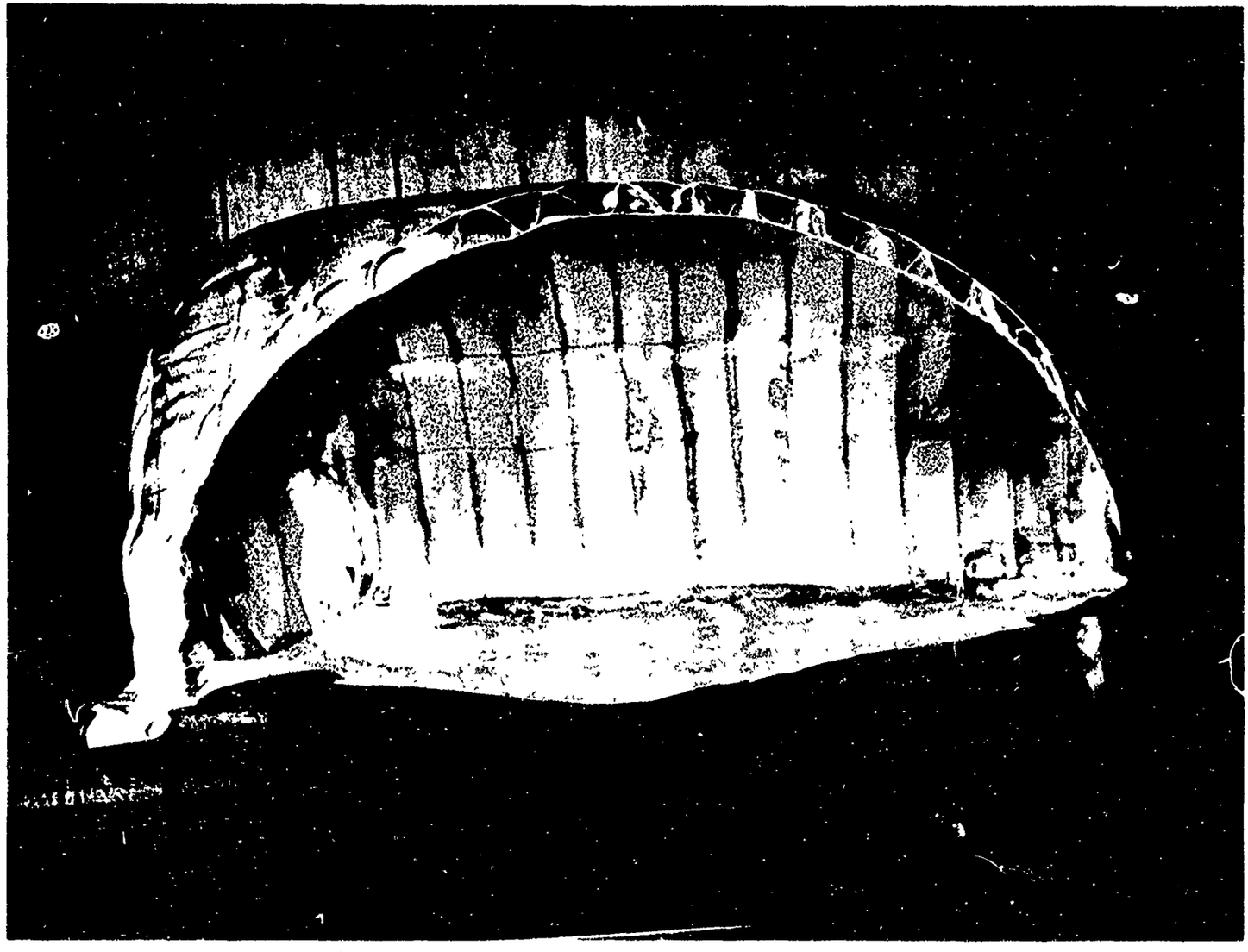

Figure 44 - A Corrugated Roof Configuration With Faces Attached For The Aerospace Maintenance Dock

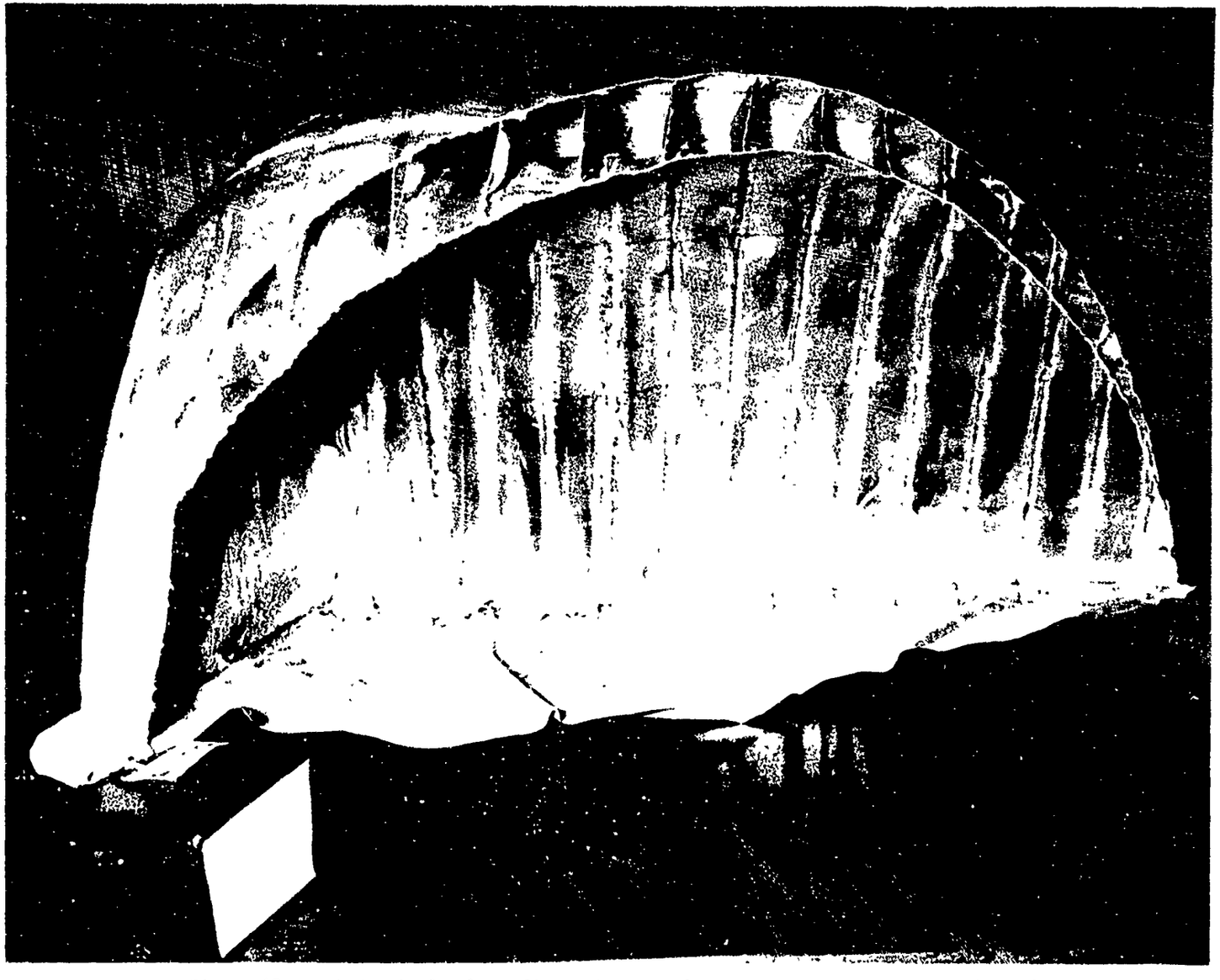

Figure 45 - A Vertical Web Configuration For The Aerospace Maintenance Dock Roof

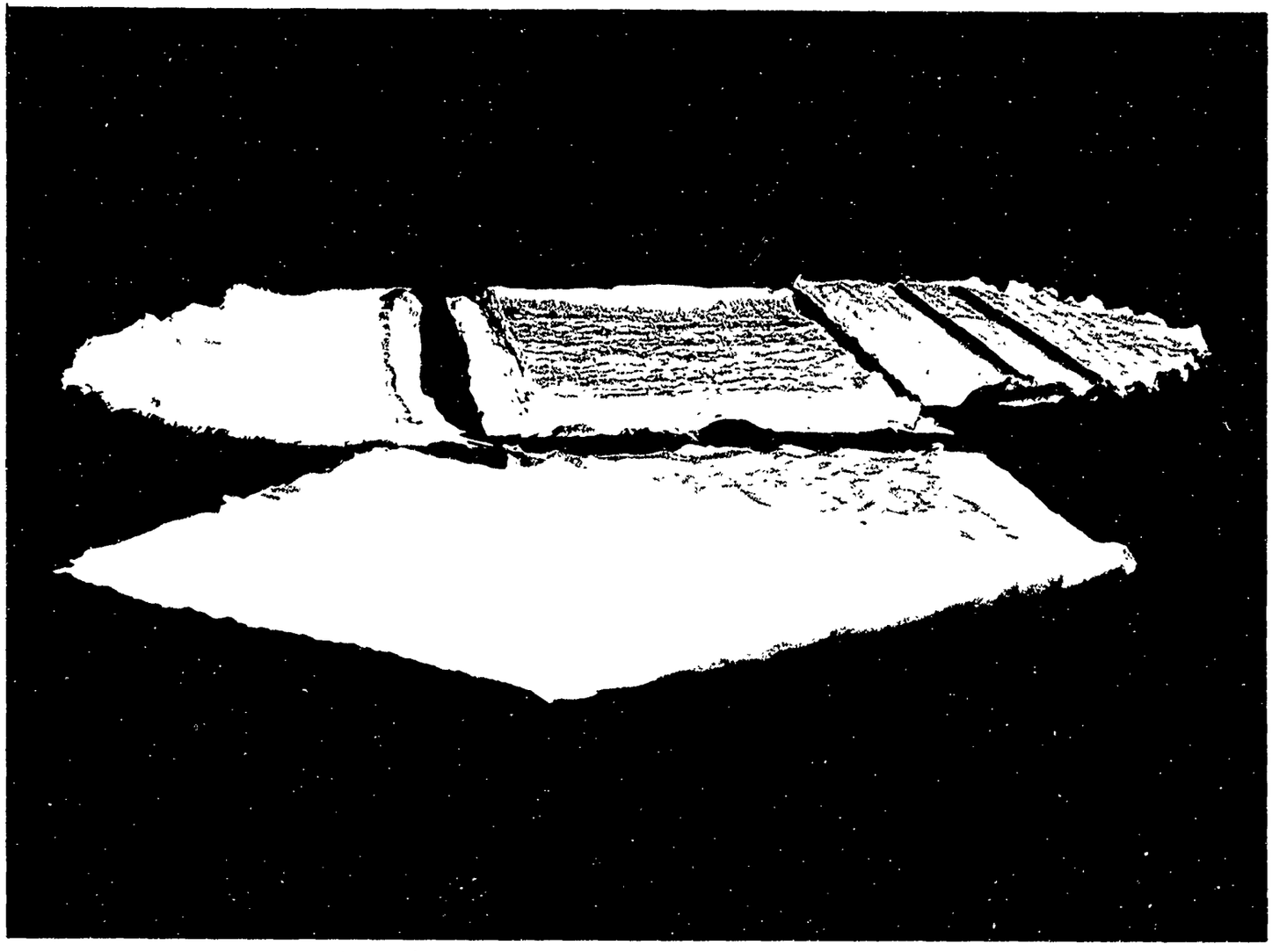

Figure 46 - The Four Components For The Model Aerospace Maintenance Dock Before Assembly

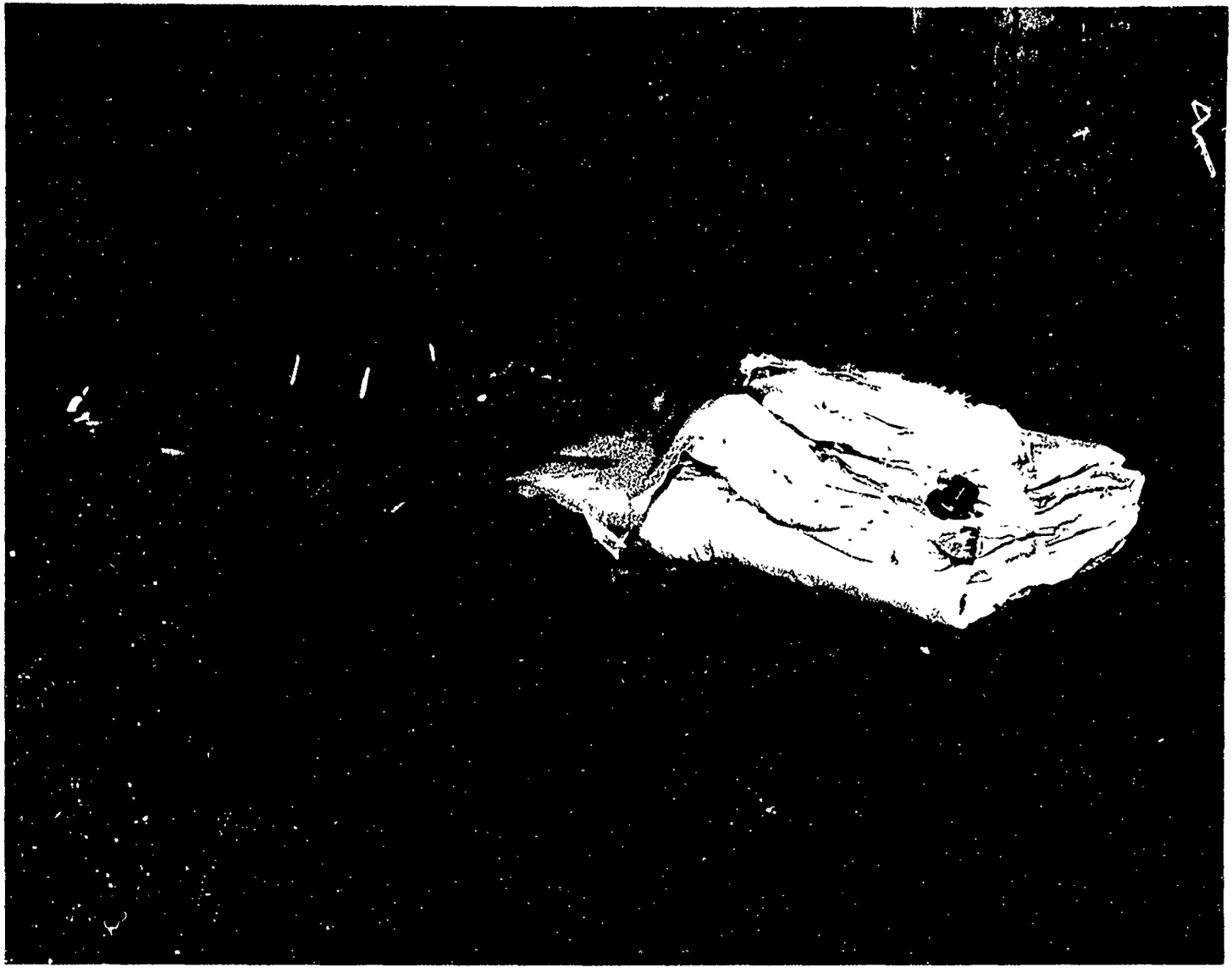

Figure 47 - Folded Aerospace Maintenance Dock Model Inserted Into Resin Impregnation Envelope

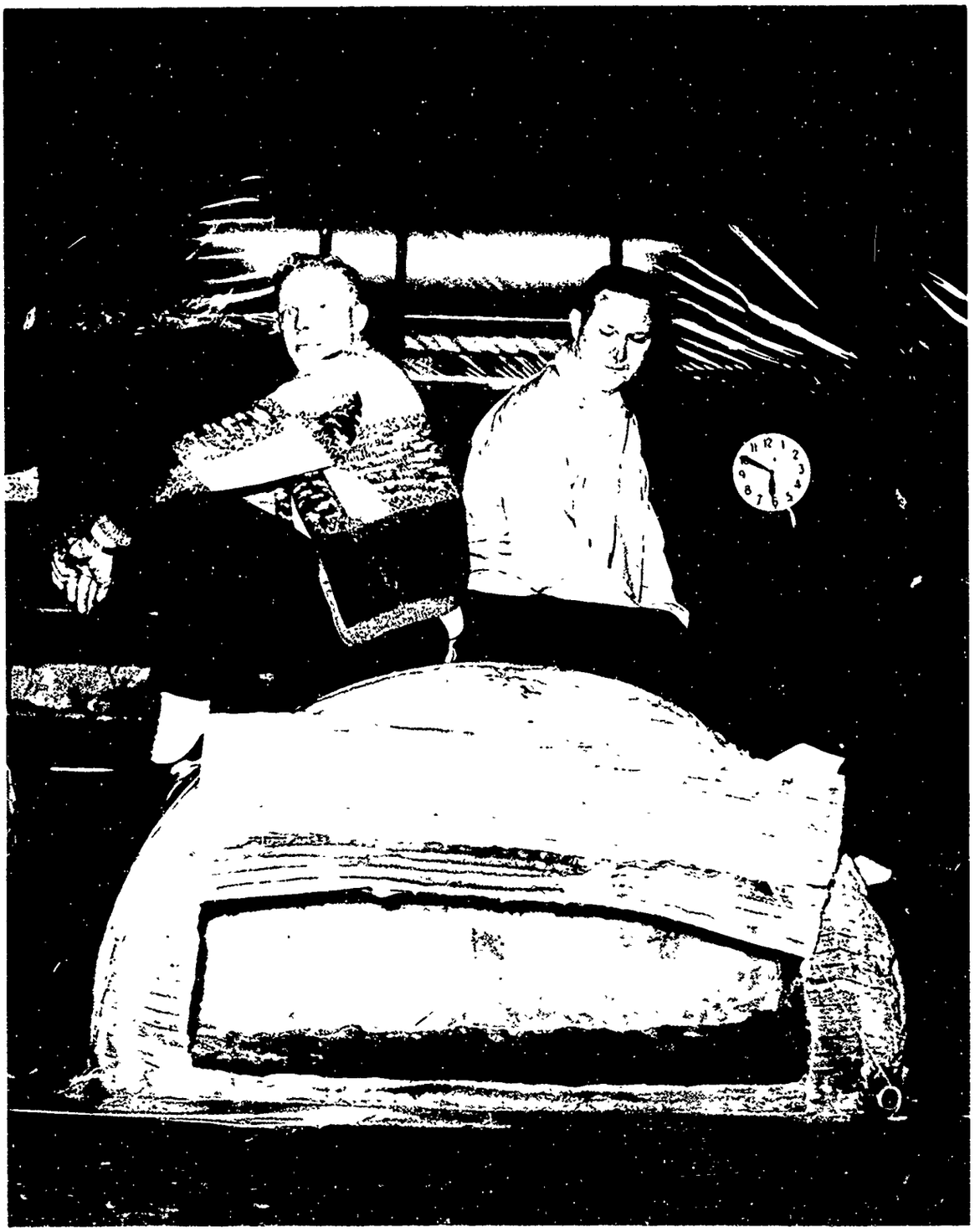

Figure 48 - Deployed And Rigidized Aerospace Maintenance Dock Model

c) Material Handling Techniques

Also out of the model studies, came optimum material handling techniques. Among the most important techniques were marking and cutting. Since all of the models involved fabricating intricate, three dimensional components from flat fabric, a method of marking off pieces on the flat fabric and then cutting them out for assembly was developed.

During marking, care had to be taken to keep the fiberglass fabric from sliding and distorting the pattern. Also, it was necessary to use a marking pen that would not later prematurely catalyze the rigidizing resin.

Before any of the fiberglass fabrics could be cut, they had to be processed to prevent raveling. This was accomplished by running a special (zig-zag) sewn seam just inside and parallel to the edge to be cut. The zig-zag seam bound the material adjacent to the cut edge and prevented raveling. Starching the fabrics before they were cut was also effective in minimizing raveling. However, it was difficult to remove the starch from the fabric in order to get a good resin impregnation.

3. Seam Strength Study

A seam strength study was an important part of the final design of the aerospace maintenance dock. It was from the results of this study that seaming materials and configurations were chosen. From previous work with the models of the aerospace dock, it was learned that the sewn seams were only critical to the performance of the structure prior to rigidization. After the resin was cured, the bonding action of the resin made all joints as strong as the base material.

Prior to rigidization, however, all of the sewn seams had to restrain the unfolding and inflation pressures. For the most part, these seams were made by sewing with a relatively heavy thread in an industrial type sewing machine. The seam testing program was conducted with linen, nylon, and fiberglass thread. These threads were used to construct single and double lap and fin seams in two types of fiberglass cloth. The joints were impregnated with urethane resin and tested in the wet condition as tensile specimens in an Instron testing machine.

The results are reported in Table 37. The table lists the maximum loads sustained by each seam in lbs per inch. However, the allowable load for limit design conditions was not taken as more than one-half of the ultimate maximum load since excessive slippage and deformation of the seams were present at the maximum loads. The results are the average of three or more test samples. Sketches of the joints are shown in Figure 49.

It was found, that the thread type did not make any appreciable difference on the seam strengths. Since the nylon thread was found to be better suited to the sewing machines, it was used in sewing the aerospace maintenance dock. There were no failures in the thread itself, but only by excessive slippage of the seam on the fabric.

TABLE 37

SEWN SEAM STRENGTHS

Sketch Number	Description of joint	Fiberglass cloth type	Cloth edge condition	Average maximum load - lbs/inch	Number of test samples
1	Lap joint, Single seam	#181	zig-zag with cotton thread	10	9
1	Lap joint, Single seam	#181	selvaged edge	15	3
1	Lap joint Double seam	#181	as cut	7*	9
1	Lap joint, Single seam	#H-51	as cut	3	3
2	Fin joint, Single seam	#181	as cut	7	9
2	Fin joint, Single seam	#181	selvaged edge	22	3
2	Fin joint, Double seam	#181	as cut	14	9
2	Fin joint, Single seam	#H-51	as cut	8	2

* seams had 1/4" edge distance in spots and slid off the edges

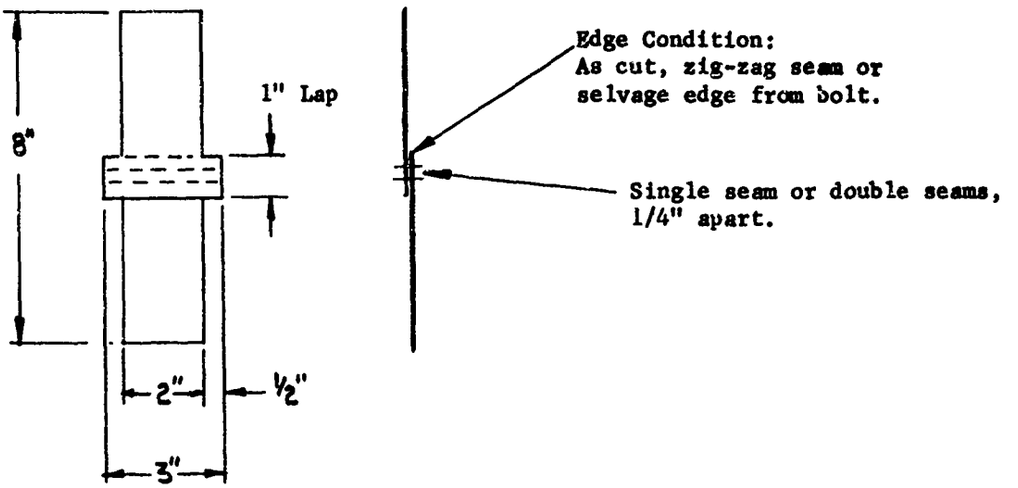

Lap Seams

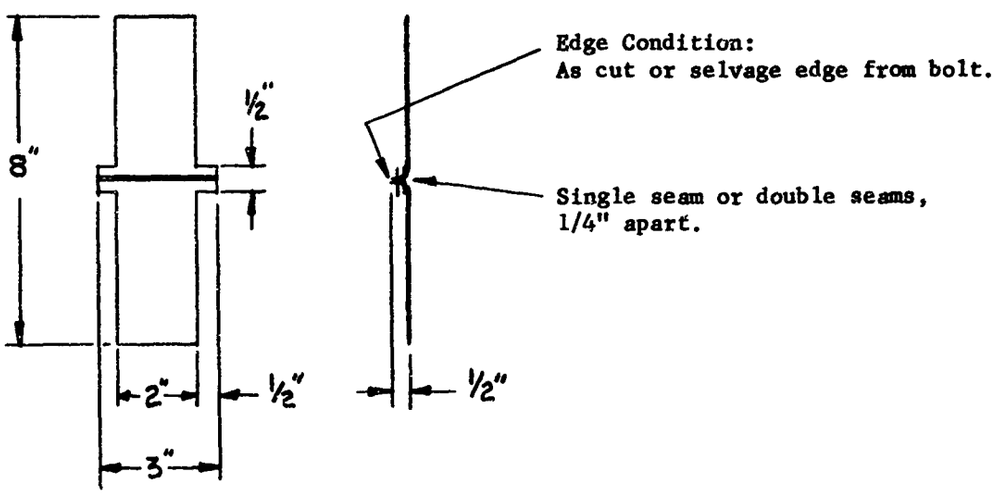

Fin Seams

Figure 49 - Seam Configurations

4. Fabrication of The 13 x 15 Foot Aerospace Maintenance Dock

The fabrication of the aerospace maintenance dock itself was no longer a development effort. Rather, it was a matter of drawing from previous efforts to design and construct the end item. The fabrication of the dock was concentrated into three areas - design, preparing drawings and materials, and assembling materials.

a. Design

The design of the final 13 by 15 ft, structure was very similar to the 52 x 30 inch model. The web configurations and orientations were identical to the model; however, different fabric weaves and depths of sandwich sections were used.

The roof of the final structure was constructed of three different types of fiberglass fabric. The inside facing was style #181 fabric. The webs were continuous 4 inch wide woven fiberglass tapes (Hess-Goldsmith Style 64-T) and the outside facing was style #181 fabric lined with style #402 fabric for porosity control. The depth of the roof section was 3 inches. The webs were spaced 3 inches apart by sewing them to the inside facing at this spacing. However, they were sewn to the outside facing 3-5/16 inches apart. This, and an excess of material in the outside facing, permitted the inflation pressure to blow the outside facing into cylindrical sections between webs. The curved cylindrical sections were important to the design of the outside facing because of their superior load carrying characteristics.

All of the components of the roof (facings, webs) were continuous in the circumferential direction. Thus, except for joining the roof to the floor, the roof contained no longitudinal seams. This provided more assurance of a successful inflation of the structure because there were no sewn seams subjected to circumferential inflation stresses after the roof was secured to the tie down anchors.

The rear wall of the structure was constructed of the same materials and sandwich configuration as the roof. The rear wall differed from the roof in that the webs were sewn to both the inside and outside facings 3-5/16 inches apart. Thus, by providing excess facing material in the rear wall, both facings were permitted to assume cylindrical sections between webs during inflation and rigidization. In the final configuration, the webs were spaced 3 inches apart.

All of the seaming in the rear wall was oriented vertically, parallel to the webs. During inflation, it was subjected to very small stresses. The front wall of the structure was constructed of a 3 inch deep sandwich section with a triangular web core configuration. The triangular configuration permitted the web to be continuous in two directions and thus allow some biaxial stress resolution. The facings were constructed of the same material as used in the roof and rear wall, however, the web was style #181 fabric. The flutes of the web were oriented horizontally to give the greatest stiffness to the door and surrounding wall. Again, as in the rear wall, excess facing material was provided so that the facings would blow into continuous cylindrical sections between attachments to the triangular web. All of the seaming in the front wall was oriented horizontally. The seaming in this wall also was not subjected to any appreciable inflation stresses.

The floor was constructed of a single layer of style #402 fiberglass fabric. None of the seaming in the floor was subjected to large inflation pressures because it was all oriented parallel to the width of the structure.

A formal stress analysis was conducted on all of the load carrying components of the aerospace maintenance dock. The theory that is discussed in a preceding section was utilized for this purpose. All of the components of the dock from the fluted core sandwich sections to the catenary load tapes showed positive margins of safety against the ultimate design loads.

b. Drawings and Materials

Sewing patterns and assembly drawings were prepared for each of the end walls, the roof, and the floor of the aerospace maintenance dock. The sewing patterns contained seam locations, dimensions, and other information necessary to mark, cut, and sew the fiberglass fabric into the desired configurations. The assembly drawings served as illustrated instructions for assembling the various configurations into the final structure.

The information contained on the sewing patterns was transferred to the various fiberglass fabrics with marking pens for cutting and sewing operations. Each edge to be cut was first bound with a zig-zag seam to prevent ravelling. After the pieces were marked and cut, the porosity control liner fabrics were sewn to all of the outside facings. The facings and webs were then sewn together to form the sandwich sections of the roof or end walls.

c. Material Assembly

The outside facings of both end walls were sewn to the outside facing of the roof with circumferential fin seams. The inside facings of these pieces were then joined in the same manner.

Both facings of the end walls and the roof were sewn to the floor in parallel fin seams. These seams were separated by the depth of the roof and wall section (3 inches). All but the inner facing of the roof were joined with single fin seams. This facing was joined to the floor with a double fin seam because of the hoop tension stresses present in this seam before the dock could be secured to the ground anchor tie downs. The fabrication of the aerospace maintenance dock is shown in Figure 50.

Subsequently, the fabricated dock was vacuum impregnated, temporarily folded, inflated, and rigidized with in house funds. Figure 51 shows the folded, impregnated dock while the rigidized structure is seen in Figure 52.

Figure 50 - Fabrication Of The Aerospace Maintenance Dock

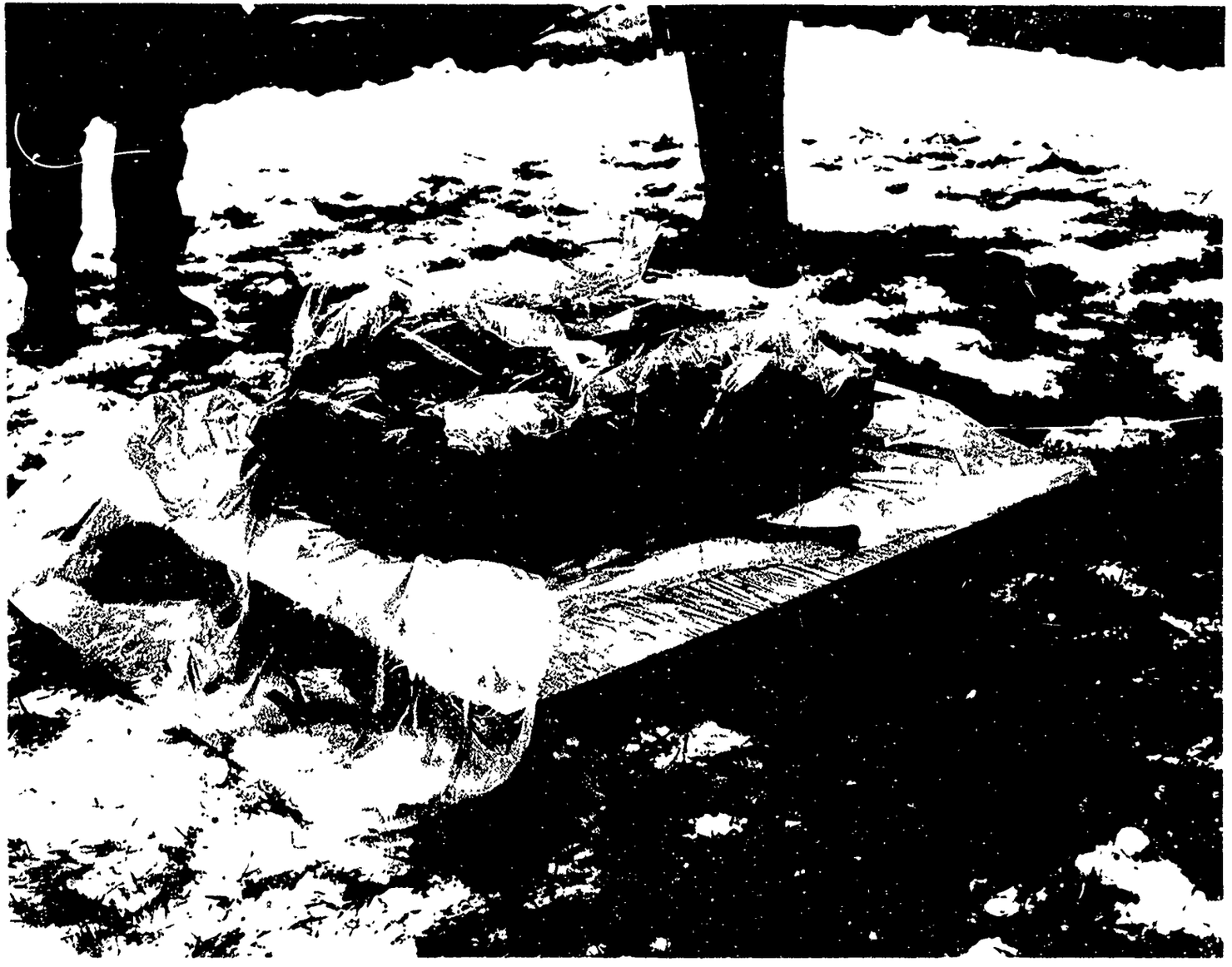

Figure 51 - 13 x 15 Foot Aerospace Maintenance Dock Impregnated and Packaged

Figure 52 - Rigidized 13 x 15 Foot Aerospace Maintenance Dock

SECTION 6

CONCLUSIONS

A. The resin research improved the vapor cured urethane system and demonstrated the feasibility of an alternate vapor cured system.

1. A trend was established that showed that with continued research it is possible to achieve increased physical strengths with decreased cure times.

2. A polyester resin which was catalyzed with a peroxide vapor was improved under this effort.

B. The development of improved solar collectors was possible by selecting materials and techniques that proved to be optimum in constructing and rigidizing smaller size collectors. In particular:

1. It appears that large diameter solar collectors can be successfully fabricated and deployed from completely flexible, foldable plastic films, fabric sandwich material, and a gas cured rigidizing resin.

2. The pressure that is used to inflate the aluminized Mylar film during fabrication is critical to the appearance of the reflective surface after the solar collector is rigidized.

3. The flexible layer developed during this effort does not completely mask the irregular surface of the rigidized fabric sandwich material. This is also attributed to solvent attack on the flexible layer.

4. A scheme of vacuum impregnating the fabric sandwich material with predistributed resin and an impermeable, contoured cover film appears to be the most effective for large solar collectors.

5. An improved reflective surface was obtained by changing the arrangement of the drop threads in the fabric sandwich material from parallel rows to a random pattern.

C. From the development of the 13 foot diameter by 15 foot long terrestrial shelter (aerospace maintenance dock), the following items were concluded:

1. A practical (if approximate) theory of stress resolution can be applied in designing structures of this nature. The theory developed under this effort correlated fairly well with test results.

2. Fabricating this and similar structures from flat fabric is not entirely satisfactory at this time. However, it is the best solution to many types of structures.

3. Larger sized structures similar to the aerospace dock appear to be feasible to fabricate, without any appreciable development effort.

SECTION 7

RECOMMENDATIONS

A. On the basis of the resin research completed under this effort, it is recommended that:

1. Aryl isocyanates be studied to improve the reactivity of the vapor cured urethane system. Included in this study should be chloro-m-phenyl diisocyanate and several new poly aromatic diisocyanates.

2. The plasticizer additive study should be continued and evaluated for improvements to the properties and performance of the resin system.

3. Polyfunctional polyester polyols be compared to the recently developed polyether polyols for physical strengths.

4. Amido-polyols and urido-polyols be evaluated.

5. Metallic catalysts should be investigated to increase prepolymer reactivity without jeopardizing shelf stability.

6. Modifications be made to polyester based resins in order to increase co-polymerization reaction rates.

7. Reactive nonvolatile monomers be synthesized.

8. Vinyl type monomers be evaluated for increased reactivity.

B. On the basis of the present development of the inflatable, self-rigidizing solar collector, the following recommendations are made:

1. An exact system analysis of the solar collector as an expandable space structure should be made. This analysis should define the various elements of the space environment and design methods to successfully deploy, rigidize, and utilize an inflatable, self-rigidizing solar collector in space.

2. An effort to improve the flexible layer in order to reduce distortions in the reflective surface should be continued.

3. Refinements to the current method of impregnating the fabric sandwich material with predistributed resin envelopes should be made.

C. The following recommendations are made on the basis of the study conducted to develop an inflatable, self-rigidizing aerospace maintenance dock.

1. An effort should be made to improve the substrate fabric. During this study, it was necessary to work with fiberglass substrate fabrics that were designed for other applications. An optimum fabric for application to thin walled, inflatable structures, should be constructed of larger yarn filaments, less porous and easier handling weaves, and sandwich material with integrally woven webs and facings throughout.

2. As an alternative to integrally weaving facings and webs, an improved method of seaming and joining the substrate material should be investigated.

3. Inflatable, self-rigidizing structures should avoid configurations containing flat surfaces (other than the floor). The flat end walls of the aerospace maintenance dock unnecessarily complicate the fabrication of the dock.

4. A shelf life study should be conducted on large structures to see if the outgassing and impregnation methods that successfully prolong the shelf life of small samples can be applied to the larger sized structures.

SECTION 8

REFERENCES

1. Ning Chien, Yin Feng, Hung-Ju Wang, and Tien-To Siao, "Wind-Tunnel Studies of Pressure Distribution on Elementary Building Forms", Iowa Institute of Hydraulic Research, State University of Iowa, Iowa City, 1951.

2. Anonymous, "Plastics for Flight Vehicles - Part I - Reinforced Plastics", MIL-HDBK-17, Armed Forces Supply Support Center, Washington, D.C., 5 Nov. 1959.

3. Syracuse University, "Materials Design Handbook Division I Structural Plastics", ML-TDR-64-141 AF Materials Laboratory WPAFB, Ohio, May 1964.

4. Handbook of Textile Fibers, Harris Research Labs, Inc., 1955.

5. MIL-HDBK-5, Aug., 1962.

6. F. W. Forbes, "Expandable Structures", Flight Accessories Laboratory, Directorate of Aeromechanics, ASD, WPAFB, Dayton, Ohio.

7. Schwendeman, Robertson, Salyer "Gelatin As A Possible Structural Material For Space Use", ASD-TDR 63-444, Wright-Patterson Air Force Base, Ohio.

8. N. Fried, "The Compressive Strength of Parallel Filament Reinforced Plastics - The Role of the Resin", paper presented at the 18th Annual meeting of the S.P.I. in Chicago, Feb. 1963.

9. "Handbook of Structural Stability Part IV - Failure of Plates and Composite Elements", NACA TN-3784, Aug. 1957.

10. S. P. Timoshenko and J. M. Gere, "Theory of Elastic Stability", McGraw Hill, 1961.

11. A. B. Burns and R. F. Crawford, "Buckling of Beryllium Plates and Cylinders", Astronautics and Aerospace Engineering, Oct. 1963, pp 36-41.